PHOTOSYNTHETIC ADJUSTMENTS OF *AMARANTHUS* VARIETIES IN RESPONSE TO GROWTH IRRADIANCE

A Thesis

Submitted to the College of

Graduate and Postdoctoral Studies

In Partial Fulfillment of the Requirements

For the Degree of Master of Science

In the Department of Plant Sciences

University of Saskatchewan

Saskatoon

By

Elena Benic

PERMISSION TO USE

In presenting this thesis in partial fulfillment of the requirements for a Postgraduate degree from the University of Saskatchewan, I agree that the Libraries of this University may make it freely available for inspection. I further agree that permission for copying of this thesis in any manner, in whole or in part, for scholarly purposes may be granted by the professor or professors who supervised my thesis work or, in their absence, by the Head of the Department or the Dean of the College in which my thesis work was done. It is understood that any copying or publication on use of this thesis or parts thereof for financial gain shall be given to me and to the University of Saskatchewan in any scholarly use which may be made of any material in my thesis.

Requests for permission to copy or to make other use of materials in this thesis in whole or in part should be addressed to:

Head of the Department of Plant Sciences
University of Saskatchewan
Saskatoon, Saskatchewan S7N 5A8
Canada

OR

Dean
College of Graduate and Postdoctoral Studies
University of Saskatchewan
107 Admission Place
Saskatoon, Saskatchewan S7N 5A2
Canada

ABSTRACT

Increased concern of food security has created a demand for crops that exhibit high yields under conditions that require a minimal input of resources, such as light. *Amaranthus* is a C4 plant that has multiple uses, including that of a food source in many parts of the world. The objective of this research was to evaluate the photosynthetic performance of red and green vegetable varieties of *Amaranthus blitum* grown under high light (HL; 500 µmol m^{-2} s^{-1}) photosynthetic photon flux density (PPFD) and low light (LL; 70 µmol m^{-2} s^{-1} PPFD). Under HL growth irradiance, the red variety accumulated more biomass than the green variety before flowering. This was accompanied by a 1.2-fold increase of photosynthetic efficiency, a 1.5-fold increase of photosynthetic capacity (maximal rates of O_2 evolution), a 1.5-fold increase of dark respiration rate, a 1.3- fold increase in light compensation point and a 1.7-fold increase of light saturation point. These values were supported by a 2.5- and 2.6-fold higher content of chlorophyll and carotenoids, respectively. A 4.7-fold greater betalain content was also observed. In addition, exposure to a photoinhibitory irradiance (1450 µmol m^{-2} s^{-1} PPFD) at 2°C for 4 hours demonstrated the red variety exhibited increased tolerance to photoinhibition in comparison to the green variety when measured at the level of maximal photochemical efficiency of photosystem II. Further, this may be a result of the screening of light and shielding of chloroplasts by betalains that accumulate predominantly in the abaxial mesophyll and supported by a 1.2-fold increase in the red variety lower mesophyll cells thickness than in the green variety, leading to a thicker leaf. The granal index in bundle sheath cells under high light irradiance in the red variety was 2.0-fold greater than in the green variety, supported by 3.1-fold greater ratio of the length of appressed/non-appressed thylakoids and a 2.0-fold increase in thylakoids/granum. These results suggest that under HL growth irradiance, the granal index and stackness (thylakoids/granum) enhances photosynthetic efficiency and capacity. In contrast, under LL growth irradiance both varieties performed photosynthetically similarly. Collectively, these results indicate that the red variety possesses a greater photoacclimatory capacity than the green variety under HL growth irradiance, whereas neither variety expressed an advantage under the LL growth irradiance in this study.

ACKNOWLEDGEMENTS

I would like to express my deepest gratitude and appreciation to Dr. Gordon R. Gray and Dr. Karen K. Tanino for their encouragement, scientific guidance, patience and financial support during my studies.

I would also like to thank my graduate committee members: Dr. Rosalind A. Bueckert (chair), Dr. Robert H. Bors and Dr. Art Davis for providing their diverse backgrounds to support me during this project, as well as deep thanks to Dr. Simon D. X. Chuong for being the External Examiner and for his imput to the completion of this work.

Special thanks to the staff of the Department of Plant Sciences, especially: Dr. Yuguang Bai (head), Carolyn Ouellet, Gloria Gingera and Marlene Freeman. Special thanks to the many members of Dr. Tanino's Lab for their time, advices and support with specific note of Dr. Ian Willick, Kaila Hamilton, Eric Rae, Dr. Prakash Venglat, Pankaj Banik, Gowribai Valsala, Rensong Liu, Dr. Masoomeh Etehadnia, Dr. Tawhidur Rahman and Abdul Halim. Quality plant care was made possible by the phytotron team.

Special thanks to Dr. Guosheng Liu from Department of Biology for advice and help in preparation of samples for TEM, to Larhonda Sobchishin from WCVM imaging center using TEM. Microscopy techniques were learned from the imaging team at NMBU with special recognition of Drs. YeonKyeong Lee, Hilde Kolstad, Lene Cecilie Hermansen and Jorunn Olsen. Special thanks also to Dr. Chris Ambrose for his advice and support.

Without the numerous and generous funding sources this project would have not been possible: Special thanks to Saskatchewan Ministry of Agriculture, Natural Sciences and Engineering Research Council of Canada, Saskatchewan Innovation & Opportunity Scholarship, Rene Vandeveld Postgraduate Scholarship and Daniel Geddes Graduate Scholarship in Plant Sciences, as well as the Department of Plant Sciences.

Finally, I would like to recognize my husband Kresimir Benic, and friends (especially Tatiana Mashkova) for their interest and unwavering support over the course of the project.

DEDICATION

This thesis is dedicated to my beloved husband Kresimir Benic, son Jakov, and daughters Azra and Judita for their love, support and incredible patience.

TABLE OF CONTENTS

Page

LIST OF TABLES

LIST OF FIGURES

LIST OF ABBREVIATIONS

Asp	Aspartate
ATP	Adenosine triphosphate
BSC	Bundle sheath cells
Car	Carotenoid
Chl	Chlorophyll
CP	Cytoplasmic protrusions
CI	Crystalline inclusions
Cyt b_6f	Cytochrome b_6f complex
DAS	Days after sowing
D1	Reaction centre D1 protein of PSII
DW	Dry weight
EC	Epidermal cells
ETR	Relative linear electron transport rate through PSII
F_m	Maximal fluorescence in the dark-adapted state
F_0	Minimal fluorescence in the dark-adapted state
F_v	Variable fluorescence in the dark-adapted state ($F_m - F_0$)
F_v/F_m	Maximal photochemical efficiency of PSII
FW	Fresh weight
GI	Granal index
HL	High light
H_2O_2	Hydrogen peroxide
LA	Leaf area
LCP	Light compensation point
LEC	Lower epidermal cells
LHCI	Light harvesting complex I
LHCII	Light harvesting complex II
LL	Low light
LMC	Lower mesophyll cells
LSP	Light saturation point
LT	Leaf thickness
MC	Mesophyll cells
NAD-ME	Nicotinamide adenine dinucleotide-Malic Enzyme
NPQ	Non-photochemical quenching
O_2	Oxygen
OAA	Oxaloacetate
OEC	Oxygen evolving complex
PAR	Photosynthetically active radiation
P_{680}	Reaction centre Chl of PSII
$P_{max}O_2$	Maximal rate of O_2 evolution
PEP	Phosphoenolpyruvate
PEPC	Phosphoenolpyruvate carboxylase
PR I	Peripheral reticulum I
PR II	Peripheral reticulum II

PPFD	Photosynthetic photon flux density
PSI	Photosystem I
PSII	Photosystem II
Q_A	Primary plastoquinone electron acceptor of PSII
q_L	Coefficient of photochemical quenching
R_{dark}	Rate of dark respiration
RC	Reaction centre
RGR	Relative growth rate
ROS	Reactive oxygen species
Rubisco	Ribulose-1,5-bisphosphate carboxylase-oxygenase
RuBP	Ribulose-1,5-biphosphate
SD	Standard deviation
SE	Standard error
SI	Stomatal index
SLA	Specific leaf area
UEC	Upper epidermal cells
UMC	Upper mesophyll cells
VB	Vascular bundle
3-PGA	3-phophoglycerate
$\Phi_{app}O_2$	Apparent quantum yield of O_2 evolution
Φ_{PSII}	Effective quantum yield of PSII electron transport
ΔpH	Proton gradient across the thylakoid membrane

CHAPTER 1

1.0 INTRODUCTION

Amaranthus is a dicotyledonous C4 plant from the Amaranthaceae family, genus *Amaranthus* L*. Amaranthus* plants are highly studied as a model C4 plant of the nicotinamide adenine dinucleotide-dependent malic enzyme (NAD-ME) subtype. Being C4 plants, they possess a high photosynthetic performance by eliminating the competing photorespiration process (Long 1999, Sage 1999), and as such, require less nitrogen and water than C3 plants which makes these plants an environmentally sustainable crop (Hocking and Meyer 1991). Moreover, *Amaranthus* is used as a nutritious grain and fresh leafy vegetable in many parts of the world, viewed as a "future food security crop", especially in African countries. However, food security is also a huge issue even in highly developed countries. The high cost of electricity has created interest in the greenhouse industry for lower light tolerant crops which can be produced as a secondary crop. Based on previous experiments under greenhouse conditions on several vegetable *Amaranthus* spp. and varieties (Tanino *et al*. 2014), the red and green varieties of *Amaranthus blitum* spp. appeared to accumulate greater biomass than other species and varieties. However, when plants were grown under reduced light, the red variety appeared to show greater plasticity of carbon assimilation than the green variety, based on biomass accumulation. Light in greenhouse conditions was modulated by using shade cloth (Tanino *et al*. 2014). For this research, the red and green varieties of *Amaranthus blitum* were selected to primarily evaluate the photosynthetic adjustments in response to growth irradiance, and secondarily the role of betalain pigments in enhancing photoprotection. Their phenotype suggested that these two varieties possessed the biggest difference in betalain accumulation, particularly the betacyanin pigment, responsible for the appearance of red color of leaves, stem and flowers.

Light is one of the most important environmental factors regulating the development of the photosynthetic apparatus in higher plants. In high light (HL) or low light (LL), plants develop sun or shade leaves, respectively (Anderson 1986). There has been extensive research done in C3 plants examining photosynthetic performance

when grown at HL or LL (Boardman 1977, Lichtenhaler 1981, Givnish 1988) as well as how C4 plants respond to HL (Hong *et al.* 2005, Sage and McKown 2006, Tazoe *et al.* 2006). However, few studies have been conducted to evaluate how these plants photosynthetically perform and adjust to LL growth conditions because of the assumption that C4 plants are adapted for warm, dry, HL open spaces. Nevertheless, there are C4 species which persist in heavily shaded environments (Pearcy and Calkin 1993, Brown 1997, Long 1999). Generally, plants grown under LL are characterized by large, thin leaves with a low stomatal density. Ultrastructurally, they possess a reduced number of chloroplast and an increased stacking of the thylakoid membranes, lower contents of chlorophyll (Chl), carotenoid (Car) when expressed on an area basis and a lower Chl *a/b* ratio. In addition, most indicators of photosynthetic performance such as photosynthetic efficiency (apparent quantum yield of oxygen ($\Phi_{app}O_2$)), photosynthetic capacity (maximal rate of O_2 evolution ($P_{max}O_2$)), dark respiration rate (R_{dark}), light compensation point (LCP) and light saturation point (LSP) are also decreased in LL in comparison to HL grown plants (Björkman 1981, Lichtenthaler 1981, Lambers *et al.* 1998, Sage and McKown 2006).

Long term growth under prevailing environmental conditions induce acclimation. Plants are able to photoacclimate to different light environments due to adjustments of their photosynthetic apparatus at the physiological, biochemical, structural and ultrastructural levels. These include, but are not limited to, leaf surface structures (trichomes and stomates) and anatomy, changes in the light harvesting antenna size, the screening of photoradiation, the dissipation of excess energy as heat, chloroplast morphology and ultrastructure, as well as thylakoid architecture. These responses have been well documented for many plant species (Boardman 1977, Anderson 1986, Anderson *et al.* 1995, Voznesenskaya *et al.* 1999, Chow *et al.* 2005, Walters 2005, Takahashi and Badger 2011). Björkman (1981) emphasized that C4 plants such as *Flaveria*, *Zea mays* and *Amaranthus* spp. can acclimate to LL, but may not complete their life cycle. Whereas in the C4 plants the advantages of C4 photosynthesis are well established, however their photoacclimatory responses are largely unknown.

The specific values of LL irradiance are relative. In the Tanino *et al.* (2014) study,

LL under commercial greenhouses ranged from 40 to 140 µmol m^{-2} s^{-1} PPFD, depending upon the season as well as location within the greenhouse. In other studies, LL was not defined at a specific irradiance but varied depending upon the plant (Tazoe *et al.* 2006, Yamori *et al.* 2009). Acclimation to LL under a broad range of irradiance was evaluated only in a few studies (Leong and Anderson 1984a, 1984b, Bailey *et al.* 2001, 2004).

Overall, the increased concern about food security and increased population will provide an advantage for LL crops which have the potential to be either exploited as food bearing plants for 'windowsill farming' or increasing efficiency in greenhouse production as a second crop grown in the shade between plants or underneath benches in commercial greenhouse production. Understanding the physiological basis for LL photoacclimation using *Amaranthus* as a model plant is a first step towards the development of LL crops of high yield and quality that will be beneficial to the consumer, vegetable breeding programs, and the greenhouse industry.

1.1 Hypothesis and Objectives

1.1.1 Hypothesis

The red variety of *Amaranthus blitum* will have greater photosynthetic performance ($\Phi_{app}O_2$ and $P_{max}O_2$) and greater tolerance to photoinhibition in comparison to the green variety when grown under HL and LL growth irradiance.

1.1.2 Overall Objective

The aim of this research was to test and evaluate the photosynthetic performance and the role of betalain pigments in enhancing photoprotection of two varieties (red and green) of *Amaranthus blitum* as a consequence of long term photosynthetic adjustments to HL and LL growth irradiance (photoacclimation). The irradiance range for photoacclimation was for HL (500 µmol m^{-2} s^{-1} PPFD) and LL (70 µmol m^{-2} s^{-1} PPFD). This was accomplished by identifying and evaluating which growth and developmental, biochemical and physiological, and anatomical and ultrastructural adjustments allowed one variety to photosynthetically outperform the other variety at

either HL or LL growth irradiance. Additionally, the role of betalains as a mechanism of photoprotection was also evaluated.

1.1.3 Specific Objectives

The photoacclimation responses of the red and green varieties of *Amaranthus blitum* were assessed in three areas at either growth irradiance:

i) Growth and developmental adjustments

This was examined through a growth kinetics analysis.

ii) Physiological and biochemical adjustments

This was examined through determination of $\Phi_{app}O_2$, $P_{max}O_2$, photoinhibitory responses and pigmentation composition.

iii) Anatomical and ultrastructural adjustments.

This was examined through leaf surface structures and anatomy, as well as organelle ultrastructure.

CHAPTER 2

2.0 LITERATURE REVIEW

2.1 Photosynthesis

Photosynthesis is a biological process whereby the sun's energy is captured and stored by a series of events that convert the energy of light into the biochemical energy needed to power life. All life on earth depends directly or indirectly on this energy which provides our food and energy resources. Photosynthesis converts light energy (photons), carbon dioxide (CO_2), and water (H_2O) into oxygen (O_2) and carbon containing compounds such as sugar (sucrose). This process occurs primarily in leaves in an organelle known as a chloroplast. Within the thylakoid membranes of this organelle the light dependent reactions take place and generate adenosine triphosphate (ATP) and nicotinamide adenine dinucleotide phosphate (NADPH). These compounds are then used in the photosynthetic carbon reduction reactions which occur in the chloroplast stroma to reduce CO_2 to carbohydrates (Baker 2008, Hopkins and Hüner 2008, Ruban 2009).

2.1.1 Leaf Structure and Anatomy

Photosynthesis takes place mostly in the leaves of plants. The anatomy of the leaf is highly specialized for light absorption and for efficient use of the light energy. Essentially, leaves must absorb as much light as possible and to deliver light to all the chloroplasts (Terashima *et al.* 2001). Furthermore, of all the energy reaching the earth only 5% is used in synthesis of carbohydrates, whose efficiency is directly dependent on leaf anatomy (Hopkins and Hüner 2008, Taiz *et al*. 2015). Leaves are typically laminar or blade-like structures, composed of various kind of tissues, including epidermis, mesophyll, bundle sheath and vascular bundle. The leaf is typically of determinate growth with dorsiventral symmetry. Because the leaf blade is flat, the epidermis is separated between the leaf margins into an upper (adaxial) and lower (abaxial) epidermal cells (EC) layer. The upper epidermal layer is typically transparent to visible light, and the cells commonly have a planoconvex shape. The transparency and shape allow the EC to act as lenses that can collect and focus the light (Vogelmann 1993,

Myers *et al.* 1994). The convexity is more characteristic when plants are grown under reduced light levels. The light that enters the mesophyll is two to three times greater than the incident light, and even can be ten times greater in some extremes cases (Vogelmann *et al.* 1996a).

In C3 plants, the major photosynthetic cells are the mesophyll cells (MC). Most C3 dicotyledonous leaves contain two types of mesophyll, namely the palisade and spongy mesophyll. The palisade mesophyll consists of one to three layers of rather tightly packed, elongated, cylindrical cells with the long axis perpendicular to the surface of the leaf. Below is the spongy mesophyll which consists of more loosely packed irregular cells with an extensive network of air spaces. However, dicotyledonous C4 plants (such as the *Amaranthus* plants in this study) have a special anatomy known as Kranz anatomy. Plants exhibiting this anatomy utilize both MC and bundle sheaths cells (BSC). The BSC are the major photosynthetic cells. Differentiation of the two cell types is essential for operation of Kranz anatomy (Hatch and Slack 1970, Hatch 1987, Dengler and Nelson 1999, Heckmann 2016). A typical Kranz anatomy includes an outer layer of chloroplast-containing MC for initial carboxylation, and an inner layer of large, distinctive BSC that surround the vascular bundle (VB) for carbon reduction (Sage 2004). The arrangement, thickness, shape, density of the cells in every tissue and the arrangement of the chloroplasts in the cells, as well the connectivity between the tissues affect the optical properties of leaves. The optical properties of the leaves are dynamic over different time scales and may include changes in the leaf position, leaf structure as well as chloroplasts movement (Vogelmann *et al.* 1996b, Hopkins and Hüner 2008, Baránková *et al.* 2016). These may help to optimize the absorption of incident quanta to maximize the energy utilization in photosynthesis or/and to avoid harmful over excitation.

2.1.2 Stomata and Trichomes

Stomata are minute openings present in the epidermal layer of leaves, stems and other organs that facilitate gas exchange. They exert control over the fluxes of gases (vapor H_2O, CO_2, O_2) between the leaf and the atmosphere. Air enters through the stoma by gaseous diffusion providing the CO_2 and O_2 used in photosynthesis and

respiration, respectively. The O_2 produced by photosynthesis is released by diffusion to the atmosphere as well as water vapor in a process called transpiration. The stoma itself is bordered by a pair of unique cells called guard cells. In most cases the guard cells are in turn surrounded by specialized, differentiated EC called subsidiary cells. The stoma, guard cells and the subsidiary cells are collectively called the stomatal complex or stomatal apparatus (Esau 1977, Hopkins and Hüner 2008, Taiz *et al.* 2015). There are numerous stomatal complex configurations in dicotyledonous plants based on composition and cellular orientation (Metcalfe and Chalk 1950). The number, size and distribution of the stomata is variable dependent on species and growth conditions. Dicotyledonous plants usually have more stomata on the abaxial than on the adaxial side of the leaves (Fricker and Wilmer 1996). The guard cells possess the capacity to undergo reversible turgor changes that in turn regulate the size of the stoma. When the guard cells are fully turgid the stoma is open, and when flaccid the stoma is closed. The turgidity of the guard cells is modulated by the blue light which regulates ion pumping into the guard cells and sensed by photoreceptors (phototropins) present in the guard cells (Taiz *et al.* 2015).

Trichomes of plants are epidermal outgrowths of various types covering most aerial plant tissues. Trichomes are found in a very large number of plant species and are composed of a single cell or multicellular structures that can be grouped based on morphology (Esau 1977). Unicellular or multicellular trichomes may be glandular or non-glandular as well as branched or unbranched. The size and density of trichomes may be modulated by different biotic and abiotic factors, all of which increase the fitness of the plant to the environment. Functionally, trichomes may be simple hairs or more specialized such as glandular secreting trichomes. Trichomes are important for plant growth and development in many ways. Even simple trichomes can change leaf reflectance, thereby reducing leaf temperature. Trichomes can also help to reduce excessive transpiration (Mauricio and Rausher 1997, Wagner *et al.* 2004, Schilmiller *et al.* 2008). Glandular trichomes can secrete and/or store large quantities of secondary metabolites as defence compounds for biotic stresses such as insect predation, fungi and other pathogens, as well as herbivory (Tattini *et al.* 2000, Puterka *et al.* 2003, Yu *et al.* 2010, Weinhold and Baldwin 2011, Glas *et al.* 2012, Yu and Pichersky 2014, Spring

et al. 2015). Trichomes can also be used as protection against ultraviolet (UV) radiation in plants exposed to high solar radiation, such as olive (*Olea europaea*), sunflower (*Helianthus annuus*) and *Phillyrea latifolia,* a Mediterranean plant (Tattini *et al.* 2000, Liakopoulos *et al.* 2006, Spring *et al.* 2015).

2.1.3 Chloroplasts

The chloroplast is the subcellular organelle where photosynthesis takes place. The chloroplast is surrounded by a double envelope membrane, which consists of inner and outer lipid membranes. The structure of the chloroplast consists of internal membranes known as thylakoids. A stack of thylakoids forms a granum, and many stacks are known as granal lamellae or appressed thylakoids. The adjacent grana are connected by unstacked thylakoids known as stromal lamellae or non-appressed thylakoids. The fluid which surround the thylakoid membranes and is inside the inner membrane is known as stroma (Fig. 2.1). All thylakoid membranes within a chloroplast form a continuous network that encloses a single luminal space (Shimoni *et al.* 2005). The chloroplast also contains its own DNA, RNA, and ribosomes.

2.1.3.1 Peripheral Reticulum

The peripheral reticulum (PR) is a system of tubes and vesicles continuous with the chloroplast inner membrane (Wise and Harris 1984). There are three morphological PR types: PRI, is characterized by a single or double row of tubules parallel to the chloroplast envelope; PRII, is characterized as groups of densely packed tubules neither isolated to any one area of the chloroplst's periphery nor assembled into discrete rows or bundles, and PRIII, best described as discrete, isolated bundles or units of reticulating tubules (Wise and Harris 1984). It has been suggested that the PR may play a role in photosynthetic performance by increasing surface area of the chloroplasts inner envelope membrane, thereby influencing metabolite exchange between the plastid and the cytoplasm (Held and Saur 1971, Westphal *et al.* 2003, Wise 2006, Brautigan and Weber 2011, Szczepanik and Sowinski 2014).

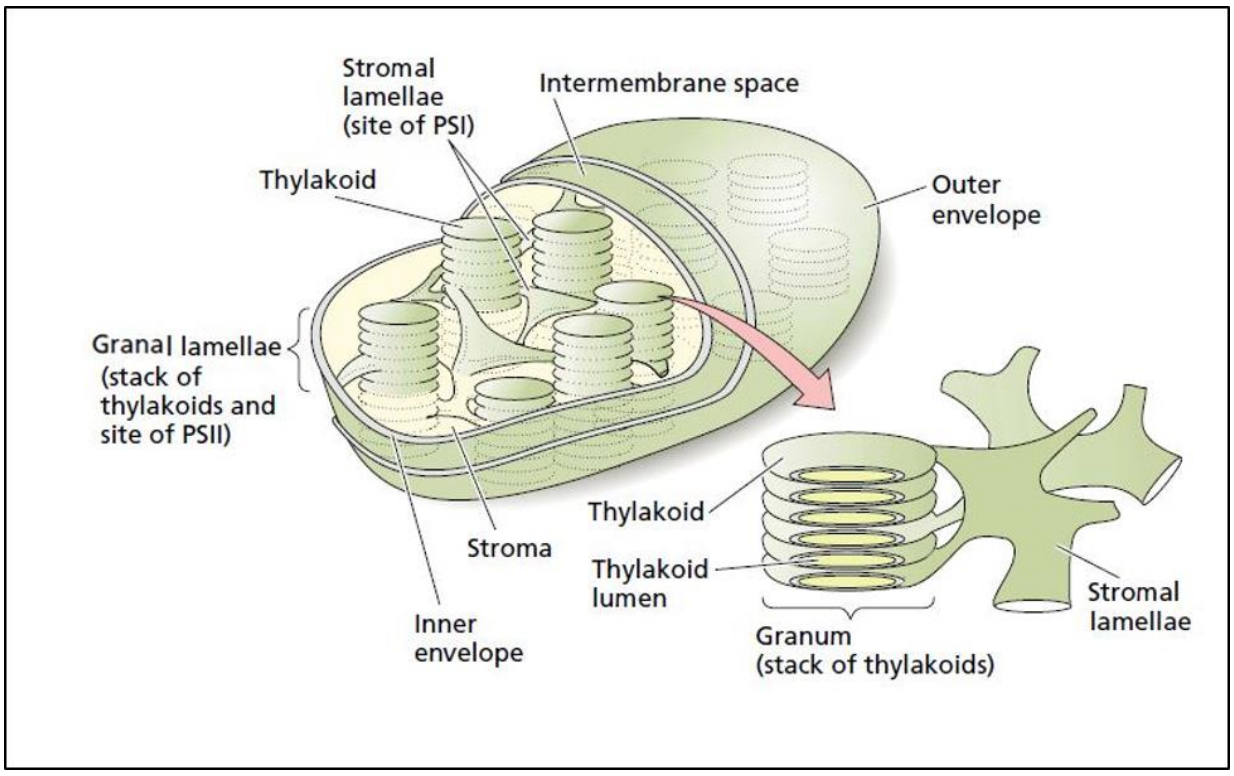

Figure 2.1 Schematic diagram of the overall organization of the chloroplast. Modified from Taiz *et al.* (2015).

2.1.3.2 Cytoplasmic Protrusions

A cytoplasmic protrusion (CP) is cytoplasm surrounded by a distorted portion of a chloroplast. In other research papers, this feature is named “cytoplasmic invagination” and are observed in response to viral infection (Ushiyama and Matthews 1970, Jang *et al.* 2013). While the function of these structures is unknown, it has been hypothesized they serve to increase chloroplast transport and, in some manner, affect photosynthetic performance (Larkin *et al.* 2016).

2.1.3.3 Crystalline Inclusions

Crystalline Inclusions (CI) are accumulations of granular material in the stroma between the thylakoid membranes of chloroplast. These granules are assembled into crystals (Esau 1975). Early studies about CI suggests that they consist of Rubisco (Sprey 1977, Sprey and Lambert 1977), however the immunocytochemical study of Shojima *et al.* (1987) illustrated that the CI are not accumulations of Rubisco. It is assumed that the CI may consist of different components, depending on cell type (Ueno 2001).

2.1.4 Microbodies

Microbodies are a class of spherical organelles, surrounded by a single membrane and their matrix is granular or fibrillar (Frederic and Newcomb 1969, Esau 1977). Their matrix is rich in enzymes and other proteins, but they do not contain genetic material, which indicates that they cannot self-replicate. As such, they are structurally simple but biochemically diverse. Commonly they are localized in the MC (C3) and/or in the BSC (C4) where they are closely associated with chloroplasts, mitochondria or oil bodies. In plants, there are two well known microbodies, peroxisomes and glyoxysomes. Peroxisomes, play an important role in the process of photorespiration and contain large quantities of the catalase enzyme that can form a crystalline core (CY) in the matrix. Glyoxysomes occurs in lipid storing cells where they play a role in lipid metabolism (Taiz *et al.* 2015).

2.1.5 Light Dependent Reactions

The light dependent reactions of photosynthesis occur in the thylakoid membranes of the chloroplast. The thylakoids harbor four large multimeric protein supracomplexes; photosystem II (PSII), photosystem I (PSI), the cytochrome b_6f complex (Cyt b_6f) and the ATP synthase complex (Dekker and Boekema 2005, Nelson and Junge 2015). In addition to these major complexes, the thylakoid membranes also contain the lipophilic electron carrier plastoquinone (PQ), while the mobile electron carrier plastocyanin (PC) resides in the lumenal space.

Photosynthesis is initiated with light absorption, primarily by Chl bound to proteins known as light-harvesting (or antennae) complexes. This, in turn, drives electron transport through carriers within the chloroplast thylakoid membrane. The light-harvesting complex II (LHCII) antenna is associated with PSII and is a trimeric integral membrane complex that contains three major PSII light-harvesting Chl *a/b*-binding proteins (LHCB1, LHCB2, LHCB3). Three minor monomeric Chl *a/b*-binding proteins (LHCB4, LHCB5, LHCB6) are also associated with PSII (Jansson 1999). Similarly, PSI also possesses an antenna known as light-harvesting complex I (LHCI) (Nelson and Yocum 2006, Amunts *et al.* 2010). Both LHCI and LHCII facilitate efficient energy harvesting to the PSI and PSII core complexes, respectively. Furthermore, LHCII can transiently associate with PSI, controlled by an elegant system of phosphorylation/dephosphorylation.

Photosystem II is a multi-component pigment-protein complex that is responsible for O_2 evolution and plastoquinone reduction (Nickelsen and Rengstl 2013, Järvi *et al*. 2015). Components of PSII include the reaction center core proteins D1 and D2 (PsbA and PsbD), core antenna proteins CP43 (PsbC), CP47 (PsbB), cytochrome b_{559} (PsbE/PsbF), numerous chloroplast and nuclear encoded low-molecular-mass (LMM) proteins (Nickelsen and Rengstl 2013) and the extrinsic oxygen evolving complex (OEC) proteins (PsbO, PsbP, PsbQ) (Bricker *et al.* 2012). In addition, more than 60 auxiliary proteins or enzymes involved in the assembly, stability and repair of PSII complexes are present (Mulo *et al.* 2008, Nixon *et al.* 2010, Nickelsen and Rengstl 2013, Pagliano *et al.* 2014, Järvi *et al.* 2016). Photosystem II converts light energy into potential energy required to split water and subsequently evolve molecular O_2 (Debus

1992). This takes place when light excitation of the primary donor (P_{680} - reaction centre Chl of PSII), comprising a special pair of Chl *a*, results in electron transfer to pheophytin, followed by electron transfer to the acceptor quinones (Q_A and Q_B). The resulting cation radical of P_{680}^+ receives electrons via a redox-active tyrosine of D1, from the manganese cluster (Mn_4CaO_5). The Mn_4CaO_5 converts two water molecules into one molecular O_2 and four protons through a light driven cycle consisting of five intermediates called S states (Vinyard *et al.* 2013). Electrons derived from water splitting in PSII are ultimately transferred via the Cyt b_6f to PSI, where the reduction of nicotinamide adenine dinucleotide phosphate ($NADP^+$) into NADPH occurs, also referrred to as linear electron transport. Linear electron transport generates a proton gradient across the thylakoid membrane (ΔpH) through the combination of protons generated by the water splitting complex associated with PSII and proton translocation associated with electrons passing through the Cyt b_6f complex. The ΔpH together with a membrane potential ($\Delta\psi$) formed across the thylakoid membrane drives ATP production by the ATP synthase (Malkin and Niyogi 2000).

In addition to linear electron transport, cyclic electron transport can also occur which drives the production of ATP but not NADPH (Hopkins and Hüner 2008, Yamori and Shikanai 2016). The role of PSI cyclic electron transport is essential for increasing the ATP/NADPH ratio as well as for protecting both photosystems from damage caused by chloroplast overreduction (Shikanai 2007, Takahashi and Badger 2011). PSI cyclic electron transport can sustain a large ΔpH under conditions in which linear electron transport is limited. This is a requirement for the induction of photoprotective mechanisms such as non-photochemical quenching (NPQ; Niyogi 1999, Müller *et al.* 2001).

The arrangement of PSII and PSI are such that they are spatially separated in the thylakoid membranes. The PSII reaction center, along with its antenna chlorophylls is located predominantly in the granal lamellae (Andersson and Andersson 1980, Albertsson 2001, Dekker and Boekema 2005). The distance between neighbouring granal thylakoids is about 3.5 nm, resulting in the exclusion of the PSI and the ATP synthase from the grana, as their protrusions are larger (Abrahams *et al.* 1994, Amunts *et al.* 2007, Kirchhoff 2014). The PSI reaction center and its associated antenna

pigments, as well as the ATP synthase enzyme that catalyzes the formation of ATP, are found almost exclusively in the stromal lamellae and at the edges of the granal lamellae (Andersson and Andersson 1980, Albertsson 2001, Dekker and Boekema 2005). The separation of PSII, PSI, and ATP synthase introduces a lateral heterogeneity in the thylakoid membrane of plants. The distribution of the Cyt b_6f of the electron transport chain that connects the two photosystems is still under debate. Initially assumed to be evenly distributed across the thylakoid membranes (Allen and Forsberg 2001). Recent studies show an enrichment of Cyt b_6f in the stroma lamellae as well as in the nanodomains within PSII in granal regions (Johnson *et al.* 2014, Tomizioli 2014).

Thylakoid architecture and granal stacking play a crucial role in allowing the plants to acclimate to different growth irradiance. Granal lamellae formation facilitates photosynthetic light harvesting and its regulation via NPQ, thus protecting PSII from photodamage (Anderson 1999, Horton 1999). Granal stacking has also been described as a way to physically separate the slow-working PSII from the fast-working PSI, hence avoiding a spillover of excitation energy (Trissl and Wilhelm 1993). In addition, the lateral heterogeneity caused by granal formation avoids competition between linear and cyclic electron flow (Allen *et al*. 1981, Albertsson 2001, Bendall and Manasse 1995) as well as increasing the diffusion rate of plastoquinol (Kirchhoff *et al.* 2002). However, granal stacking results in a requirement for the long-range diffusion of electron carriers between PSII and PSI (Mullineaux 2008, Kirchhoff *et al.* 2011) and crowding can restrict the rapid diffusion of damaged PSII to lumen, where its repair takes place (Kirchhoff *et al*. 2008, Mulo *et al.* 2008). Lateral heterogeneity also has an impact on the stoichiometry of PSII/PSI. The PSII/PSI ratio is about 1.5:1, but it can change when plants are grown under different light conditions (Anderson *et al*. 1988, Bailey *et al.* 2001, Ballottari *et al.* 2007).

2.1.6 Photosynthetic Measurements

Photosynthetic performance can be measured through several methods that are well established. The methods used in this research, photosynthetic O_2 evolution and Chl fluorescence, are briefly described below.

2.1.6.1 Photosynthetic O_2 Evolution

This method involves constructing a light-response curve based on evolution of O_2 at different irradiance (Fig. 2.2). This can be determined in the gas or liquid phase. As a result of electron transport, water is oxidized releasing O_2 in the presence of light. The O_2 evolved is detected polarographically using a Clark-type electrode. Many photosynthetic parameters can be derived from these curves, indicated in Fig. 2.2. The $P_{max}O_2$ corresponds with the upper asymptote, $\Phi_{app}O_2$ is the initial slope of the light-response curve. The LCP, and R_{dark} are the values from the intersection on the X- and Y-axes, respectively. The LSP represents the inflection point of the curve.

2.1.6.2 Chlorophyll Fluorescence

The light absorbed by Chl can be utilized photochemically to drive photosynthesis (coefficient of photochemical quenching (q_L)), dissipated as heat (NPQ) or re-emitted as fluorescence (Fig. 2.3). These three pathways are in competition such as any increase in efficiency of one will result in a decrease in the yield of other two. Hence, by measuring the yield of Chl *a* fluorescence, information about changes in photochemistry and heat dissipation can be obtained (Krause and Weis 1991, Maxwell and Johnson 2000, Gray *et al*. 2003, Baker 2008).

Chlorophyll fluorescence is widely used not only for evaluation of photosynthetic performance but also as an indicator of the physiological competence of plants (Baker and Rosenqvist 2004). When plants are exposed to abiotic and biotic stresses, a decrease in the maximal photochemical efficiency of PSII (F_v/F_m) is frequently observed. The measure of F_v/F_m provides a simple and rapid way of monitoring stresses such as heat (Srinivasan *et al.* 1996), salt (de Lucena *et al.* 2012), drought (Kościelniak *et al.* 2005), nutrient deficiency (Durães *et al*. 2001, Kalaji *et al.* 2014), herbicides (Korres *et al*. 2003) and water availability in plants (Germ *et al*. 2005).

2.1.7 Photosynthetic Carbon Reduction

The photosynthetic carbon reduction cycle (Calvin cycle) occurs in the chloroplast stroma. It is a sequence of reactions all plants use to reduce CO_2 to organic

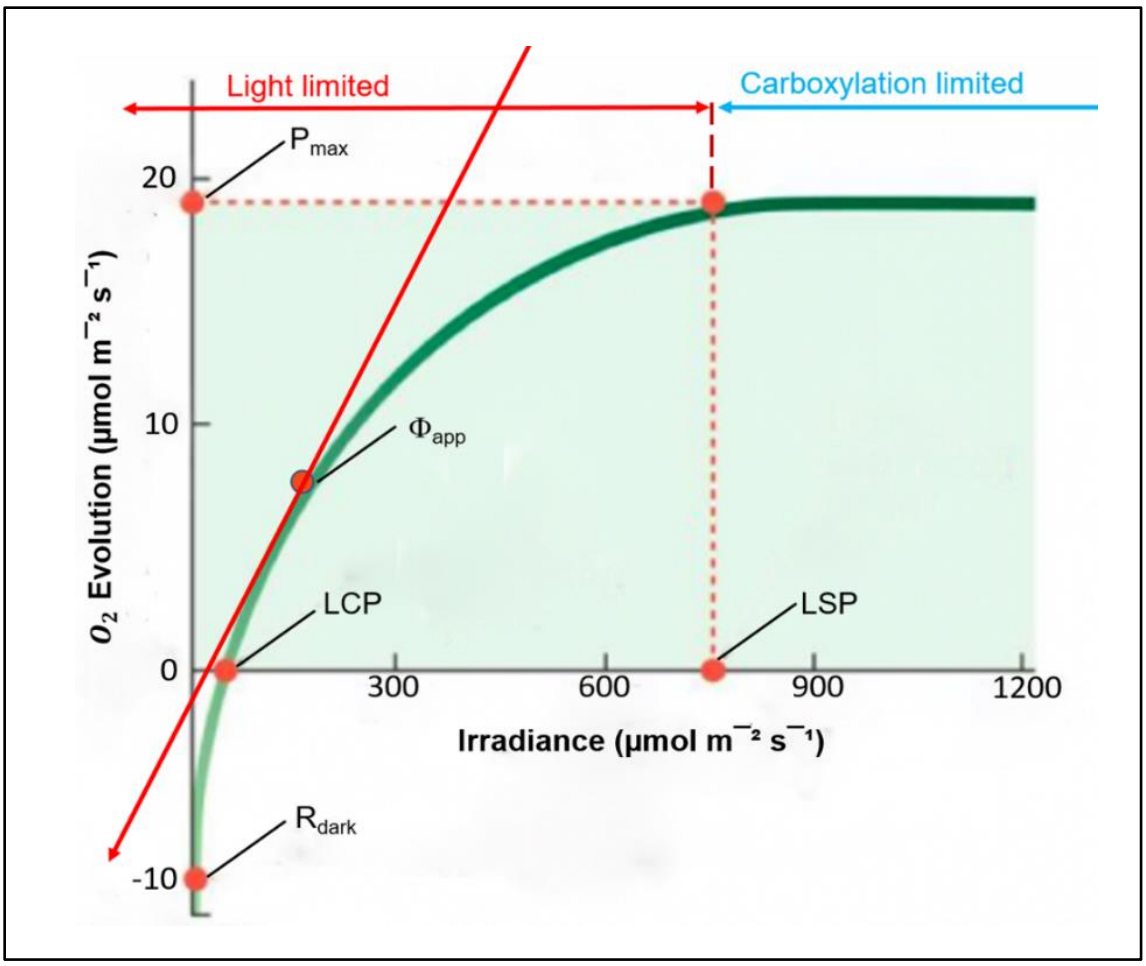

Figure 2.2 Typical light response curve of O_2 evolution and derived parameters. $\Phi_{app}O_2$, apparent quantum yield of O_2 evolution; LCP, light compensation point; LSP, light saturation point; $P_{max}O_2$, maximal rate of O_2 evolution; R_{dark}, rate of dark respiration. Modified from Bowman *et al.* (2017).

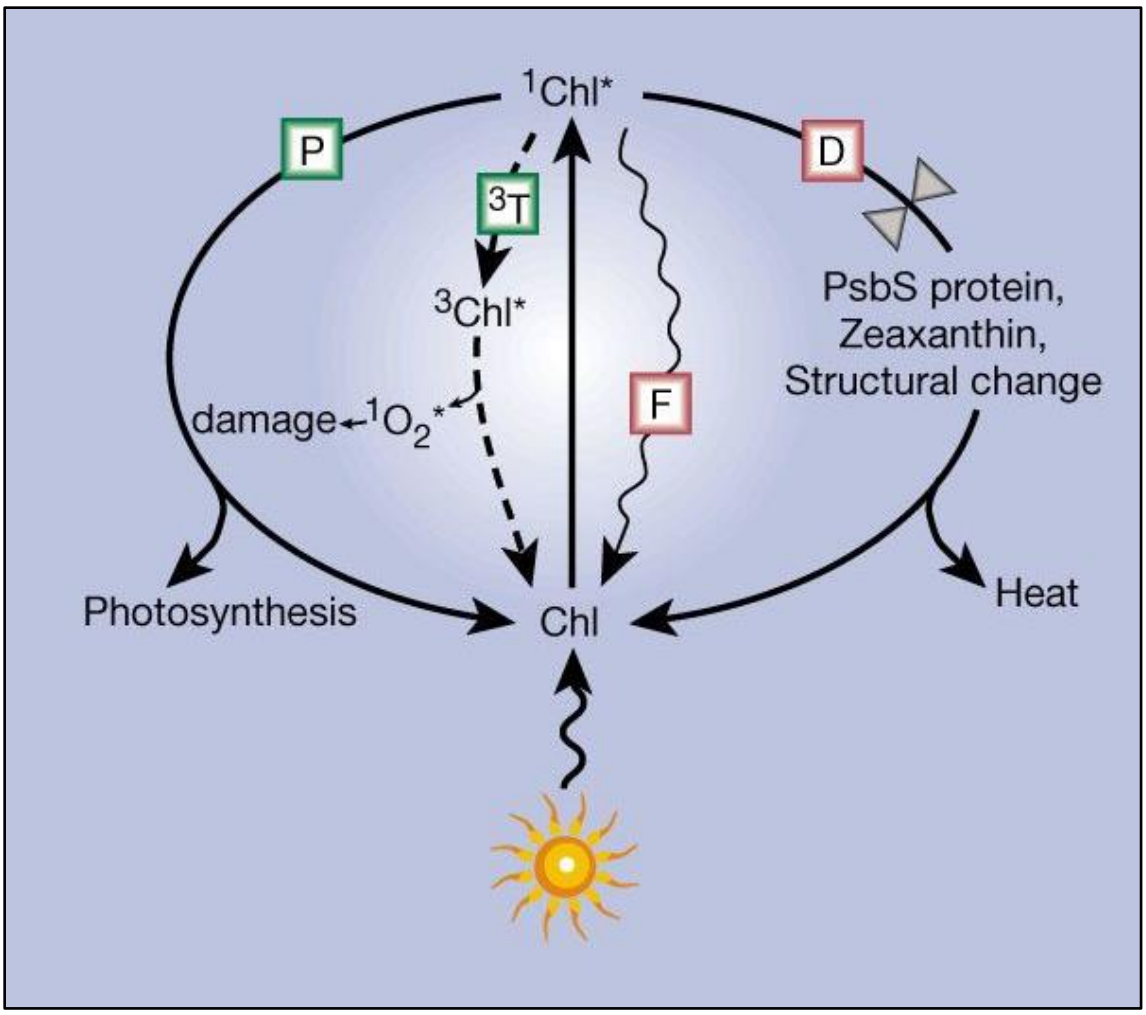

Figure 2.3 Fates of sunlight absorbed by the light-harvesting chlorophyll complexes of PSII. Chl, chlorophyll; ^{1}Chl*, excited singlet chlorophyll; ^{3}Chl*, excited triplet chlorophyll; P, photochemistry (green); D, safe dissipation of excess excitation energy as heat (red); F, fluorescence; ^{3}T, triplet pathway, leading to the formation of singlet oxygen ($^1O_2$*) and photooxidative damage. From Demming-Adams and Adams (2000). Permission obtained from publisher.

carbon. The fixation of CO_2 is directly dependent on the enzyme ribulose-1,5-bisphosphate carboxylase-oxygenase (Rubisco), which catalyzes the addition of a CO_2 molecule to an acceptor molecule ribulose-1,5-bisphosphate (RuBP). The Calvin cycle consists of three stages: carboxylation, reduction, and regeneration. Carboxylation consists of the fixation of CO_2 in the presence of Rubisco. Rubisco is catalyzing the addition of a CO_2 molecule to the acceptor molecule RuBP, leading to the production of two molecules of 3-phosphoglycerate (3-PGA). In the reduction phase, ATP and NADPH are consumed in conversion of 3-PGA to glyceraldehyde-3-phosphate (G3P). The obtained product after having been converted to dihydroxyacetone phosphate (DHAP) is ready to be exported to the cytoplasm for sucrose biosynthesis (Taiz *et al.* 2015). Regeneration is a complex series of reactions that are responsible for the regeneration of the CO_2 acceptor RuBP to ensure the continuous fixation of CO_2. The excess carbon can be stored as starch in the chloroplast or transported to other parts of the plant. Only ATP is used in these series of reactions (Hopkins and Hüner 2008).

Plants can be subdivided into C3 or C4 photosynthetic carbon reduction, which refers to the first stable carbon compound generated in the respective processes. In C3 plants, the fixation of CO_2 to the acceptor molecule RuBP is catalyzed by the enzyme Rubisco and results in 3-PGA, a 3-carbon compound. The energy needed to complete the reduction of one molecule of CO_2 is 3 ATP and 2 NADPH (Hopkins and Hüner 2008). In contrast, the leaves of C4 plants have a special anatomy known as Kranz anatomy (Fig. 2.4A) and photosynthetic carbon reduction occurs as a result of the coordinated function of MC and BSC, generating a 4-carbon compound. The principles of photosynthesis in C4 plants are illustrated in Fig. 2.4B. There are different subtypes of this process that vary in the enzymes, compounds and cellular organelles involved, however, the process remains similar.

The *Amaranthus* plants used in this study belong to the NAD-ME (malic enzyme) subtype (Fig. 2.5). In the cytoplasm of the MC, CO_2 is converted by carbonic anhydrase (CA) to carbonic acid (HCO_3^-). Carbonic acid and phosphoenolpyruvate (PEP) which are combined through the action of phosphoenolpyruvate carboxylase (PEPC) to form oxaloacetate (OAA), a C4-acid compound, and orthophosphate (Pi). Oxaloacetate is converted to aspartate (Asp) by Asp aminotransferase in the cytoplasm of the MC. The

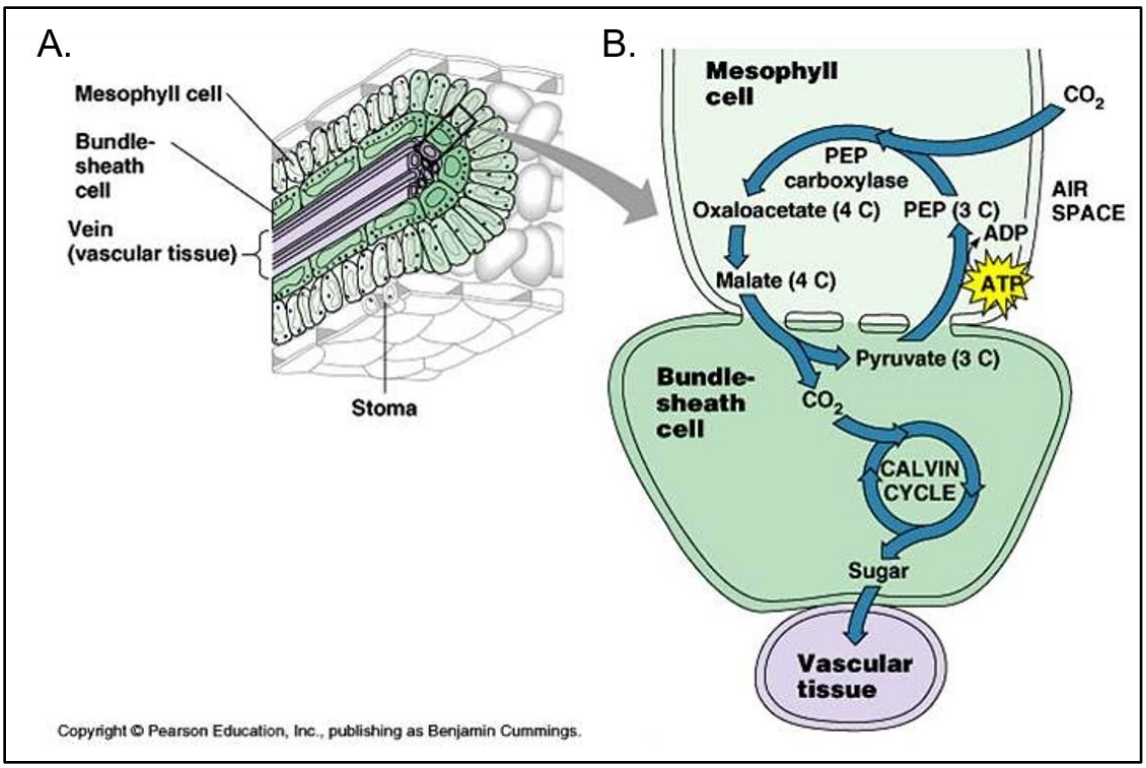

Figure 2.4 C4 leaf anatomy (**A.**) and a general schematic of C4 photosynthesis (**B**). ADP, adenosine diphosphate; ATP, adenosine triphosphate; PEP, phosphoenolpyruvate; 3/4C, three/four carbon acid. Modified from Reece *et al.* (2010).

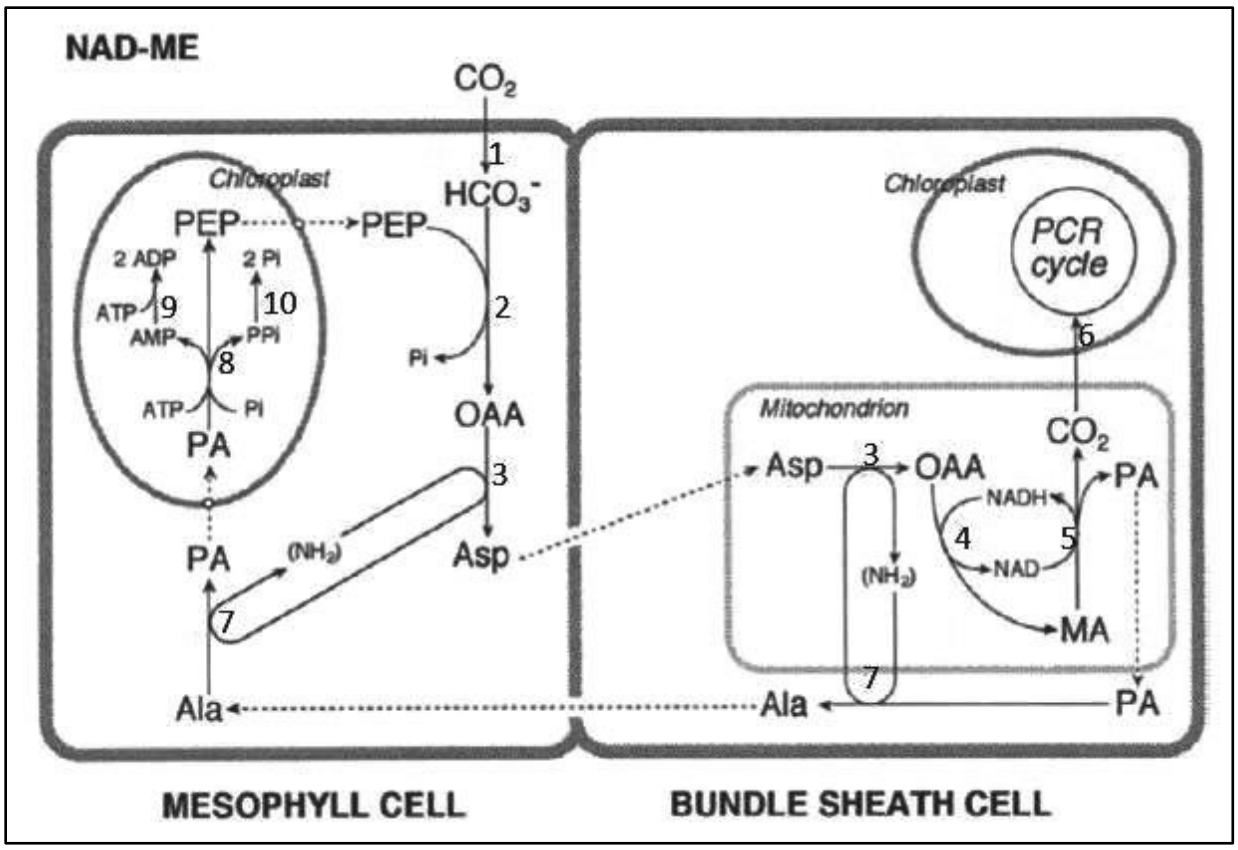

Figure 2.5 The C4 photosynthetic pathway demonstrating the NAD-ME (nicotinamide adenine dinucleotide-dependent malic enzyme) sub-type. Ala, alanine; Asp, aspartate; MA, malate; OAA, oxaloacetate; PA, pyruvate; PEP, phosphoenolpyruvate; Pi, orthophosphate; PPi, pyrophosphate. Enzymes are as follows: 1, carbonic anhydrase; 2, PEP carboxylase; 3, aspartate aminotransferase; 4, NADH-malate dehydrogenase, 5, NAD-ME-malic enzyme, nicotinamide adenine dinucleotide-dependent malic enzyme; 6, Rubisco; 7, alanine aminotransferase; 8, pyruvate phosphate dikinase; 9, adenylate kinase; 10, pyrophosphatase. Modified from Sage and Monson (1999).

Asp pass through the plasmodesmata to bundle sheath cells (BSC) into mitochondria. In mitochondria Asp is deaminated by Asp aminotransferase to OAA, which is reduced to malate by NAD-ME dehydrogenase. Malate is then decarboxylated by NAD-ME into CO_2 and pyruvate. The released CO_2 is refixed by Rubisco in the Calvin cycle of BSC chloroplasts and pyruvate is converted to alanine which is shuttled to the MC chloroplast for regeneration of PEP (Hatch 1987, Sage 2004, Sommer *et al.* 2012). The energy needed for the complete reduction of one molecule of CO_2 is 5 ATP and 2 NADPH in subtype NAD-ME (Hatch 1987, Sage 2004).

Whereas the energy cost is greater than in C3 plants, the spatial separation of the reactions in C4 plants allows for the concentration of CO_2, thereby minimizing the process of photorespiration (oxygenation by Rubisco) and potential carbon loss. Since Rubisco can operate under high CO_2 concentrations in the BSC, it works more efficiently than in C3 plants. Consequently, C4 plants need less of this enzyme, which is by far the most abundant protein in the leaves of C3 plants. This leads to a better nitrogen-use efficiency of C4 plants compared to C3 plants, since the rate of photosynthesis per unit nitrogen in the leaf is increased (Oaks 1994). Additionally, C4 plants exhibit better water-use efficiency than C3 plants. Because of the CO_2 concentration mechanism, C4 plants can acquire enough CO_2 even when their stomata are not fully open. Thus, water loss by transpiration is reduced (Long 1999). Overall, the C4 mechanism results in better photosynthetic performance under conditions of low CO_2 or high temperature (Sage 1999).

2.1.8 Photorespiration

Photorespiration, also known as the oxidative photosynthetic carbon cycle, occurs in three organelles: chloroplast, peroxisome and mitochondrion. This process starts in the chloroplast stroma under conditions whereby Rubisco acts as an oxygenase and reacts with O_2 and RuBP. The oxygenase activity of Rubisco yields 3-PGA which returns to the Calvin cycle and 2-phosphoglycolate (2PG), which upon the action of phosphoglycolate phosphatase forms glycolate. This glycolate flows from the chloroplast to peroxisome where it is converted to glyoxylate by the enzyme glycolate oxidase. This reaction also liberates hydrogen peroxide (H_2O_2) which is converted to

H_2O and O_2 by the enzyme catalase. Glyoxylate is converted to glycine by glutamate: glyoxylate aminotransferase and is then exported to the mitochondria. In the mitochondria, under the activity of enzymes glycine decarboxylase complex and serine hydroxymethyltransferase, glycine is transformed to serine with the concurrent release of the CO_2 and ammonium (NH_4^+). Serine is then transported back to the peroxisome and converted to glycerate by the action of serine:2-oxoglutarate aminotransferase and hydroxypyruvate reductase. Finally, the glycerate from the peroxisomes and the NH_4^+ from the mitochondria return to the chloroplast in a process that recovers part of the carbon and all the nitrogen lost in photorespiration. Here the glycerate is phosphorylated to 3-PGA and incorporated back in the Calvin cycle. The nitrogen is recovered in the stroma through the incorporation of NH_4^+ into glutamate via glutamine synthetase and glutamate synthase (GS/GOGAT) cycle (Fig. 2.5; Taiz *et al.* 2015).

2.2. Photostasis and Photoinhibition

2.2.1 Photostasis

Plants have developed elaborate mechanisms for acclimation, defense and repair in response to environmental stress. The chloroplast is recognized as a global sensor of stress and acts by perceiving energy imbalances between sources and sinks (Falkowski and Chen 2003, Ensminger *et al.* 2006, Wilson *et al.* 2006). The maintenance of cellular energy balance is called photostasis. The balanced photostatic state exists when light capture through photosynthetic light harvesting (source) is equal to energy utilization by carbon, nitrogen and sulfur assimilation processes (sink). Any factor which affects source or sink relationship has the potential to shift this energy balance. If the stress is severe, a significant change in photostasis may result in the death of the plant. However, plants survive by restoring photostasis through modulation either of the source, sink or both. While the mechanism by which this occurs is species- and organism-specific, in many cases it involves decreasing the rate of energy harvesting through changes in the absorptive cross section of PSII and dissipative processes such as NPQ or increasing the sink processes that are determined primarily by carbon and nitrogen metabolism (Hüner *et al.*1998, Ensminger *et al.* 2006, Biswal *et al.* 2011).

2.2.2 Photoinhibition

Photoinhibition is defined as a light-dependent decrease in photosynthetic efficiency and/or capacity. It can occur at any irradiance when light exceeds the requirements for photosynthesis (Fig. 2.6; Powles 1984, Krause 1988, Osmond 1994, Hopkins and Hüner 2008). This decrease is associated primarily with damage to the reaction center of PSII which is susceptible to photoinhibition under visible and UV light (Aro *et al.* 1993, Melis 1999).

Many mechanisms have been suggested to explain PSII photoinhibition including over reduction of the acceptor side of PSII as well as inactivity of the donor side of PSII or excess light damage to the D1 polypeptide of PSII reaction center (Vass *et al*. 1992, Aro *et al.* 1993, Anderson *et al.* 1998, Melis 1999). Photoinhibition is also widely considered to be an important mechanism to protect PSII from over-excitation through the down regulation of PSII photochemistry (Hüner *et al.* 1993, van Wijk and van Hasselt 1993, Krause 1988, Krause 1994a). Currently, a two-step mechanism of photodamage to PSII is favoured whereby step one is the light induced inactivation at the Mn_4CaO_5 of the OEC, and step two is inactivation of the PSII reaction centers by light absorbed by Chl. Inactivation of the OEC occurs in UV and visible light releasing a manganese ion to the thylakoid lumen, and as a result making it unable to reduce P_{680}^+ which results in oxidative damage of PSII reaction centers (Hakala *et al.* 2005, Ohnishi *et al.* 2005).

Plants evolved different photoprotective mechanisms to excess irradiance (photoinhibition). Direct photodamage can be alleviated by leaf and chloroplast movement. Phototropins have been shown to initiate chloroplast movement to the periphery of the cells. This results in their positioning parallel to the incident light, resulting in reduced light absorption (Kong and Wada 2014). The attenuation of incident light can also occur by the accumulation of photoprotective pigments in the upper epidermal cell layer or in the abaxial mesophyll parenchyma (Takahashi *et al.* 2010). In the long term, plant morphological changes can also occur. These changes under HL, usually result in reduced leaf area, increased leaf thickness (LT) based on increased adaxial and/or abaxial MC elongation, as well as by eventual addition of a layer of palisade cells (Kim *et al.* 2005, Mishra *et al.* 2012). In addition, an increased

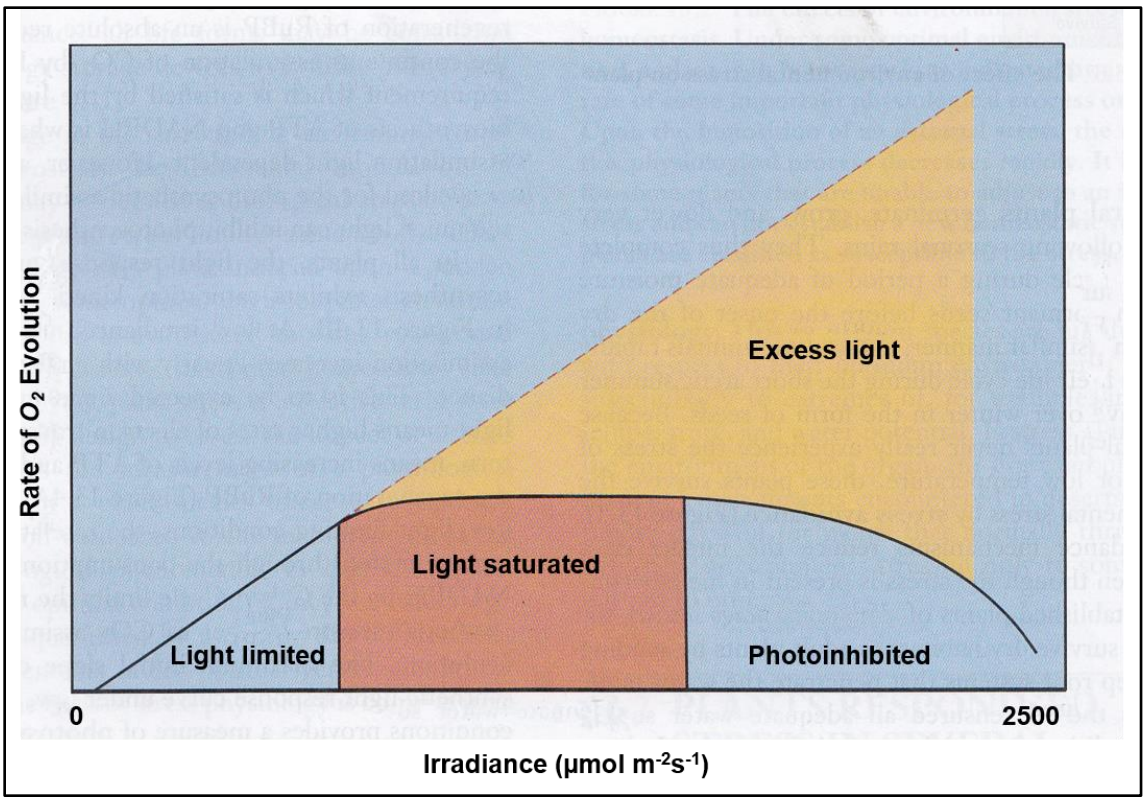

Figure 2.6 Light response curve of O_2 evolution demonstrating light limiting, light saturating, and photoinhibitiory conditions. Modified from Hopkins and Hüner (2008).

stomatal index (SI), trichome density and epicuticular wax content and composition also contribute to the photoprotective mechanism (Fricker and Wilmer 1996, Tattini *et al.* 2000, Wagner *et al.* 2004, Liakopouos *et al.* 2006, Zarinkamar 2007, Schilmiller *et al.* 2008, Tsutsumi *et al.* 2017). Changes in chloroplast ultrastructure are evident with less stacking (appression) in chloroplast of plants under HL (Boardman 1977). A common mechanism for coping with excess excitation energy involves NPQ, a process that takes place in the external antennae of PSII (Li *et al.* 2000). The energy-dependent component of the process involves the xanthophyll cycle comprising of three carotenoids: violaxanthin (V), antheraxanthin (A) and zeaxanthin (Z)s the xanthophyll cycle. The xanthophyll cycle consists of epoxidation of V to Z via A, which allows an efficient dissipation of excess light into heat (Demming-Adams and Adams, 1992). The q_E is dependent on a ΔpH across the thylakoid membrane which can be generated by linear and cyclic electron flow (Takahashi and Badger 2011). The low pH in the lumen induces protonation of PsbS protein, which in turn induces conformational changes in minor antenna complexes (LHCB4, LHCB5 and LHCB6). Conformational changes imply that the minor antenna complexes bind one molecule of Z and one of Chl, that accept energy transfer from excited chlorophylls. Zeaxanthins are able to return to their ground state by dissipating energy as heat (Horton and Ruban, 2004). Other mechanisms involve enhancing the turnover of PSII, such as phosphorylation and dephosphorylation of PSII core proteins, thus maintaining PSII functionality despite increased damage to the D1 protein (Aro *et al.* 1993, 2005, Tyystjärvi and Aro 1996, Bellafiore *et al.* 2005, Tikkanen *et al.* 2008a, 2008b, 2010). Furthermore, plants can avoid reactive oxygen species (ROS)-mediated damage by activating a multi-layer network of enzymatic and non-enzymatic antioxidants to maintain ROS at basal levels (Foyer and Noctor 2009).

Damaged PSII reaction must be disassembled and repaired. However, only the damaged D1 protein is removed and replaced whereas the other components of the PSII reaction center are recycled. In the past, it has been assumed that damage to PSII was accelerated by the environmental stresses that limit the photosynthetic fixation of CO_2. Currently, it is believed that oxidative stress, as well as cold and salt stress, actually exert their effect by inhibiting repair of the photosynthetic machinery (Gombos *et al*. 1994, Nishiyama *et al.* 2001, Allakhverdiev *et al.* 2002, Allakhverdiev and Murata

2004). The combination of low temperature and high irradiance conditions act synergistically and lead to photoinhibition and photooxidation. This occurs because of an increase in the proportion of closed PSII reaction centers due to slower rates of photosynthetic carbon fixation reactions, as well as restricted rates of D1 protein turnover, decreased xanthophyll cycle activity and inadequate rates of removal of ROS (Krause 1994b, Ensminger *et al.* 2006, Wilson *et al.* 2006, Biswal *et al.* 2011).

2.3 Photoacclimation

Light is one of the most important requirements for plant growth and under natural field conditions light quantity and quality is highly heterogeneous (Chen *et al.* 2016). Plants have to cope with highly variable light regimes to ensure further growth and development. This is achieved through photoacclimation. Photoacclimation is the process whereby adjustments are made to the structure and function of the photosynthetic apparatus in response to changes in growth irradiance and/or light quality (Hopkins and Hüner 2008).

During evolution, two kinds of species have evolved: the light demanding plant (HL tolerant) and the shade demanding plant (LL tolerant). Low light tolerant species can survive and grow under as little as 1-2% of full sunlight (Augspurger 1984, Chen *et al.* 2014). Usually such plants exhibit a lower P_{max}, reduced Φ_{app}, as well as reduced LCP, LSP, R_{dark}, relative linear electron transport rate through PSII (ETR), but increased Φ_{PSII} than the same plants grown under HL (Boardman 1977, Bazzaz 1979, Givnish 1988, Valladares *et al*. 2000, Valladares and Niinemets 2008). At the chloroplast level, LL tolerant plants present a larger LHCI and LHCII and a decreased Chl *a/b* ratio, but a greater leaf area (LA) and pigments content per leaf fresh weight (FW; Lichtenhaler *et al.* 1981, Leong and Anderson 1984a, Anderson and Osmond 1987, Givnish 1988, De la Torre and Burkey 1990, Bailey *et al*. 2001). At the anatomical level, LL tolerant plants have reduced LT, lower area and length of MC, reduced number of cells per LA, as well as lower number of chloroplasts per unit area, thus determining a reduced LT, but with increased granal index (GI) and stackness (Givnish 1988, Lee *et al.* 2001, Oguchi *et al.* 2005, Tazoe *et al*. 2006, Skillman *et al*. 2005). All these parameters are opposite for the HL tolerant plants, with the exception of GI and thylakoids per granum.

Photoacclimation is a very complex process and the fact that photosynthesis has the ability to respond to a broad range of environmental stimuli allowed Anderson *et al*. (1995) to hypothesize that acclimation to any environmental stress receives stimuli from photosynthesis itself. As such, photoacclimation serves as a homeostatic mechanism, to correct the deleterious consequences of environmental changes, thereby maintaining efficient photosynthesis (Walters 2005). Plants have developed different mechanisms to sense the environment. Therefore, when an imbalance alters the photostatic state and this energy imbalance is sensed by plants, cellular, physiological and developmental changes are made to reestablish the lost photostasis. In response to changes in irradiance, short-term photoacclimation involves NPQ (Ruban *et al.* 2012). Short-term photoacclimation occurs when plants are shifted to HL, that results in increased phosphorylation of PSII core proteins, whereas the level of LHCII phosphorylation decreases. It is known that PSII phosphorylation in HL facilitates the unpacking of PSII-LHCII complexes required for proper processing of the damaged PSII centers and thus, prevents oxidative damage of the photosynthetic apparatus (Tikkanen *et al.* 2008a, Fristedt *et al.* 2009, Kirchhoff *et al.* 2011). Furthermore, the D1 protein needs to be dephosphorylated before its proteolytic degradation upon PSII turnover (Koivuniemi *et al.* 1995).

Short-term photoacclimation when plants are shifted to LL results in decreased phosphorylation of PSII core proteins, whereas the phosphorylation of LHCII proteins increases (Rintamäki *et al.* 1997, 2000). Phosphorylation of LHCII can result in the association of LHCII with the PSI core. In this manner, both photosystems are energetically connected through a shared light-harvesting system composed of LHCII trimers (Grieco *et al.* 2015) and there is efficient excitation energy transfer between the two photosystems (Yokono *et al.* 2015). Moderate phosphorylation of both PSI core and LHCII proteins is needed to provide the granal membranes with sufficient fluidity as well as sufficient energy transfer from LHCII to PSI (Tikkanen *et al.* 2008b, Grieco *et al.* 2012, Wientjes *et al.* 2013). Overall, the phosphorylation of thylakoids membranes is a dynamic redox regulated process, dependent on the interplay of two kinases (state transition 7 and 8 (STN7 and STN8; Bellafiore *et al.* 2005, Bonardi *et al.* 2005, Vainonen *et al.* 2005, Tikkanen *et al.* 2006) and two phosphatases (thylakoid-associated

phosphatase38/protein phosphatase1 (TAP38/PPH1) and PSII core phosphatase (PBCP); Pribil *et al.* 2010, Shapiguzov *et al.* 2010, Samo *et al.* 2012). Moreover, the ∆pH across the thylakoid membrane regulates these kinases and phosphatases.

Long-term photoacclimation in response to HL is also accompanied by a regulation in the amount of LHC proteins and the PSII/PSI ratio (Anderson 1986). Under HL conditions, photoacclimation results in a reduced amount of LHC proteins, whereas the PSII content increases compared to PSI. However, under LL conditions the opposite is observed, where the PSII/PSI ratio reflects a lower amount of PSII complexes, but they are associated with a larger amount of LHCII proteins and decreased amounts of Rubisco and Cyt b_6f (Anderson *et al*. 1988, Bailey *et al.* 2001, Ballottari *et al.* 2007).

2.4 *Amaranthus* Plants

2.4.1 Taxonomy

The taxonomy of the genus *Amaranthus* L. is considered “difficult” (Costea and DeMason 2001). Frequent outcrossing and hybridization has caused a large number of accessions resulting in nomenclatural disorder and misapplication of names that has created intricate problems in its taxonomy (Costea and DeMason 2001, Das and Iamonico 2014, Iamonico 2014a, 2014b, 2016a, 2016b). The studies of Sauer (1967, 1976, 1993) based on morphological features allowed for the delineation of two subgenera: *Acnida* L., which includes the dioecious weed species and *Amaranthus* L., which includes the monoecious weed species, and all vegetable and grain species (Sauer 1967). There is currently no consensus about the taxonomy of the *Amaranthus* L. genus, and as such, the classification by Sauer (1967) usually prevails. The number of *Amaranthus* species varies in the literature. The genus *Amaranthus* L. according to The Plant List (2013) consists of 105 species. However, these 105 species were verified from 455 species, which indicates that many synonyms or non-accepted names of the species are used. For this study, the red and green varieties of *Amaranthus blitum* were used. These belong to the family Amaranthaceae.

2.4.2 Utilization and Nutritional Importance

Most of the *Amaranthus* species are annual weeds, and only a few are valued as

grains (pseudocerials) and vegetables. Some ornamentals with beautiful foliage also belong to this species.

The grain *Amaranthus* spp. are *A. hypochondriacus*, *A. caudatus* and *A. cruentus*. Traditionally, the grain amaranths were used as flour, popped seeds, cooked into a gruel, and roasted (Marx 1977). Today they are more used as crackers, sweet rolls, amaranth-containing spread, mixed grain pilaf, pancakes, hot cereals, several sorts of bread, tortillas, dumplings and muffins (Saunders and Becker 1984). The flour is often added to maize or wheat, to create a balanced source of proteins (Alvarez-Jubete *et al*. 2010). Amaranth grain is gluten free (Petr *et al*. 2003) and rich in minerals including magnesium, calcium, potassium, phosphorus, iron and sodium (Bressani 2003, Alvarez-Jubete *et al*. 2009) and bioactive substances (Klimczak *et al.* 2002). The protein content was reported between 12.4 and 16.8% (Bejosano and Corke 1998), however in the most recent research study of 1309 accessions (Shukla *et al.* 2017) a wider range was reported (7.8 to 18.0%). The lysine level (a limiting amino acid in most cereal grains) of grain amaranth is twice that of wheat protein, three times that of corn and comparable to milk protein (National Research Council, 1984). Starch is the most abundant component of grain amaranth seeds, comprising about 62% (Becker *et al*. 1981). The diameter of the starch granules is very small which allows it to be used in food and non-food applications, such as a fat replacement ingredient and for producing biodegradable films (Lindeboom *et al.* 2004). The amount of oil in grain *Amaranthus* varies between 5.1 to 7.7% depending on species and contains a high level of squalene (3.6 to 6.1%) which is important in the cosmetic and technology industries (He *et al.* 2002).

Vegetable *Amaranthus* spp. have recently gained importance as a promising food crop owing to its resistance to heat, drought, diseases and pests and high nutritional value of its leaves, stem and seeds (Polturak and Aharoni 2018). Different edible species of *Amaranthus* are consumed widely as leafy vegetables across the world due mainly to their lower price and nutritional composition. *Amaranthus* is a rich source of protein, vitamin C, dietary fiber (Shukla *et al.* 2003, Kadoshnikov *et al.* 2008) and minerals such as calcium, iron, zinc and magnesium (Shukla *et al.* 2006). As a vegetable, amaranths are nutritionally more valuable than most spring and summer

vegetables on a FW basis (Allemann *et al.* 1996). However, breeding of *Amaranthus* as a leafy vegetable has not been reported (Grubben 2004, Natural Resources Conservation Service, USDA, 2018). Several species of *Amaranthus* have been reported to contain various bioactive phytochemicals such as Car, flavonoids and phenolic acids (Amin *et al.* 2006). *Amaranthus* has been well documented to possess important pharmacological properties including anticancer (Sani *et al.* 2004, Al-Mamun *et al.* 2016), anti-inflammatory (Tyszka-Czochara *et al.* 2016), and antioxidant activities (Amin *et al.* 2006, Ozsoy *et al.* 2009, Al-Mamun *et al.* 2016).

Amaranthus blitum is a weed, spread over the world from the tropics to temperate areas, most likely originating from the Mediterranean region. *A. blitum* is well adapted to temperate climates. It has a number of weedy forms with leaves varying greatly in size and color. The leaves, petioles and young tips are used as salads and as potherbs (Larkcom 1991). It is present in many African countries and is mostly a protected weed in backyards and home gardens, sometimes produced for sale at the market. Cultivated types are present in Central and East Africa, likely originating from India where it is an important vegetable. It is also a popular home garden vegetable in southeastern Europe where it is used as a substitute for spinach (*Spinacia oleracea*) during the hot dry summer months. Many cultivated types are larger, more erect and more succulent than weedy types. Mediterranean cultivated types are robust, erect, simple or little-branched plants (up to 1 m tall) with large leaves. The African or Asian (Indian) cultivated types are generally much smaller (up to 50 cm), strongly branched and erect or prostrate. In most African floras, the species name *A. lividus* is used. However, current nomenclature suggests that *A. blitum* should be used (The Plant List 2013).

2.5 Betalain Pigments

2.5.1 Biosynthesis

Betalains are a group of water-soluble nitrogenous pigments, present in most families (such as Amaranthaceae) of the order Caryophyllales, where they replace the anthocyanins as pigments (Stafford 1994, Brockington *et al.* 2011, Gandia-Herrero and Garcia-Carmona 2013). Their name comes from the Latin name of the common beet

(*Beta vulgaris*), from which betalains were first extracted. Betalains are comprised of the yellow-orange betaxanthins and the red-violet betacyanins. The betalain biosynthetic pathway consists of several enzymatic and spontaneous reaction steps and is shown in Fig. 2.7 (Harris *et al*. 2012). Betalains are thought to be synthesized in the cytoplasm and endoplasmic reticulum, based on subcellular localization of their key biosynthetic enzymes (Tanaka *et al.* 2008, Christinet *et al.* 2004, DeLoache *et al.* 2015).
Betalains are synthesized from tyrosine, an aromatic amino acid that is mainly produced in plants through the shikimate pathway (Herrmann 1995, Tanaka *et al.* 2008, Harris *et al.* 2012). Tyrosine is initially hydroxylated to form 3,4-dihydroxy-L- phenyalanine (L-DOPA). The second step in the biosynthetic pathway is conversion of L-DOPA to betalamic acid, the chromophore molecule for both betacyanins and betaxanthins. Betalamic acid can condense with an additional amine, or amino-groups.
and form yellow betaxanthin pigments. These reactions are spontaneous. The formation of betacyanins consists of L-DOPA being converted to cyclo-DOPA which can spontaneously condense with betalamic acid. Many molecular species of betacyanins can be obtained as a result of glycosylation or acylation.

2.5.2 Roles and Applications of Betalains

Betalains are the sum of betacyanins and betaxanthins and classified based on their structural characteristics and light absorption properties. Betalains replace the anthocyanins in the majority of families of the order Caryophyllales and are structurally and biosynthetically distinct from anthocyanins. Betalains can be produced in a wide range of plant organs and cell types including leaves, trichomes, stems, flowers, fruits, seeds and roots (Gandia-Herrero and Garcia-Carmona 2013). Like the anthocyanin pigments, betalains have been proposed to play important roles in plant photoprotection and as scavengers of ROS in response to numerous biotic and abiotic stress factors (Solovchenko and Merzljak 2008). The photoprotective function of betalains under low temperature and heat stress was demonstrated in earlier studies (Wang and Liu 2007, Hayakawa and Agarie 2010). The presence of betacyanins in epidermal and mesophyll

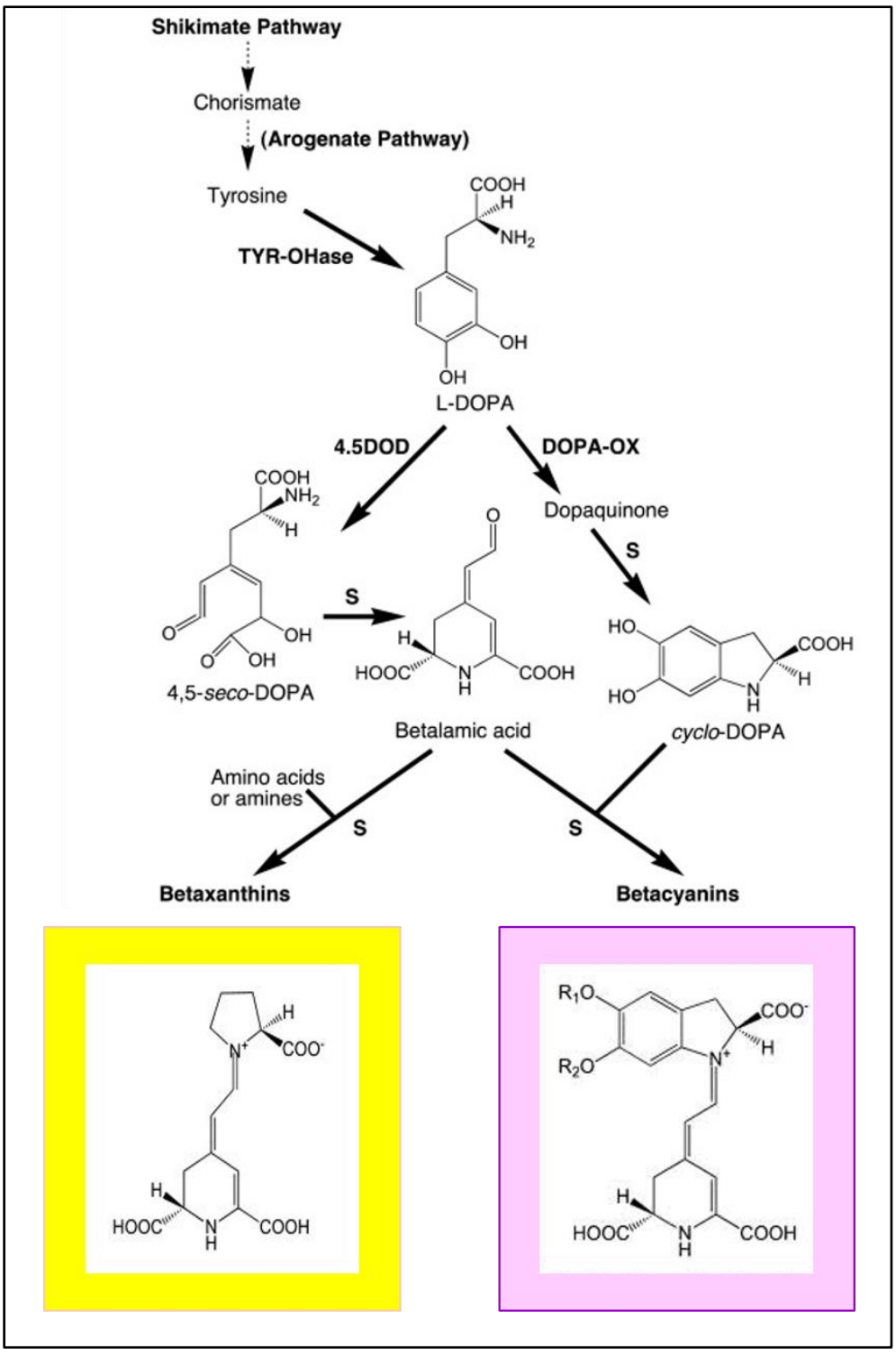

Figure 2.7 The betalain biosynthetic pathway. S, spontaneous condensation reactions. Modified from Harris *et al.* (2012).

cells and their role in attenuating excess incident light was demonstrated by Gould *et al.* (1995) and later by Nakashima *et al.* (2011) who showed two to three-fold reductions in leaf transmittances of visible light in betacyanic leaves in comparision to acyanic leaves. Betalain localization appears to be species-specific. In some species they accumulate primarily in the upper epidermal and adaxial sub-epidermal layers, but in others, in the abaxial mesophyll layer (Vogt *et al.* 1999, Ibdah *et al.* 2002, Wybraniec *et al.* 2010). The latter is proposed to protect the deeper tissues from photodamage due to green and yellow light (Koizumi *et al.* 1998, Vogelmann and Han 2000, Hughes *et al.* 2005, Oguchi *et al.* 2011, Takahashi and Badger 2011). In addition, some betacyanins have been demonstrated to have a high ROS scavenging activity (Cai *et al.* 2001, 2003, Neill and Gould 2003, Wang *et al.* 2006). Apart from their protective effects, betalains can also act as visible signals to attract insects, birds and animals for pollination and seed dispersal (Tanaka *et al.* 2008).

Additionally, betalains serve roles in the food industry as food colourants and replacements for synthetic pigments (Petit-Paly *et al.* 1994, Cai *et al.* 2005, Herbach *et al.* 2006, Stintzing and Carle 2007). Due to their strong antioxidant activity, the potential health promoting properties of betalains have been intensely studied (Cai *et al.* 1998a, 1998b, Escribano *et al.* 1998, Butera *et al.* 2002, Strack *et al.* 2003, Stintzing and Carle 2004, Wang *et al.* 2006, Wu *et al.* 2006, Azeredo 2009, Nagatsu and Sawada 2009, Georgiev *et al.* 2010, Tenore *et al.* 2012, Gandia-Herrero and Garcia-Carmona 2013, Vidal *et al.* 2014, Gengatharan *et al.* 2015, Gandia-Herrero *et al.* 2016, Khan 2016). The metabolic pathway is also of interest as L-DOPA is a precursor for dopamine-mediated biosynthesis of high value metabolites (Kuklin and Conger 1995, Solomon *et al.* 1996, Kulma and Szopa 2007, Nomura and Kutchan 2010, Beaudoin and Facchini 2014, Ehrenworth and Peralta-Yahya 2017). Other studies with betalains have explored their potential use in dye-sensitized solar cells, textile dyes, chemical biosensors and as fungicides (Zhang *et al.* 2008, Sivakumar *et al.* 2009, Calogero *et al.* 2012, Guesmi *et al.* 2012, DeLoache *et al.* 2015, Cabanes *et al.* 2016, Polturak *et al.* 2016, 2017, Gannesan and Karthik 2017).

CHAPTER 3

3.0 MATERIALS AND METHODS

3.1 Plant Materials and Growth Conditions

Seeds of red and green varieties of *Amaranthus blitum* were obtained locally from Mr. M. P. M. Nair (Low Light Tolerant Plants, LLT® Plants Inc.) and stored at 4°C until use. Seeds were germinated in 10 cm pots (Kord Products, Toronto, ON, Canada) containing Sungrow Sunshine LG3 Mix Germinating soil medium (Sun Gro Horticulture Canada Limited, Seba Beach, AB, Canada). The soil medium was placed in a container and watered to field capacity. Pots were filled to 15 mm from the top and seeded with 4 to 5 seeds approximately 1 mm below the soil surface. Pots were placed in a plastic tray and covered with a transparent plastic lid to maintain the humidity. On the third day the cover was removed. Seedlings were thinned on the eighth day after sowing (DAS) to one seedling per pot. Plants were watered with plain tap water as required and beginning on day 11, a fertilizer solution (1 g/L, NPK, 20-20-20) was used (Plant Products Inc., Leamington, ON, Canada).

Plants were grown in controlled environment chambers (Conviron Model E8H, Controlled Environments Limited, Winnipeg, MB, Canada), with light provided by fluorescent lamps (T8HO; Philips Electronics Ltd, Markham, ON, Canada), in the University of Saskatchewan, College of Agriculture and Bioresources Phytotron facility. The chamber settings were 25/22°C (day/night) temperatures with a relative humidity (RH) of 50% and a 16/8 h (light/dark) cycle. Irradiance values were adjusted to 500 or 70 $\mu molm^{-2}\ s^{-1}$PPFD at pot level determined using a light meter (LI-250; Li-Cor Biosciences, Lincoln, NE, USA) and light sensor (MULT-164.47, LI-Cor, Inc). The 500 $\mu mol\ m^{-2}\ s^{-1}$ PPFD was referred to as the HL growth irradiance, and 70 $\mu mol\ m^{-2}\ s^{-1}$ PPFD as the LL growth irradiance. All experiments were performed on fully expanded fourth leaves as determined by growth analyses (see section 3.2) unless otherwise indicated. Sampling occurred at similar times after the start of the photoperiod.

3.2 Growth Analyses

3.2.1 Absolute Growth Parameters

The aerial portions of the whole plant were cut at the base of the stem and fourth leaves were harvested for the determination of fresh weight (FW) and dry weight (DW). Fresh weight was determined using an analytical balance (NewClassic MF, model MS204S; Mettler Toledo, Langacher, Greifensee, Switzerland). Samples were placed in a drying oven (Precision Scientific Thelco, Model 17, Boston, USA) for a minimum of 48 h at 115°C or until constant weight was obtained for the determination of DW. Leaf water content was estimated as described by Ceccato *et al.* (2001) as:

*Leaf Water Content (%) = ((FW-DW)/FW) * 100*

The leaf area (LA) of the fourth leaf was obtained using *Fiji*-ImageJ, a distribution of the popular Open Source software ImageJ (National Institute of Health, USA; Schindelin *et al.* 2012, Rueden *et al.* 2017). For all growth parameters under HL, the sampling interval occurred daily from the 16th to the 26th DAS and at LL the sampling period was at three or five day intervals, depending on plant growth rate, from the 28th to the 55th DAS.

3.2.2 Relative Growth Parameters

The aerial portions of the whole plant and fourth leaf relative growth rates (RGRs) were calculated over the entire sampling period of the plant or fourth leaf which corresponded with 10 days under HL (from 16th to the 26th) and 27 days under LL (from 28th to the 55th), as described by Hoffmann and Poorter (2002) using the equation:

$$RGR = (lnDW_2 - lnDW_1)/(t2 - t1)$$

where DW represents dry weight and t represents time.

Specific leaf area (SLA) was calculated for the fourth leaf as LA/DW, where LA represents leaf area and DW represents dry weight.

3.3 Photosynthetic Measurements

3.3.1 Photosynthetic O_2 Evolution

Leaf discs (10-cm^2) from fourth leaves were used for the determination of photosynthetic O_2 evolution. Measurement occurred in the gas phase at 25°C with an electrode chamber (model LD2; Hansatech Instruments Ltd., King's Lynn, UK) as described by Gray *et al.* (1994). Before collecting any data, the electrode responsiveness was tested and calibrated according to the manufacturer's instructions (Hansatech Intruments LTD.**,** 2006). The data were collected using an Oxylab control unit (Hansatech) along with O2view software (v 2.06, Hansatech). Light-response curves were generated by using a LH36/2R light source (Hansatech) which provided 10 irradiance values from 0 to 650 µmol m^{-2} s^{-1} PPFD (0, 10, 35, 50, 70, 125, 250, 375, 500, 650) over a 30 min period. The temperature was maintained at 25°C by using a circulating water bath (model RC6 CS; Lauda Dr. R. Wobser GmbH and Co. KG, Lauda-Königshofen, Germany) and CO_2 was provided from capillary matting saturated with 1.0 M $NaHCO_3$.

Several photosynthetic parameters were derived by using the O2view software (Hansatech) and the O_2 evolution light-response curves (see Fig. 2.2), as described by Walker (1987). The $P_{max}O_2$ corresponded with the upper asymptote of the hyperbolic light-response curve. The LCP was calculated as the x-intercept, which represents the irradiance at which the rate of photosynthesis equals the rate of respiration. The LSP represents the inflection point of the curve, which indicates at which irradiance the photosynthesis saturates. The R_{dark} was calculated as the y-intercept of the curve and represents the rate of O_2 efflux for plant metabolism in the dark, while the $\Phi_{app}O_2$ was calculated from the slope of the light response curve in the light-limiting portion (from 10 to 125 µmol m^{-2} s^{-1} PPFD) and represents the amount of O_2 evolved per total number of quanta received.

3.3.2 Chlorophyll Fluorescence

Chlorophyll *a* steady-state fluorescence quenching parameters were determined *in planta* on detached fourth leaves at room temperature using a PAM-2000 portable chlorophyll fluorometer (Heinz Walz GmbH, Effeltrich, Germany) as described by Baerr

et al. (2005).

Leaves were dark-adapted for 10 min prior to the onset of measurement. Minimal fluorescence in the dark-adapted state (F_0) was determined by subjecting the leaf sample to a weak measuring beam. A saturating pulse of light for 800 ms was used to determine the maximal fluorescence in the dark-adapted state (F_m). The leaves then were exposed to an actinic light that was superimposed with sequential applications of a saturation pulse followed by far-red (FR) light until a steady-state level of fluorescence (F_s) was achieved (approximately 15 min). The actinic light applications corresponded to the growth irradiance at HL and LL (500 or 70 µmol m^{-2} s^{-1} PPFD). The applications of saturating pulses gave the maximal fluorescence (F_m') in the light-adapted state. Minimal fluorescence in the light-adapted state (F_0') was determined immediately after turning off the actinic source in the presence of FR background light for 4 s to ensure maximal oxidation of PSII electron acceptors. WinControl software (ver 2.00f; Heinz Walz) was used to control the timing, settings and trigger signals for the various actinic and saturating pulse light sources. Fluorescence traces were captured and analysed using the WinControl software.

The maximal photochemical efficiency of PSII was calculated as ($F_v/F_m = (F_m-F_0)/F_m$) while the effective quantum yield of PSII (Φ_{PSII}) was calculated as ($\Phi_{PSII} = F_m'-F_s)/F_m'$ (Genty *et al.* 1989). Non-photochemical quenching was calculated as (NPQ = $(F_m-F_m')/F_m'$) according to Bilger and Schreiber (1986) and the q_L was determined according to Kramer *et al.* (2004) as ($q_L = (F_m'-F_s)/(F_m'-F_0') \times F_0'/F_s$). The ETR was estimated according to Schreiber *et al.* (1994) as ($ETR = \Phi_{PSII} \times I \times 0.42$), where I is the incident PPFD on the leaf and 0.42 is the product of the spectral absorbance of the leaf (84%) and the fraction of incident photons that are absorbed by PSII (50%).

3.4 Photoinhibition of Photosynthesis

Low temperature photoinhibitory treatments were performed by floating leaf discs (10-cm^2) adaxial side up in a petri dish with deionized water. The samples were then exposed to an irradiance of 1450 µmol m^{-2} s^{-1} PPFD provided by a metal halide lamp (400W, E40 CLU1SL, Koninklijke Philips N.V., Amsterdam, Netherlands) in a cold room

at 2°C for 4 h. The irradiance was measured at the surface level of the samples using a light meter (LI-250A; Li-Cor, Inc.) and sensor (MULT-164.47, LI-Cor, Inc). Photoinhibition of photosynthesis was quantified by measuring changes in F_v/F_m with a PAM-2000 portable chlorophyll fluorometer (Heinz Walz) after dark adaptation for 10 min.

3.5 Pigment Determination

3.5.1 Chlorophyll and Carotenoids

Chlorophylls *a*, *b* and total Car content as sum of xanthophylls and carotenes (*x*+*c*) was determined spectrophotometrically from acetone extracts using a SmartSpec Plus spectrophotometer (Bio-Rad-Laboratories, Hercules, CA, USA). Leaf discs (10-cm^2) were cut using a borer and weighed to determine the FW. The samples were ground in 80% (v/v) pre-chilled acetone (HPLC Grade; EMD Millipore, Darmstadt, Germany) with a pre-chilled mortar and pestle with sand (EM Science, Merck KGaA, Darmstadt, Germany) until homogeneous. The slurry was transferred to 50 or 15 mL tubes (Sarstedt Inc. Montreal, Canada) and centrifuged for 10 min at maximum speed (4,500 rpm) at room temperature (Beckman Coulter, Allegra™ 21 Centrifuge, Brea, CA, USA). The supernatant was removed and absorbance measured at A_{663}, A_{646}, and A_{470}. Chlorophyll and Car pigments were calculated using the equations of Lichtenthaler and Welburn (1983) and expressed on a leaf FW or area basis.

3.5.2 Betalains

Betalains were determined spectrophotometrically from methanol extracts using a SmartSpec Plus spectrophotometer (Bio-Rad-Laboratories). Leaf discs (10-cm^2) were cut as described in section 3.5.1. The samples were ground in 80% (v/v) pre-chilled methanol (HPLC Grade; EMD Millipore) with a pre-chilled mortar and a pestle and sand (EM Science) until homogeneous. The slurry was transferred to 15 mL tubes (Sarstedt Inc. Montreal, Canada) and centrifuged for 10 min at maximum speed (4,500 rpm) at room temperature (Beckman Coulter). The supernatant was removed and absorbance measured at 538 nm for betacyanins and at 470 nm for betaxanthins. Betacyanin and betaxanthin contents were calculated based on the molecular extinction coefficients for

betanin (60,000 L mol^{-1} cm^{-1} in H_2O) and vulgaxanthin (48,000 L mol^{-1} cm^{-1} in H_2O) respectively (Cai 1998c, Kugler *et al*. 2004, 2007) and expressed on a leaf FW or area basis. Total betalain content was determined as the sum of betacyanin and betaxanthin.

3.6 Microscopy

3.6.1 Leaf Surface Structures

Leaf imprints were collected from the adaxial and abaxial sides of the fourth leaf on Suzuki's Universal Micro-Printing (SUMP) discs (Sump Laboratory, Tokyo, Japan) as described by Tanaka *et al*. (2005). A thin and uniform layer of the nitrocellulose solution (liquid SUMP) was applied on one side of the SUMP disc, which then was pressed on the leaf surface of interest. Afterwards, the leaf imprints were secured with double-sided tape on a glass plate for further analyses. The samples are permanent and do not require any other treatment. The leaf imprints were analysed on an inverted microscope EVOS FL (Mill Creek, Washington, United States). Six to nine fields of view were collected from each disk-imprint. The images were collected with a designated scale which allowed for the calculation of stomatal, trichome and epidermal cell densities defined as the number of stomata, trichomes or EC present per unit area of the leaf. The collected images from the imprints allowed for the determination of the type of stomata and trichomes that are present on the leaves. The stomatal index (SI) was calculated according to Salisbury (1928) as described by Royer (2001) as:

*SI (%) = (stomatal density/(stomatal density + epidermal cell density)) * 100)*

The images were analysed with *Fiji*-ImageJ public domain software (Schindelin *et al.* 2012, Rueden *et al.* 2017).

3.6.2 Leaf Anatomy

Leaf transverse and longitudinal sections (1 x 2 mm) were taken from the fourth leaf with a razor blade. The segments were either mounted in distilled water for observing betalain localization or fixed in 0.1 M cacodylate buffer (pH 7.4) containing 2.5% (v/v) glutaraldehyde for 2 h at 4°C. Samples were then post-fixed with 2% (v/v)

osmium tetroxide in the same buffer for another 2 h at 4°C followed by dehydration in an ethanol series: 25, 50, 70, 90, 100% (v/v) combined with infiltration with propylene oxide (100%) and finally embedded in Eponate 12 medium (resin Epon 812, dodecenyl succinic anhydride (DDSA) hardener, nadic methyl anhydride (NMA) hardener, benzyldimethylamine (BDMA) accelerator). The polymerization occurred over night at 60°C in a drying oven (Precision Scientific Thelco, Model 17, Bosron, USA) with modifications described by Hong *et al.* (2005).

Semi-thin leaf transverse sections (1.0 µm thick) were obtained with glass knives on an ultramicrotome (Reichert Ultracut E, Leica, Vienna, Austria). Sections were stained with 1% (w/v) Toluidine Blue-O (TBO) in 1% (w/v) $Na_2B_4O_7$ and observed under a light microscope (ZEISS AxioPlan, Carl Zeiss Microscopy GmbH, Jena, Germany).

Light micrographs were taken with a digital camera (ZEISS Axiocam 105 color) and the images were adjusted and assigned a scale through the imaging software (ZEN 2, ZEISS AxioPlan). The images were analysed with *Fiji*-ImageJ (Schindelin *et al.* 2012, Rueden *et al.* 2017). Parameters obtained included area, perimeter and maximum (max) and minimum (min) diameter of the upper epidermal cells (UEC), upper mesophyll cells (UMC), BSC, lower epidermal cells (LEC), LMC, as well the LT, and UMC and LMC layer thickness.

3.6.3 Cellular Organelles

Leaf material was prepared as described above in section 3.6.2. Leaf transverse sections (60 to 100 nm thick) were cut with a diamond knife on an ultramicrotome (Reichert Ultracut E). Sections were stained with 2% (w/v) aqueous uranyl acetate for 30 min, followed by Reynolds' lead citrate solution (Sigma-Aldrich, St. Louis, MO, USA; Reynolds 1963) and examined using a transmission electron microscope (TEM; Hitachi HT 7700, Tokyo, Japan). These data were used to demonstrate the localization of the chloroplasts, mitochondria and peroxisomes in the MC, BSC, vascular parenchyma cells (VPC) and companion cells (CC). Multiple fields of view were used to determine the area, perimeter, max and min diameter, as well revealed the shapes and arrangement of these organelles in the cells identified above. Analyses of chloroplast ultrastructure allowed measurement of appressed (App) and non-appressed (Non-App)

thylakoid length and area. Additionally, the area of the stroma was determined by subtracting the areas of thylakoid membranes, chloroplast features (CP, PR and CI), plastoglobuli, starch grains from chloroplast area. The length and area of App and Non-App thylakoid membranes and the stroma in turn allowed determination of granal index (GI), thylakoids per granum, App and Non-App thylakoid density and total thylakoid density. The GI was calculated according to Voznesenskaya *et al.* (1999) as:

*GI (%) = (length appressed thylakoids/(length total thylakoids)) * 100)*

The measurements were analyzed with *Fiji*-ImageJ (Schindelin *et al.* 2012, Rueden *et al.* 2017) and the Trainable Weka Segmentation Plugin (Arganda-Carreras *et al.* 2017).

3.7 Statistical Analyses and Experimental Design

The experiments were conducted in a completely randomized design in controlled environment chambers. Unless stated otherwise, each experiment consisted of three biological repetitions using three to six leaves from three to six individual plants. The data was analyzed by using descriptive statistics in Microsoft Excel (Microsoft Corporation, Redmond, WA, USA) and a one-way or two-way analysis of variance (ANOVA) in SigmaPlot 12 (Systat Software Inc. San Jose, CA, USA). Tests for normality (Shapiro-Wilk) and equal variance (Levene's mean test) were performed at $P = 0.05$. If a significant difference was detected, a Holm-Sidak post-hoc test at $P = 0.05$ was used to isolate the difference.

CHAPTER 4

4.0 RESULTS

4.1 Growth Analyses

Growth and development of *Amaranthus blitum* red and green varieties under HL and LL growth irradiance were noticeably different. Development under HL was very rapid and changes in phenotype were observable from one day to another (Fig. 4.1A, C). Both varieties illustrated a steep increase of aerial whole plant DW accumulation over time (Fig. 4.1A). The red variety grew and developed slightly faster than the green variety, which generated a slightly greater aerial whole plant DW accumulation during the 10 days sampling period than the green variety. The main difference between varieties under HL was the onset of the flowering period. Flowering in the red variety started at 25-26 days after sowing (DAS), while in the green variety started at 35-40 DAS.

Growth and development under LL were very slow for both varieties (Fig. 4.1B, D). Even after 55 DAS under LL, the aerial whole plant DW accumulation was 3.1- and 1.9-fold lower in red and green varieties than under HL at 26 DAS, respectively. The 26 DAS and 55 DAS represent the last day of sampling under HL and LL. However, the aerial whole plant DW accumulation between varieties during the 27 days sampling period demonstrated an opposite trend than under HL, with slightly greater accumulation in the green than in the red variety (Fig. 4.1A, B). Flowering under LL for either variety was not observed even after 80 DAS, at which point plants started to senesce.

The fourth leaf was selected for analyses based on preliminary growth experiments (data not shown). The fourth leaf DW of the red variety continued to accumulate more than the green variety until 21 DAS, after which the green variety steeply increased until 26 DAS (Fig. 4.1C). At 26 DAS both varieties reached the plateau of expansion and DW accumulation (Fig. 4.1C).

The fourth leaf DW accumulation under LL was gradual and slow, overall reflected similar trend as the aerial whole plant DW accumulation (Fig. 4.1B, C).

The fourth LA at either growth irradiance (Fig. 4.2A, B) reflected similar trends as

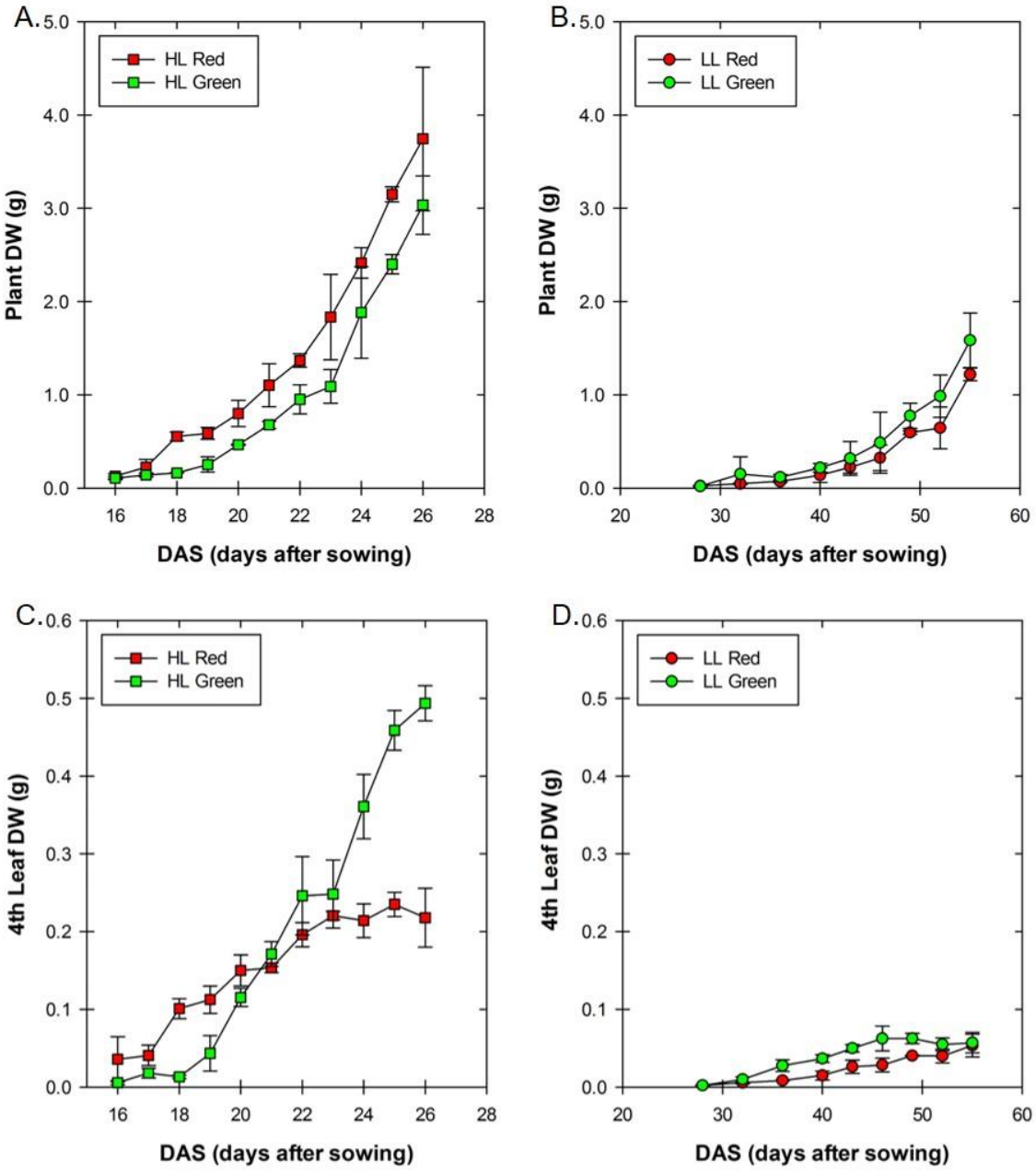

Figure 4.1 Dry weight (DW) accumulation for red and green varieties of *Amaranthus.* Plants were grown under HL (**A., C.**) and LL (**B., D.**) and DW calculated for the whole plant (**A., B.**) and fourth leaf (**C., D.**). Whole plant DW was calculated as the total aerial portion of the plant. Values represent means ± SD (*n* = 3 to 8 leaves or plants). DAS, days after sowing; HL, high light; LL, low light; SD, standard deviation.

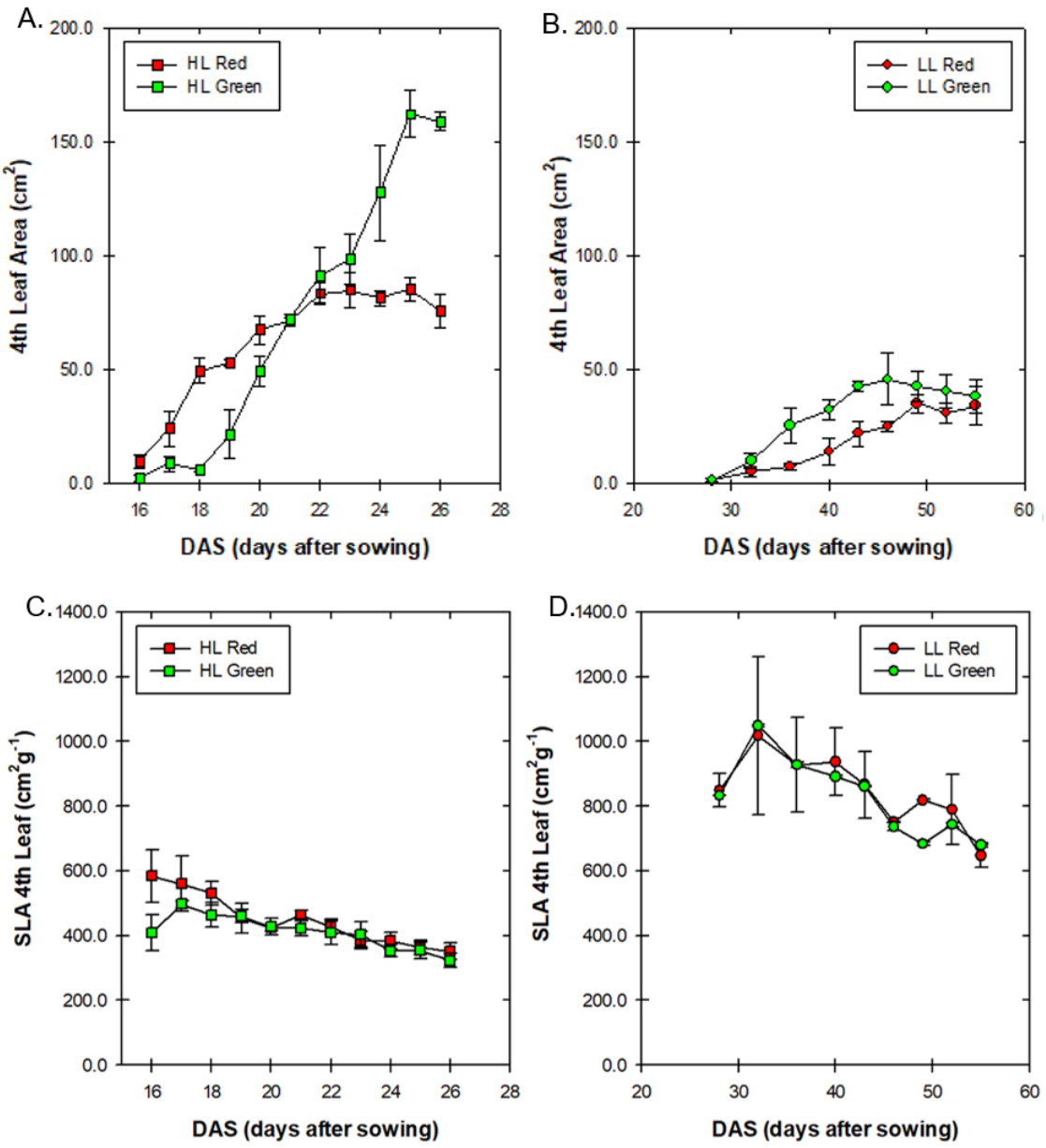

Figure 4.2 Leaf area (LA) and specific leaf area (SLA) for red and green varieties of *Amaranthus.* Plants were grown under HL (**A., C.**) and LL (**B., D.**). Leaf area (**A., B.**) and SLA (**C., D.**) were determined for the fourth leaf. Values represent means ± SD (*n* = 3 to 8 leaves). DAS, days after sowing; HL, high light; LL, low light; SD, standard deviation.

the fourth leaf DW accumulation, respectively. A similar trend between the DW accumulation and LA indicated that both varieties exhibited restricted capacity to adjust the LA under LL. The SLA of the fourth leaf under HL and LL growth irradiance suggests that the LT of the red and green varieties were significantly greater under HL than under LL growth irradiance (Fig. 4.2C, D).

The plant height at the end of the sampling period under HL (26 DAS) in both varieties was lower than under LL (55 DAS) growth irradiance but differentially responsive. The height of the red variety under HL was approximately 1.7-fold greater than the green variety (Table 4.1). Under LL (55 DAS) there was no difference in either height or leaf number between varieties. In addition, the leaf count of both varieties was different among the growth irradiance. Leaf count in the red variety under HL was greater than under LL growth irradiance. In contrast, leaf count in the green variety was lower under HL than under LL growth irradiance. However, leaf count under HL in the red variety was 1.4-fold greater than in the green variety. In contrast, under LL both varieties accumulated similar numbers of leaves (Table 4.1). Plant water content remained relatively constant for the duration of the time examined with essentially no differences between red and green varieties under both irradiance conditions (data not shown).

In order to sample at a consistent developmental phase, the DW and area of the fourth leaf was compared between varieties under HL growth irradiance over a 10 day sampling period (from 16 to 26 DAS) and under LL growth irradiance over 27 day sampling period (from 28 to 55 DAS). Based on these data, the optimal sampling times under HL for the fourth leaf was 20 and 23 DAS for the red and green *Amaranthus* varieties, respectively. Under LL, the optimal sampling time was determined to be 40 DAS for both *Amaranthus* varieties. Based on phenotypical observations (Fig. 4.3) and growth kinetics (Fig. 4.1, Fig. 4.2) both varieties under HL and LL growth irradiance at the sampling day appeared to be at similar growth stages. The relative growth rate (RGR) of the aerial whole plant in the red variety under HL growth irradiance was greater than in the green variety. However, the leaves of the green variety were significantly larger than in the red variety. Under LL growth irradiance, this trend was not observed as the growth and development in general was gradual and slow (Table 4.2).

Table 4.1 Plant height and number of accumulated leaves for the red and green varieties of *Amaranthus* grown under HL and LL. Plant material was collected at the end of sampling for growth kinetics under HL (26 DAS) and LL (55 DAS) conditions. Values followed by different letters in each column indicate a significant difference at $P = 0.05$ using a Holm-Sidak post-hoc test. Values represent means ± SD (n = 3 to 6 plants). DAS, days after sowing; HL, high light; LL, low light; SD, standard deviation.

Growth Irradiance and Variety	Plant Height (cm)	Leaf Count (#)
HL Red	16.17 ± 0.29^{b}	17.67 ± 0.58^{a}
HL Green	9.67 ± 0.47^{c}	13.00 ± 0.00^{c}
LL Red	25.97 ± 1.15^{a}	16.33 ± 0.58^{b}
LL Green	23.85 ± 2.30^{a}	16.50 ± 0.84^{b}

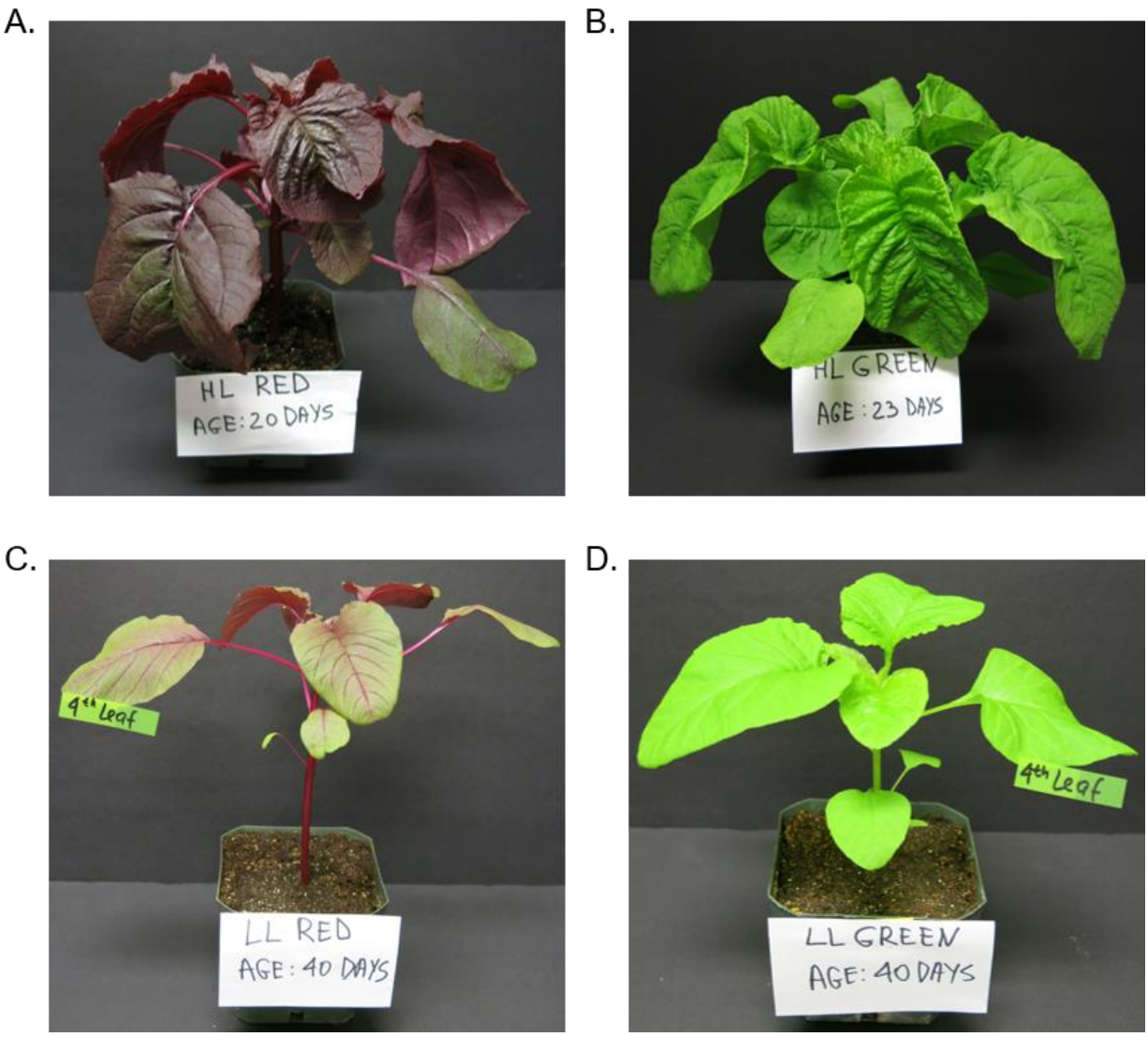

Figure 4.3 Phenotypic comparisons of *Amaranthus.* The red (**A., C.**) and green (**B., D.**) varieties of *Amaranthus* were grown under HL (**A., B.**) and LL (**C., D.**). The photographs were taken at 20 and 23 DAS for the red and green varieties under HL respectively and at 40 DAS at LL. Representative images are shown. DAS, days after sowing; HL, high light; LL, low light.

Table 4.2 Relative growth rates (RGR) for red and green varieties of *Amaranthus* grown under HL and LL. RGR was calculated for the period 16 to 20 DAS for HL red, 16 to 23 DAS for HL green and 28 to 40 DAS for LL red and green. Values were calculated based on the mean of dry weight (DW; Fig. 4.1). Values followed by different letters in each column indicate a significant difference at $P = 0.05$ using a Holm-Sidak post-hoc test. Values represent means ± SD (n = 3 to 6 leaves or plants). DAS, days after sowing; HL, high light; LL, low light; SD, standard deviation.

Growth Irradiance and Variety	Whole Plant RGR ($g\ g^{-1}\ day^{-1}$)	4^{th} Leaf RGR ($g\ g^{-1}\ day^{-1}$)
HL Red	0.47 ± 0.06^{a}	0.36 ± 0.06^{b}
HL Green	0.33 ± 0.02^{b}	0.54 ± 0.02^{a}
LL Red	0.14 ± 0.04^{c}	0.16 ± 0.03^{d}
LL Green	0.21 ± 002^{c}	0.24 ± 0.01^{c}

4.2 Photosynthesis

The photosynthetic performance of both varieties was evaluated based on the parameters derived from O_2 evolution curves (Fig. 4.4A., Table 4.3) and Chl fluorescence measurements (Table 4.4). The $\Phi_{app}O_2$ and $P_{max}O_2$ in both varieties was greater in plants grown under HL than under LL growth irradiance. The red variety under HL exhibited a 3.9- and 5.2-fold greater values of $\Phi_{app}O_2$ and $P_{max}O_2$ than under LL. A similar trend was observed for the green variety, with 3.5- and 3.4-fold greater values of $\Phi_{app}O_2$ and $P_{max}O_2$ than under LL (Table 4.3). The R_{dark} and LCP was 3.2- and 1.2-fold greater only in the red variety when compared with their counterparts grown under LL growth irradiance. Photosynthesis under HL growth irradiance in the red variety did not saturate even at 650 µmol m^{-2} s^{-1} PPFD, in contrast to the green variety which was saturated at approximately 380 µmol m^{-2} s^{-1} PPFD (Table 4.3). The LSP in the red variety for further comparision was used as 650 µmol m^{-2} s^{-1} PPFD. The LSP was 1.7-fold greater in the red variety under HL than under LL growth irradiance (Table 4.3).

Under HL growth irradiance, the red variety demonstrated a 1.2- and 1.5-fold greater values of $\Phi_{app}O_2$ and $P_{max}O_2$ than the green variety. Additionally, the R_{dark} and LCP were also greater by a 2.1- and 1.3-fold than the green variety. The LSP in red occurred at 1.7-fold greater values of irradiance than in the green variety. However, under LL growth irradiance there were no differences in any of the measured parameters between varieties with exception for LSP, which were slightly greater in the red variety (Table 4.3).

Chlorophyll fluorescence measurements showed no differences in F_v/F_m or q_L either between varieties or growth irradiance (Table 4.4). However, the NPQ values were 1.7- and 1.9-fold greater under HL for the red and green varieties, respectively. Similarly, the ETR was 5.3- and 5.8-fold greater for the red and green varieties, respectively under HL conditions (Table 4.4).

4.3 Photoinhibition

Exposure to a photoinhibitory irradiance (1450 µmol m^{-2} s^{-1}) at 2°C for 4 hours

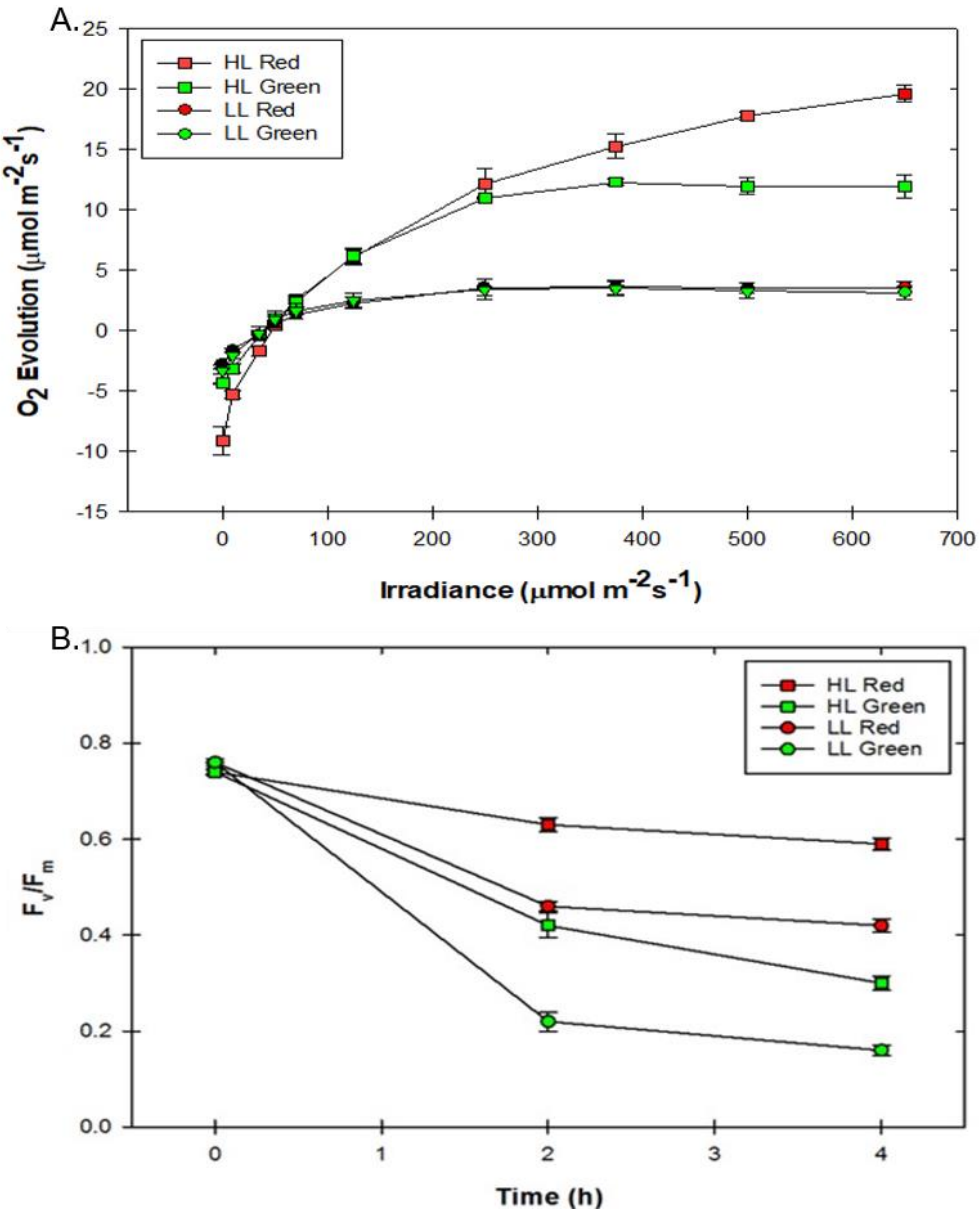

Figure 4.4 Photosynthesis and photoinhibition in red and green varieties of *Amaranthus*. Light response curves of O_2 evolution (**A.**) and photoinhibition (**B.**) were determined in the fourth leaves of plants grown under HL and LL. Values represent means ± SE (*n* = 3). Photoinhibition occurred at 2°C with a PPFD of 1450 µmol m^{-2} s^{-1} and was assessed by monitoring F_v/F_m over time. F_v/F_m, maximal photochemical efficiency of PSII; HL, high light; LL, low light; PPFD, photosynthetic photon flux density; PSII, photosystem II; SE, standard error.

Table 4.3 Photosynthetic parameters of O_2 evolution for red and green varieties of *Amaranthus.* Values were derived from O_2 evolution response curves (Fig. 4.4A) from the fourth leaves of plants grown under HL and LL and represent means ± SE (*n* = 3). Values followed by different letters in each row indicate a significant difference at *P* = 0.05 using a Holm-Sidak post-hoc test. $\Phi_{app}O_2$, apparent quantum yield of O_2 evolution; HL, high light; LCP, light compensation point; LSP, light saturation point; LL, low light; $P_{max}O_2$, maximal rate of O_2 evolution; R_{dark}, rate of dark respiration; SE, standard error.

Parameters	Growth Irradiance and Variety			
	HL Red	HL Green	LL Red	LL Green
$\Phi_{app}O_2$ ($\mu molO_2\ m^{-2}\ s^{-1}$/photon)	0.062 ± 0.005[a]	0.052 ± 0.001[b]	0.016 ± 0.003[c]	0.015 ± 0.002[c]
$P_{max}O_2$ ($\mu molO_2\ m^{-2}\ s^{-1}$)	19.63 ± 0.69[a]	12.85 ± 0.43[b]	3.75 ± 0.60[c]	3.75 ± 0.69[c]
R_{dark} ($\mu molO_2\ m^{-2}\ s^{-1}$)	-9.11 ± 1.17[a]	-4.37 ± 0.05[b]	-2.84 ± 0.04[b]	-3.04 ± 0.28[b]
LCP (μmol photons $m^{-2}\ s^{-1}$)	48.10 ± 1.58[a]	36.65 ± 2.66[b]	39.37 ± 4.92[b]	40.24 ± 8.24[b]
LSP (μmol photons $m^{-2}\ s^{-1}$)	> 650.00 [a]	380.49 ± 19.45[b]	405.14 ± 77.06[b]	300.39 ± 35.80[c]

Table 4.4 Steady-state chlorophyll fluorescence parameters for red and green varieties of *Amaranthus* grown under HL and LL. Values represent means ± SE (n = 3). Values followed by different letters in each row indicate a significant difference at P = 0.05 using a Holm-Sidak post-hoc test. ETR, linear electron transport rate through PSII; F_v/F_m, maximal photochemical efficiency of PSII; HL, high light; LL, low light; NPQ, non-photochemical quenching; PSII, photosystem II; q_L, coefficient of photochemical quenching; SE, standard error; $\Phi_{PSII,}$ effective quantum yield of PSII electron transport.

Parameters	Growth Irradiance and Variety			
	HL Red	HL Green	LL Red	LL Green
F_v/F_m	0.75 ± 0.02[a]	0.74 ± 0.01[a]	0.76 ± 0.01[a]	0.76 ± 0.002[a]
NPQ	0.79 ± 0.07[a]	0.83 ± 0.07[a]	0.46 ± 0.01[b]	0.44 ± 0.02[b]
q_L	0.76 ± 0.04[a]	0.82 ± 0.05[a]	0.90 ± 0.01[a]	0.85 ± 0.02[a]
Φ_{PSII}	0.48 ± 0.02[b]	0.50 ± 0.03[b]	0.59 ± 0.01[a]	0.60 ± 0.01[a]
ETR	81.45 ± 2.70[a]	83.76 ± 3.64[a]	15.35 ± 0.22[b]	14.46 ± 0.51[b]

(Fig. 4.4B) demonstrated that the red variety exhibited increased tolerance to photoinhibition in comparison to the green variety when measured as F_v/F_m. When grown under HL, the red variety showed only a 20% loss of F_v/F_m while the green variety exhibited a 59% loss. Similarly, plant growth under LL resulted in 45 and 79% losses of F_v/F_m in the red and green varieties, respectively (Fig. 4.4B).

4.4 Pigments

4.4.1 Chlorophyll and Carotenoids

Photosynthetic pigment analysis under HL conditions revealed the red variety had a 2.5- and 2.6-fold higher content of total Chl and Car, respectively, compared to the green variety on an area basis (Fig. 4.5A, B). A similar trend was observed under LL conditions with the red variety showing 1.8- and 2.2-fold greater increase in total Chl and Car, respectively (Fig. 4.5A, B). However, the Chl *a/b* ratio was not statistically different between varieties at either growth irradiance (Fig. 4.5C). Chlorophyll/carotenoid ratios were the same for the red variety at either growth irradiance and the green variety only under HL conditions (Fig. 4.5D). The Chl/Car ratio was 23% lower in the red variety than the green variety under LL conditions (Fig. 4.5D). With respect to growth irradiance, only the green variety expressed a decrease (25%) at HL compared to LL conditions (Fig. 4.5D). The responses were similar when expressed on a FW basis (see Table A1).

4.4.2 Betalains

The betalain pigments were significantly greater in the red variety at both growth irradiance either on a LA or FW basis (Fig. 4.6; Table A2). On an area basis, a 4.7- and 3.5-fold increase was shown in the red variety over the green variety under HL and LL growth irradiance, respectively (Fig. 4.6A). Specific profiling of the betalains indicated in the red variety under HL growth irradiance that the total betalain content consisted of 52% betacyanins and 48% betaxanthins and under LL conditions, 40% betacyanins and 60% betaxanthins. However, in the green variety, about 92% of the total betalains were attributable to betaxanthins under both HL and LL irradiance (Fig. 4.6B). With respect to growth irradiance, the content of betalain in the red variety was greater when plants

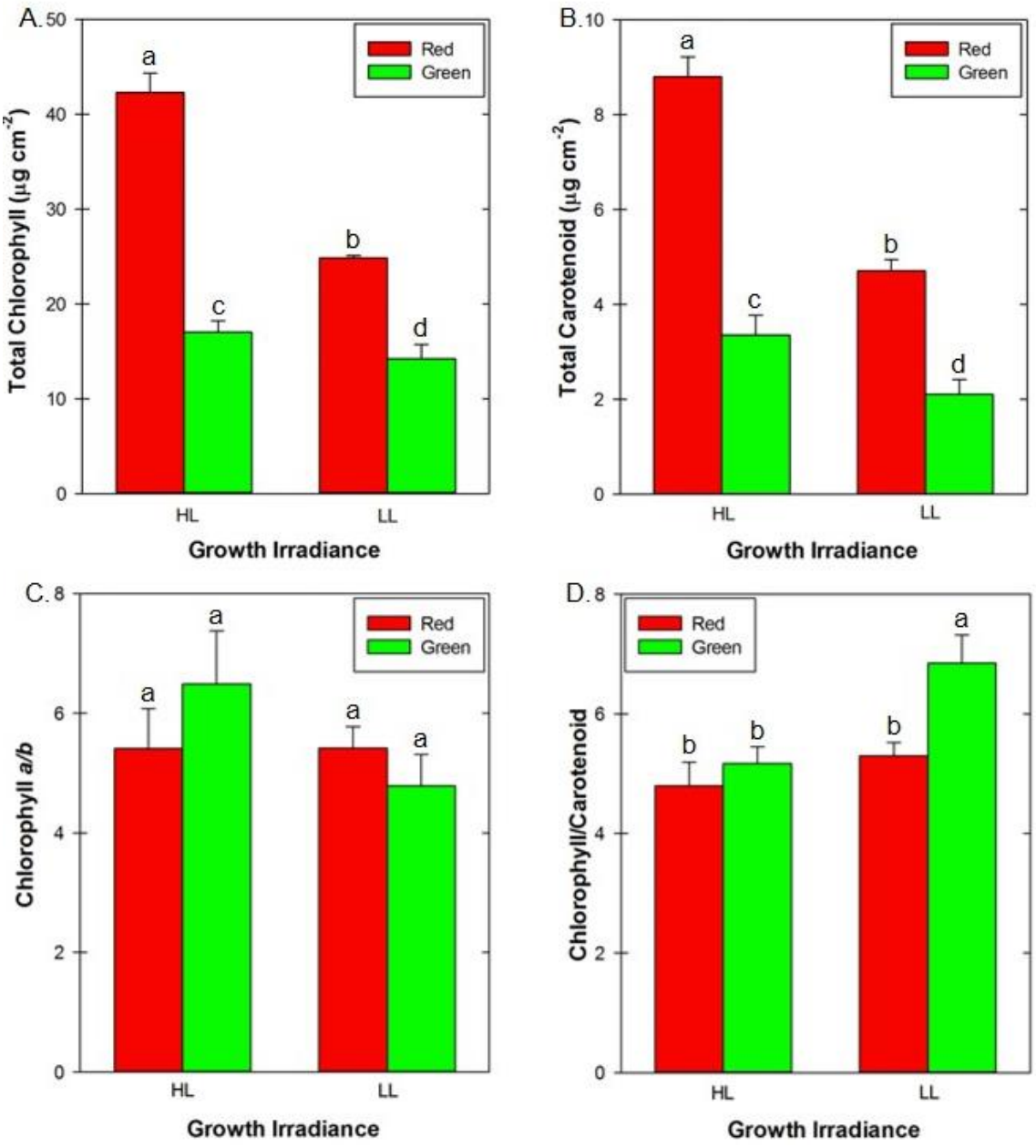

Figure 4.5 Pigment analyses for red and green varieties of *Amaranthus* based on leaf area. Total chlorophyll (**A.**), total carotenoid (**B.**), chlorophyll *a/b* ratios (**C.**) and chlorophyll/carotenoid ratios (**D.**) were determined from the fourth leaves of plants grown under HL and LL. Values represent means ± SE (n = 3). The letters above each bar indicate a significant difference at P = 0.05 using a Holm-Sidak post-hoc test. HL, high light; LL, low light, SE, standard error.

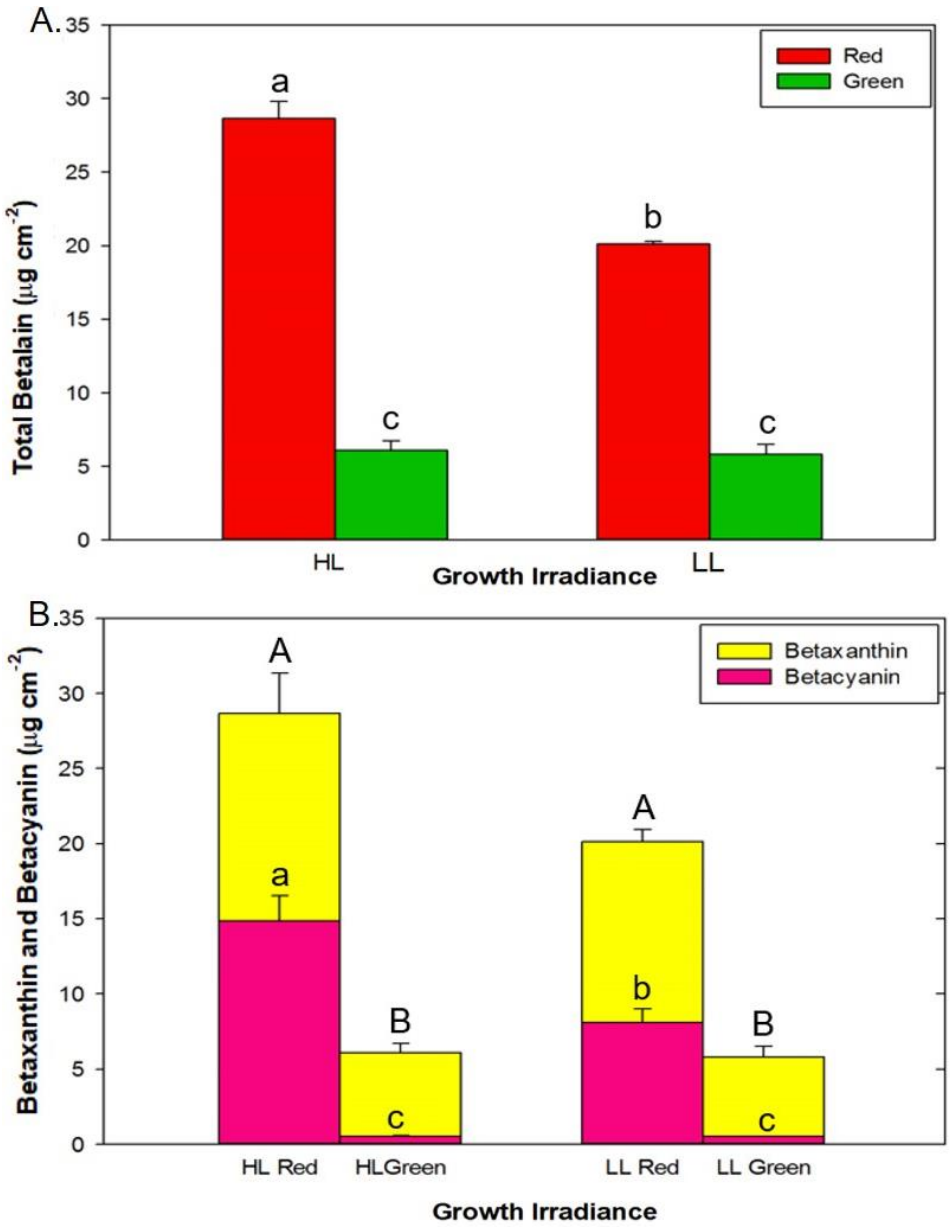

Figure 4.6 Total betalain content for red and green varieties of *Amaranthus* based on leaf area. Total betalain **(A.)** is the sum of betaxanthin and betacyanin pigments **(B.)**. The fourth leaves of plants grown under HL and LL were sampled. The letters above each bar indicate a significant difference at $P = 0.05$ using a Holm-Sidak post-hoc test. In panel **(B.)**, uppercase letters refer to betaxanthin and lowercase letters refer to betacyanin pigments. Values represent means ± SE ($n = 3$). HL, high light; LL, low light; SE, standard error.

were grown under HL. In contrast, the content of betalins in the green variety was similar at either growth irradiance. When expressed on FW basis, a similar trend was observed among varieties and growth irradiance (Table A2).

The localization of betalain pigments in the leaf in both varieties is shown in Fig. 4.7, with higher accumulation primarily on the abaxial side of the leaf blade at either growth irradiance.

4.5 Leaf Anatomy

4.5.1 Stomata and Trichomes

Leaf imprints were collected and used for the calculation of the stomatal index (SI) and stomatal and trichome density (Table 4.5, Table A3; Fig. 4.8-4.10, Fig. A1-A3). Among varieties, the SI on the adaxial side of the leaf were significantly different at either growth irradiance. The red variety exhibited 1.3- and 2.5-fold greater values than the green variety at HL and LL, respectively (Table 4.5). Despite this, the SI on the abaxial side of the leaf were not significantly different between varieties when plants were grown at HL and 1.2-fold greater in the green than in the red variety when grown under LL growth irradiance. However, with respect to growth irradiance, the red variety abaxial SI exhibited a 1.4-fold increase under HL compared to LL growth irradiance (Table 4.5) and the green variety exhibited 1.2-fold greater value under HL than under LL growth irradiance, respectively (Table 4.5). In the green variety, changes in the SI between the adaxial and abaxial sides of the leaf, at both HL and LL, were as a result of changes in stomatal density (Table A3). In addition, the red and green varieties possessed anomocytic type stomata.

Trichome density under HL growth irradiance in the red variety was approximatively 2-fold lower on the adaxial side and 2-fold greater on the abaxial side in comparison with the green variety (Table 4.5; Fig. 4.9). Under LL growth irradiance, no significant difference in trichome density was observed between the varieties on either side of the leaf. With respect to growth irradiance, the trichome density in the red variety was greater only on the abaxial side when plants grew under HL growth irradiance. In contrast, in the green variety trichome density was greater only on the adaxial side when plants were grown under HL growth irradiance. Furthermore, both varieties

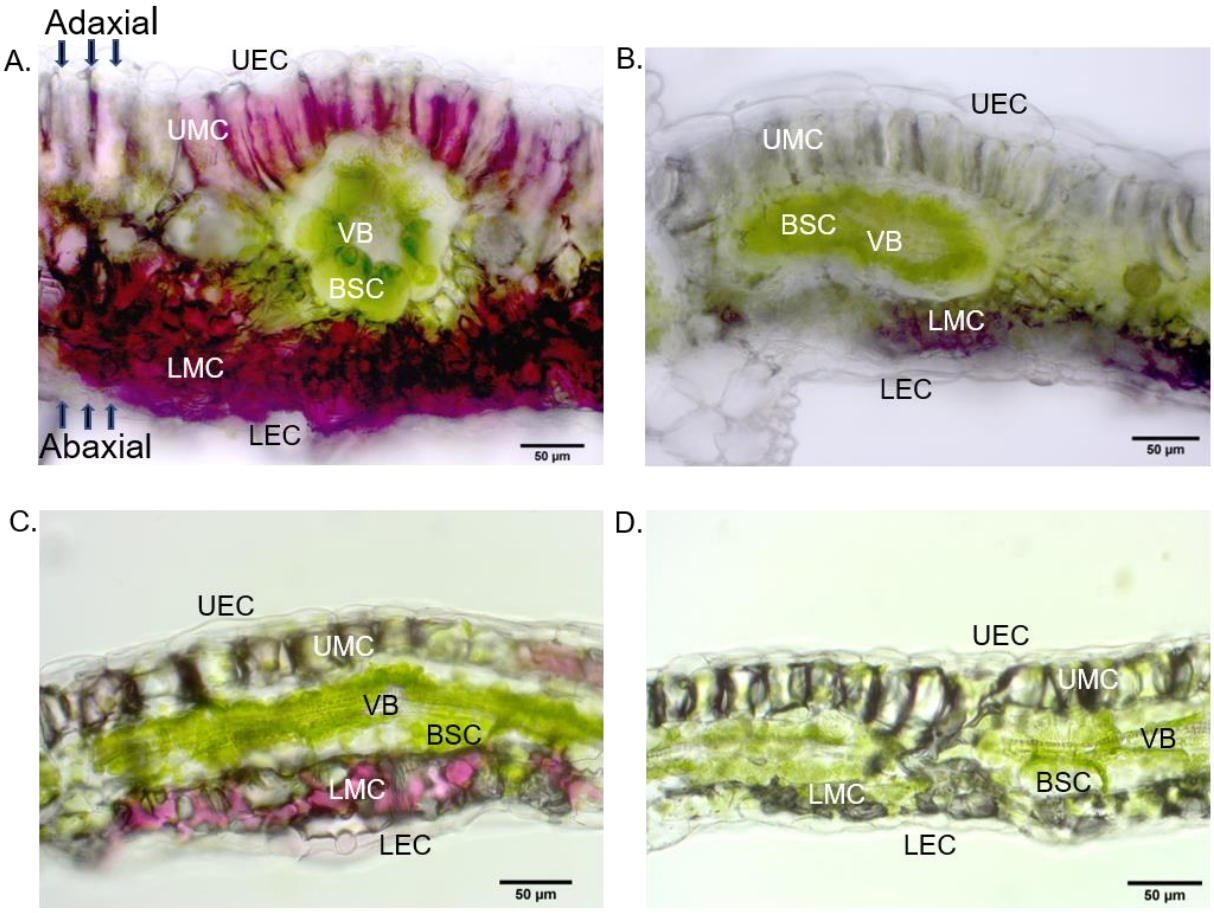

Figure 4.7 Transverse and longitudinal sections from leaves of *Amaranthus* plants showing betalain accumulation and localization. The red (**A., C.**) and green (**B., D.**) varieties of *Amaranthus* were grown under HL (**A., B.**) and LL (**C., D.**). The fourth leaves were sampled and freehand sections obtained with a razor blade, mounted in deionized water and observed under a light microscope. Transverse sections are shown for HL material (**A., B.**) and longitudinal sections for LL material (**C., D.**). Scale bars indicate 50 µm. Representative images are shown. BSC, bundle sheath cell; HL, high light; LEC, lower epidermal cell; LL, low light; LMC, lower mesophyll cell; UEC, upper epidermal cell; UMC, upper mesophyll cell; VB, vascular bundle.

Table 4.5 Leaf stomatal index and trichome density for red and green varieties of *Amaranthus.* Leaf imprints were obtained from fourth leaves of plants grown under HL and LL and used for the calculation of the stomatal index and trichome density. Values followed by uppercase letters in each column and lowercase letters in each row indicate a significant difference at $P = 0.05$ using a Holm-Sidak post-hoc test. Values represent means ± SE ($n = 3$ leaves, each consisting of 5 fields of view). HL, high light; LL, low light; SE, standard error.

Parameters and Localization	Growth Irradiance and Variety			
	HL Red	HL Green	LL Red	LL Green
Stomatal Index (%)				
Adaxial	16.41 ± 1.10^{aB}	12.54 ± 1.19^{bB}	16.24 ± 0.11^{aA}	6.03 ± 0.64^{cB}
Abaxial	22.60 ± 0.28^{aA}	22.45 ± 0.91^{aA}	15.98 ± 2.00^{cA}	19.11 ± 1.04^{bA}
Trichome Density (#/mm^2)				
Adaxial	1.55 ± 0.12^{bB}	2.92 ± 0.33^{aA}	1.43 ± 0.12^{bA}	1.83 ± 0.14^{bA}
Abaxial	2.70 ± 0.21^{aA}	1.43 ± 0.09^{bB}	1.29 ± 0.05^{bA}	1.21 ± 0.02^{bB}

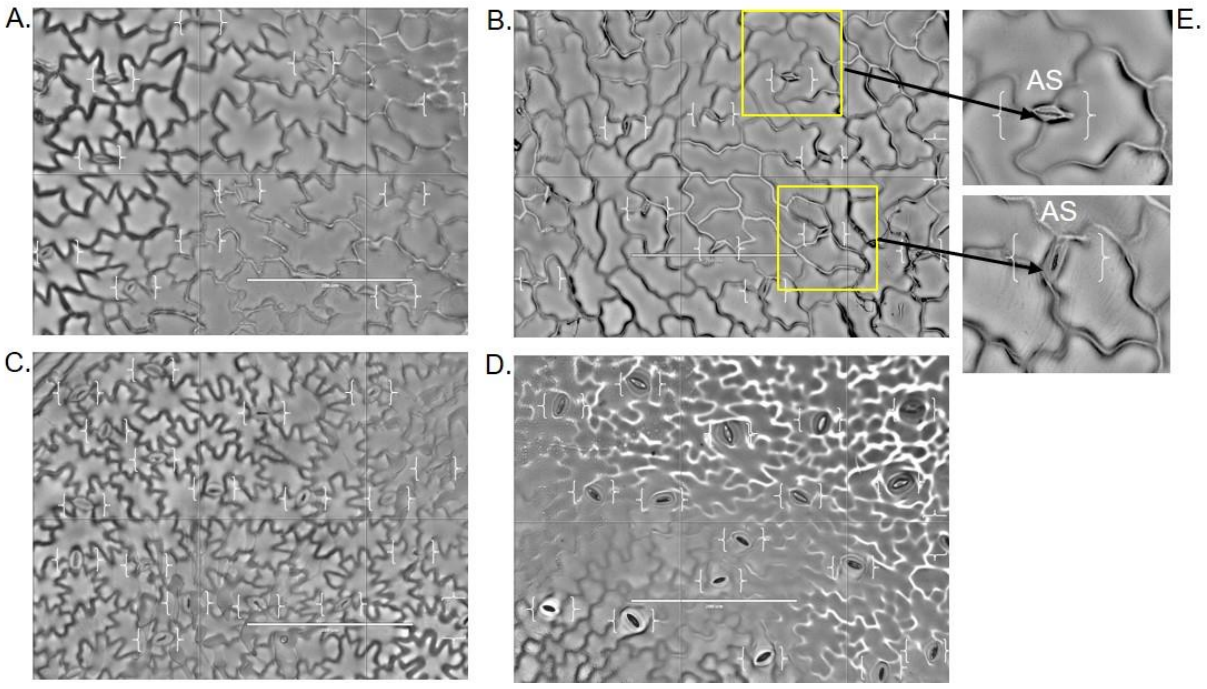

Figure 4.8 Distribution of stomata for *Amaranthus* grown under HL. Fourth leaves of the red (**A., C.**) and green (**B., D.**) varieties were analyzed on the adaxial (**A., B.**) and abaxial (**C., D.**) leaf surfaces. The insert (**E.**) shows a close up of the anomocytic stomatal complex. Scale bars indicate 200 µm. Representative images are shown. AS, anomocytic stomata; HL, high light; LL, Low light. Results under LL growth irradiance are presented in Fig. A1.

.

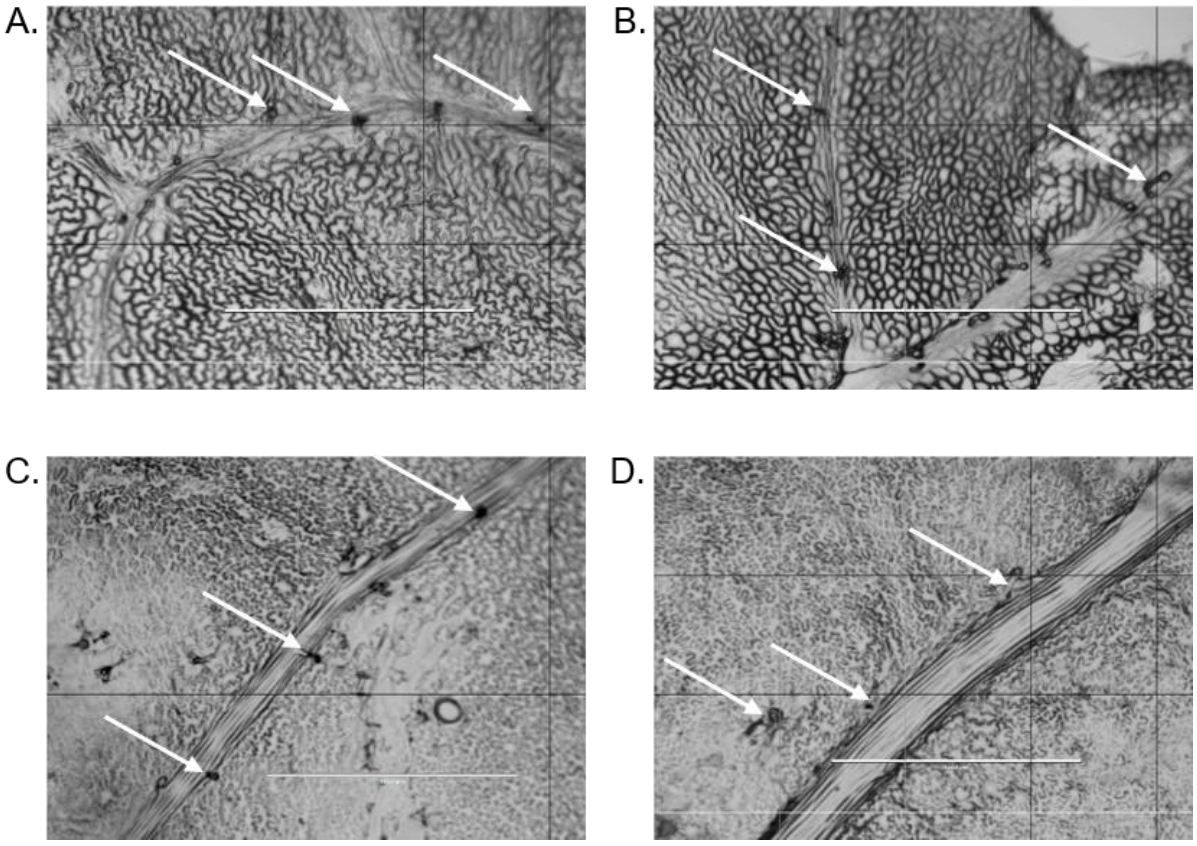

Figure 4.9 Distribution of trichomes for *Amaranthus* grown under HL. Fourth leaves of the red (**A., C.**) and green (**B., D.**) varieties were analyzed from imprints taken on the adaxial (**A., B.**) and abaxial (**C., D.**) leaf surfaces. Trichomes are indicated by arrows. Scale bars indicate 1 mm. Representative images are shown. HL, high light; LL, Low light. Results under LL growth irradiance are presented in Fig. A2.

possess short and tall glandular trichomes that are multicellular and uniseriate (Fig. 4.10, Fig. A3).

4.5.2 Leaf Structure

The images from Fig. 4.11 illustrate that both varieties exhibited features typical of NAD-ME type C4 dicot plants, with the BSC containing numerous chloroplasts in the centripetal position around the vascular bundle (VB). Based on transverse leaf sections, both varieties possessed a differentiation of mesophyll tissue in the palisade parenchyma (UMC or referred to as adaxial mesophyll layer) and spongy parenchyma (LMC or referred to as abaxial mesophyll layer), indicating increased intercellular space when compared with UMC.

Under HL, both varieties exhibited greater area of all cell types than at LL growth irradiance, with the exception of UMC areas in the green variety, which were similar. BSC areas in red and green varieties were 1.8- and 1.9-fold greater under HL than under LL, respectively (Table 4.6). Under HL, UMC area in the red variety was 1.7-fold greater than in the green variety. The UMC area in the red variety was 1.9- fold greater under HL than under LL. Under HL, LMC area in the red variety was 1.9-fold greater than in the green variety. The LMC in the red variety under HL was 2.8-fold greater than under LL growth irradiance. Under HL an increased LEC area was found in both varieties with a greater area in the red variety than the green variety. Overall, all these area increases of different cell types in the red over the green variety contributed to a slightly greater LT in the red than in the green. In contrast, under LL both varieties exhibited similar area of all cell types, which also resulted in a similar LT (Table 4.6; Fig. 4.11).

Distribution of the number of BSC around the VB was similar between varieties under HL and also between varieties under LL growth irradiance (Table 4.7). However, with respect to the growth irradiance, the red and green varieties had about a 1.4-fold greater number of BSC around the VB under HL than under LL growth irradiance (Table 4.7).

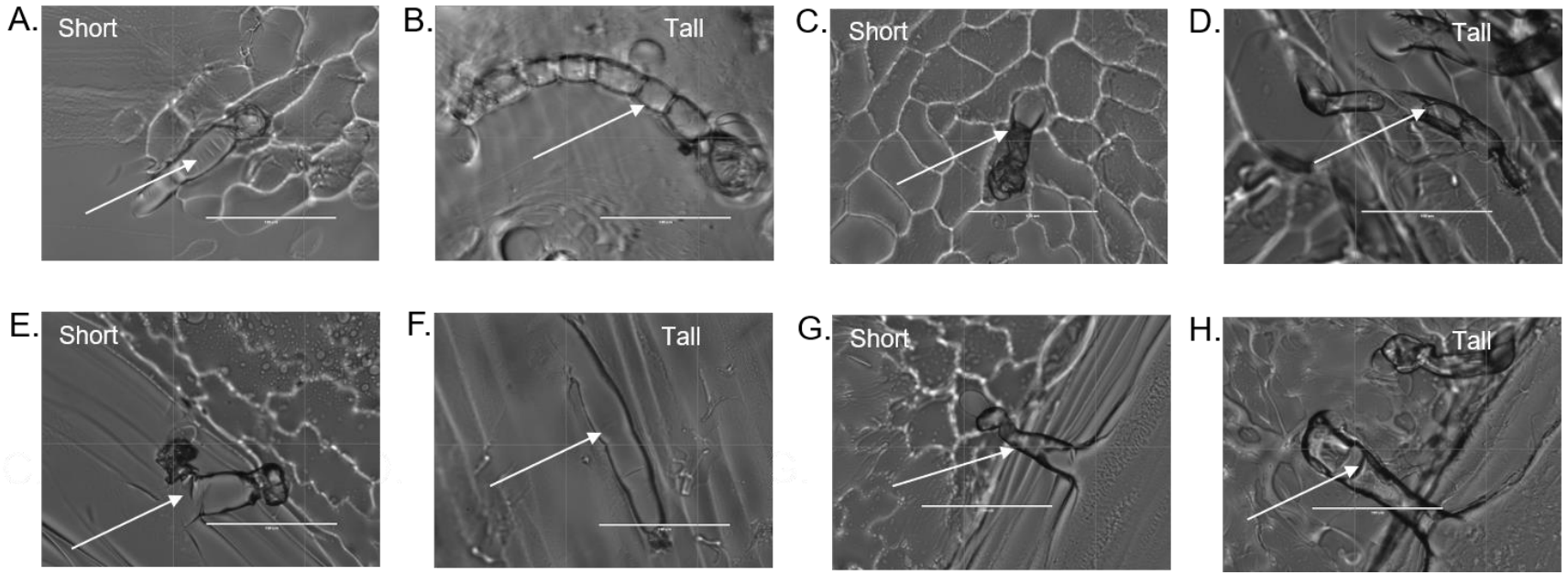

Figure 4.10 Short and tall, multicellular and uniseriate, glandular trichomes for *Amaranthus* grown under HL. Fourth leaves of the red (**A., B., E., F.**) and green (**C., D., G., H.**) varieties were analyzed from imprints taken on the adaxial (**A., B., C., D.**) and abaxial (**E., F., G., H.**) leaf surfaces. Trichomes are indicated by arrows. Scale bars indicate 100 µm. Representative images are shown. HL, high light; LL, Low Light. Results under LL growth irradiance are presented in Fig. A3.

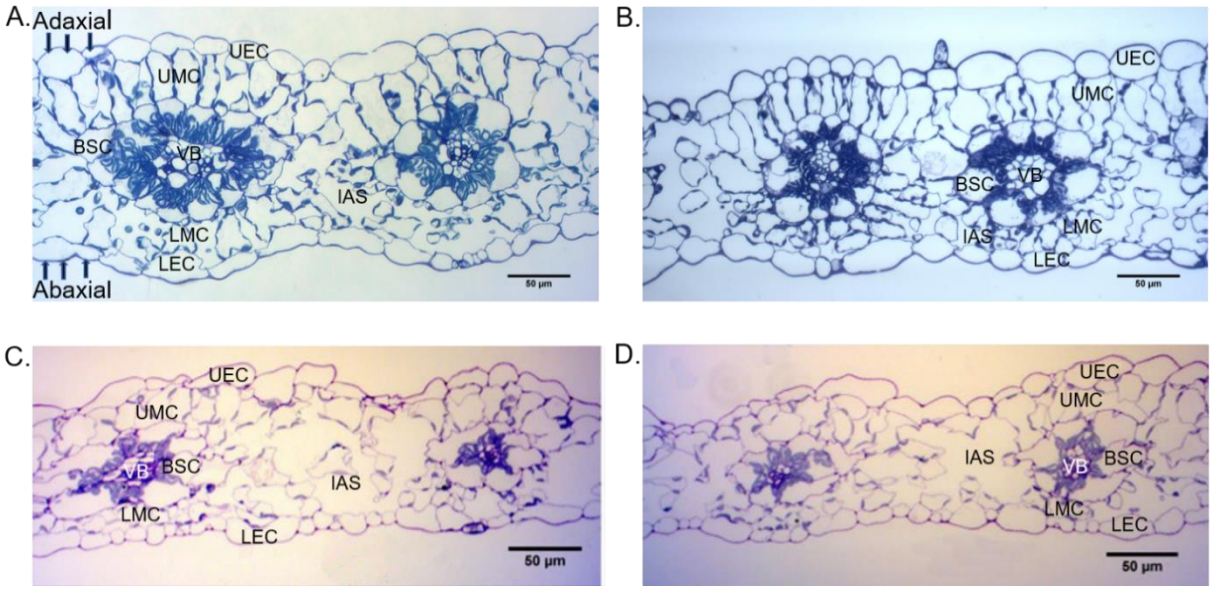

Figure 4.11 Transverse sections of fourth leaves from *Amaranthus.* The red (**A., C.**) and green (**B., D.**) varieties of *Amaranthus* were grown under HL (**A., B.**) and LL (**C., D.**). Scale bars indicate 50 µm. Representative TBO staining images are shown. BSC, bundle sheath cell; HL, high light; IAC, intercellular air space; LEC, lower epidermal cell; LL, low light; LMC, lower mesophyll cell; TBO; Toluidine blue O; UEC, upper epidermal cell, UMC, upper mesophyll cell; VB, vascular bundle.

Table 4.6 Average area of different cell types measured from transverse sectioned fourth leaves of the red and green varieties of *Amaranthus* grown under HL and LL. Values represent means ± SE (*n* = 3 leaves). One transverse section containing 2 vascular bundles (VB) was obtained for each leaf. Values followed by different letters in each row indicate a significant difference at *P* = 0.05 using a Holm-Sidak post-hoc test. BSC, bundle sheath cell; HL, high light; IAS, intercellular air space; LEC, lower epidermal cell; LL, low light; LMC, lower mesophyll cell; LT, leaf thickness; SE, standard error; UEC, upper epidermal cell; UMC, upper mesophyll cell.

Cell Type	Growth Irradiance and Variety/ Cell Area (μm^2)			
	HL Red	HL Green	LL Red	LL Green
UEC	515.94 ± 23.37^a	448.71 ± 36.26^a	256.87 ± 66.62^b	313.79 ± 27.52^b
LEC	477.23 ± 30.29^a	392.95 ± 29.07^b	229.72 ± 12.41^c	182.92 ± 28.77^c
UMC	590.35 ± 91.68^a	350.11 ± 29.72^b	311.43 ± 32.03^b	315.88 ±14.41^b
LMC	356.79 ± 70.75^a	185.48 ± 2.66^b	127.08 ± 6.27^c	106.94 ± 7.74^c
BSC	705.35 ± 10.27^a	668.43 ± 70.90^a	399.00 ± 35.28^b	358.98 ± 34.14^b
VB	1340.37 ± 221.37^a	867 20 ± 47.42^b	389.00 ± 29.75^c	234.85 ± 14.42^c
IAS (%)	18.38 ± 2.87^b	19.28 ± 1.47^b	26.33 ± 2.68^a	28.88 ± 1.00^a
LT (μm)	175.07 ± 1.77^a	164.42 ± 4.26^b	100.94 ± 4.19^c	102.25 ±1.03^c

4.5.3 Cellular Organelles

4.5.3.1 Chloroplasts

Distribution of number of chloroplasts per profile of a BSC in section under HL was 1.5- and 2.0-fold higher in red and green varieties than under the LL growth irradiance. Under HL, both varieties had similar numbers. In contrast, under LL growth irradiance, the red variety possessed 1.3-fold higher number of chloroplasts per BSC profile in section than the green variety (Table 4.7; Fig. 4.12). Moreover, it was observed that the shape of chloroplasts per BSC profile in section was also diverse between varieties under HL growth irradiance. The red variety appears to have longer chloroplasts than the green variety (Fig. 4.12; Table A5).

The area of BSC chloroplasts increased by about 40% in the red variety under HL growth irradiance compared to the other treatments and varieties. In contrast, the area of MC chloroplasts was different only in the green variety at HL, with an approximately 50% decrease than the other treatments and varieties (Table 4.8; Fig. 4.13).

4.5.3.2 Mitochondria

The area of mitochondria among the treatments, varieties and cell type was similar with the only difference observed in MC of the red variety under LL growth irradiance with an approximately 45% decrease than the other treatments and varieties (Table 4.8; Fig. 4.13).

4.5.3.3 Peroxisomes

The increased appearance of peroxisomes was observed only in the BSC of the green variety under either growth irradiance (Table.4.8; Fig. 4.14.). Their distribution varied from 1 to 6 peroxisomes per field of view under either growth irradiance. The results illustrated that area of peroxisomes was similar among the growth irradiance (Table 4.8; Fig. 4.14).

Table 4.7 Profiles of BSC in fourth leaves of the red and green varieties of *Amaranthus* grown under HL and LL. Values represent means ± SE (*n* = 3 leaves). One transverse section containing 2 vascular bundles (VB) was obtained for each leaf. Values followed by different letters in each row indicate a significant difference at *P* = 0.05 using a Holm-Sidak post-hoc test. BSC, bundle sheath cell; C; chloroplast; HL, high light; LL, low light; SE, standard error.

Parameter	Growth Irradiance and Variety			
	HL Red	HL Green	LL Red	LL Green
# BSC/VB	10.50 ± 0.58[a]	9.00 ± 0.01[a]	7.50 ± 0.01[b]	7.00 ± 0.29[b]
# C/BSC	14.60 ± 0.44[a]	14.93 ± 0.41[a]	9.53 ± 0.55[b]	7.50 ± 0.32[c]

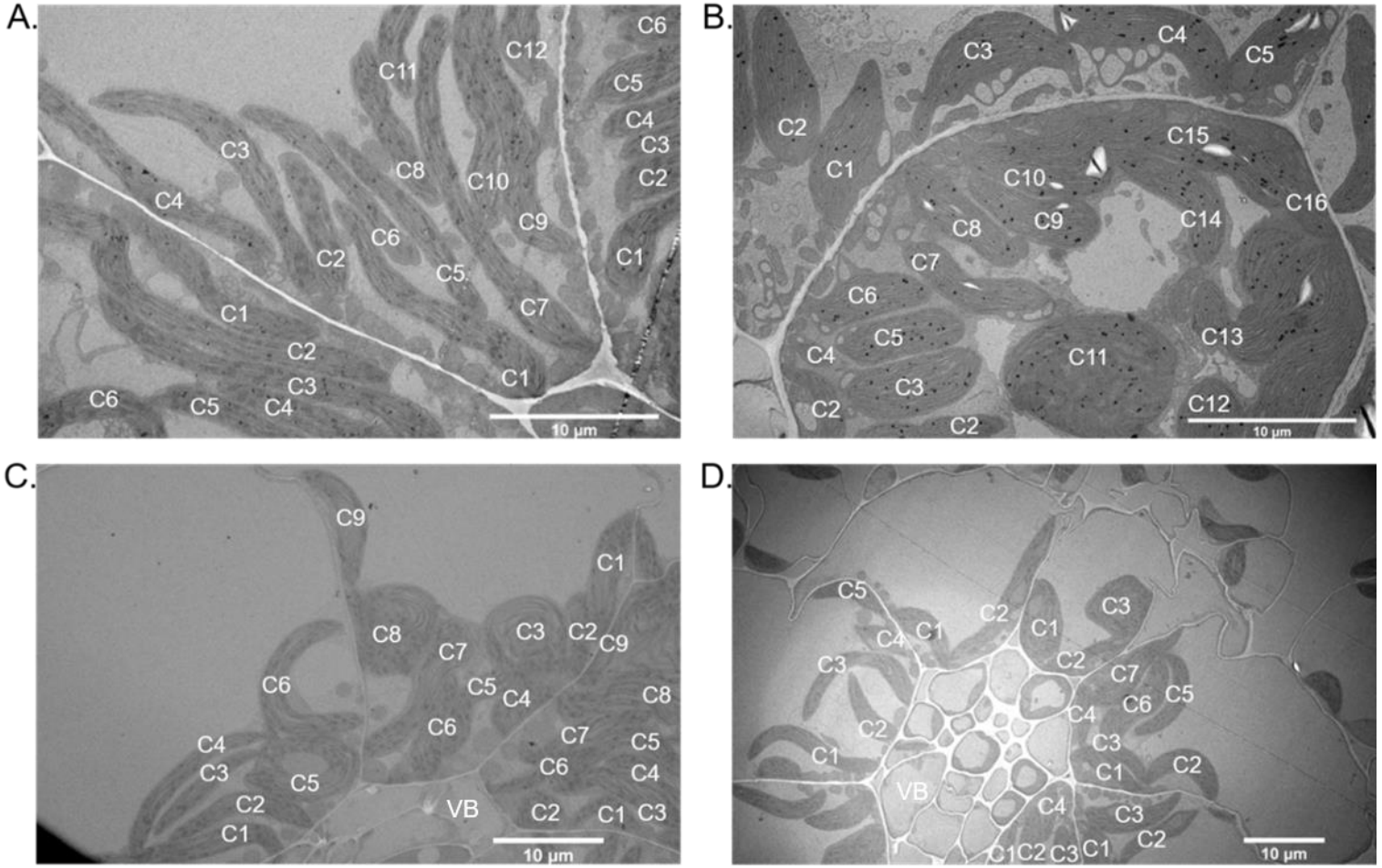

Figure 4.12 Distribution of chloroplasts (C) from profiles of BSC in sections of fourth leaves of *Amaranthus* grown under HL (**A., B.**) and LL (**C., D.**). Number of chloroplasts present are numerated as C1 to Cn of the red (**A., C.**) and green (**B., D.**) varieties. Scale bars indicate 10 µm. Representative images are shown. BSC, bundle sheath cell; HL, high light; LL, low light; VB, vascular bundle.

Table 4.8 Area of chloroplasts, mitochondria and peroxisomes from profiles of BSC and MC. Sections were obtained from the fourth leaves of the red and green varieties of *Amaranthus* grown under HL and LL. Values represent means ± SD (*n* = 7 to 54 organells obtained from multiple fields of view). Values followed by different letters in each row indicate a significant difference at *P* = 0.05 using a Holm-Sidak post-hoc test. BSC, bundle sheath cell; HL, high light; LL, low light; MC, mesophyll cell; nd, not determined; SD, standard deviation.

Organelle and Cell Type	Organelle Area (μm^2)			
	Growth Irradiance and Variety			
	HL Red	HL Green	LL Red	LL Green
Chloroplasts				
BSC	33.86 ± 17.10[a]	20.36 ± 8.59[b]	21.26 ± 9.30[b]	21.38 ± 7.19[b]
MC	12.41 ± 2.82[a]	6.06 ± 2.86[b]	13.05 ± 4.45[a]	10.88 ± 4.90[a]
Mitochondria				
BSC	0.94 ± 0.65[a]	0.86 ± 0.64[a]	1.23 ± 0.92[a]	1.34 ± 1.15[a]
MC	0.50 ± 0.30[a]	0.62 ± 0.35[a]	0.28 ± 0.16[b]	0.48 ± 0.31[a]
Peroxisomes				
BSC	nd	0.70 ± 0.51[a]	nd	1.02 ± 0.92[a]

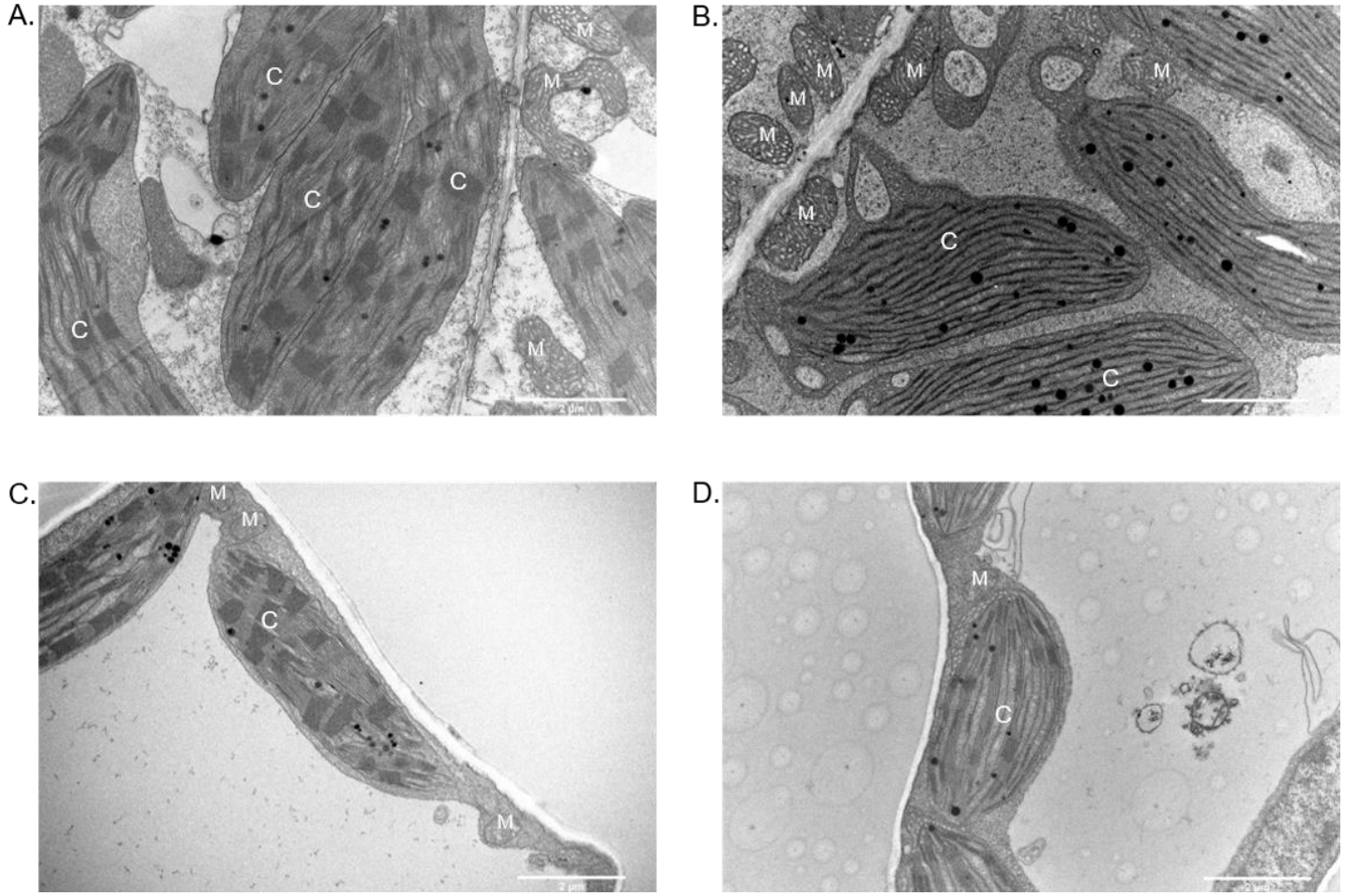

Figure 4.13 Ultrastructure of cells in leaves of *Amaranthus* grown under HL. Fourth leaf sections of the red (**A., C.**) and green (**B., D.**) varieties were analyzed from profiles of BSC (**A., B.**) and MC (**C., D.**). Scale bars indicate 2 µm. Representative images are shown. BSC, bundle sheath cell; C; chloroplast; HL, high light; LL, low light; MC, mesophyll cell; M, mitochondrion. Results under LL growth irradiance are presented in Fig. A4.

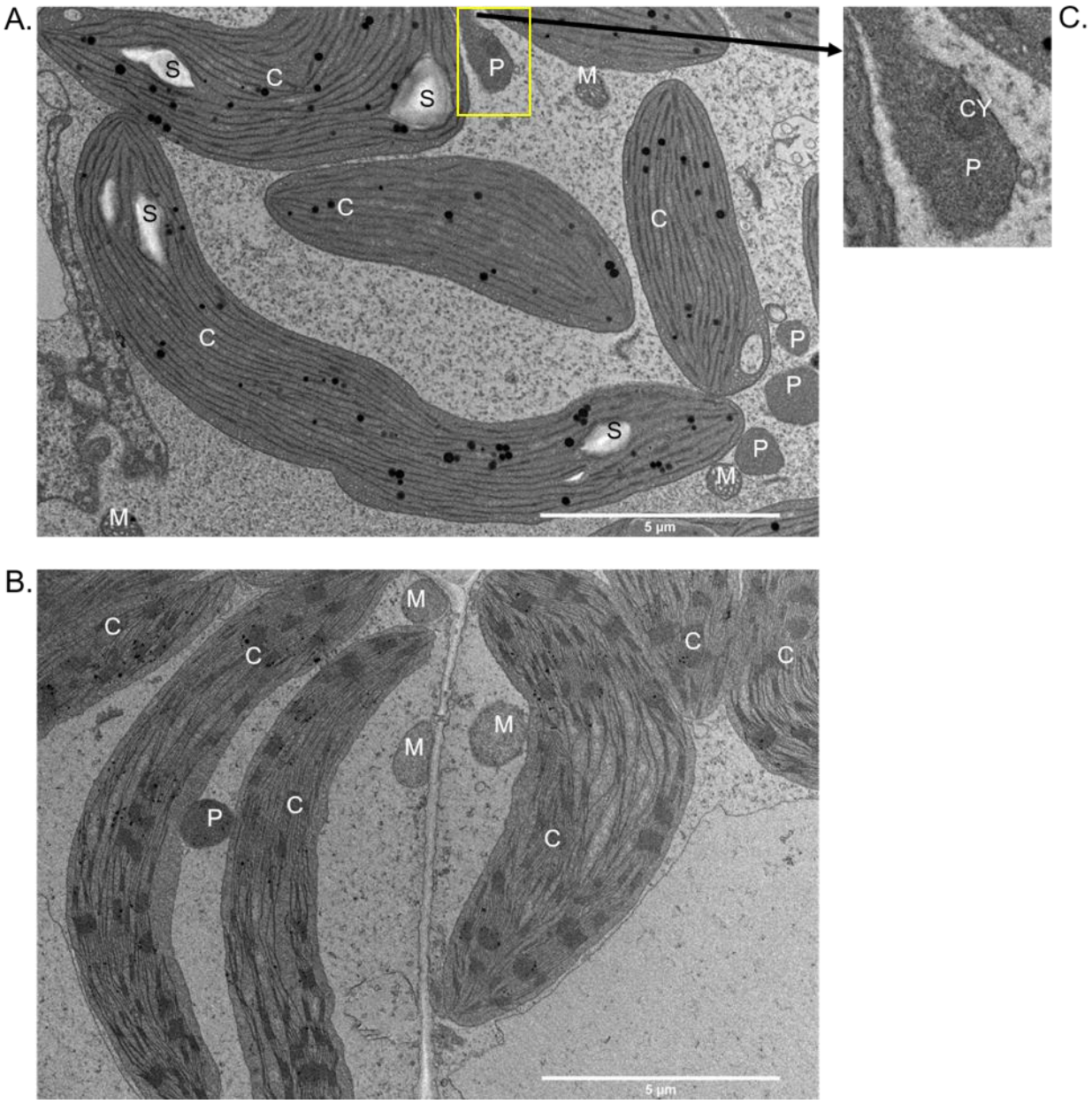

Figure 4.14 Distribution of peroxisomes (P), mitochondria (M) and chloroplasts (C) in profiles of BSC. Sections were obtained from the fourth leaves of the green variety of *Amaranthus* grown under HL (**A.**) and LL (**B.**). The insert (**C.**) shows a close up of the crystalline core (CY). Scale bars indicate 5 µm. Representative images are shown. BSC, bundle sheath cell; HL, high light; LL, low light; S, starch granule.

4.6 Chloroplast Ultrastructure

4.6.1 Thylakoid Membranes

The ultrastructural quantitative parameters of the chloroplasts are shown in Table 4.9 and Table A6 as well as the representative images shown in Fig. 4.15 and Fig. A5. The GI for BSC of the red variety under HL was 2-fold higher than that of its green counterpart (Table 4.9). There were essentially no changes in GI between varieties for BSC or MC under LL growth irradiance or MC under HL growth irradiance (Table 4.9). For the green variety, the GI was greater under LL conditions for both BSC and MC. This trend was also observed for MC in the red variety with the exception that the GI in BSC was greater under HL (Table 4.9).

Overall, minimal differences were observed between varieties and treatments for appressed, non-appressed and total thylakoid densities (Table 4.9). The exception was the green variety grown under HL that showed a significant decrease in appressed thylakoid density in the BSC (Table 4.9). Generally, the trend indicated these values were higher in MC compared to BSC (Table 4.9).

Under HL growth irradiance, the red variety showed a 3.1-fold increase in the ratio of appressed/non-appressed thylakoids for BSC in comparison to the green variety. No varietal difference was observed under HL for MC (Table 4.9). Overall, HL growth irradiance resulted in lower ratios with the exception of HL red which increased 1.5-fold compared to LL red. No difference was observed between varieties for BSC or MC when grown under LL (Table 4.9).

Thylakoids/granum in BSC and MC were significantly greater in the red variety compared to the green variety under HL (Table 4.9). Under LL, there was no difference in the BSC but the red variety showed an increase in the MC compared to the green variety. In the BSC, HL induced an increase in thylakoids/granum compared to LL for the red variety and a decrease for the green variety. In contrast, both varieties demonstrated decreases in this parameter for MC when grown under HL compared to LL (Table 4.9).

Table 4.9 Ultrastructural quantitative parameters of chloroplasts from profiles of BSC and MC. Sections were obtained from the fourth leaves of the red and green varieties of *Amaranthus* grown under HL and LL. Values followed by different letters in each row indicate a significant difference at $P = 0.05$ using a Holm-Sidak post-hoc test. Values represent means ± SD (n = 4 to 6 chloroplasts). BSC, bundle sheath cells; HL, high light; LL, low light; MC, mesophyll cells; SD, standard deviation.

Parameters and Cell Type	Growth Irradiance and Variety			
	HL Red	HL Green	LL Red	LL Green
Granal Index (%)				
BSC	52.62 ± 6.33[a]	26.22 ± 2.46[c]	42.29 ± 7.93[b]	46.40 ± 7.59[b]
MC	39.77 ± 5.82[a]	33.20 ± 6.64[a]	48.02 ± 4.97[ab]	48.55 ± 8.32[b]
Appressed Thylakoid Density (µm/µm^2)				
BSC	15.24 ± 2.93[a]	8.27 ± 1.77[b]	14.02 ± 4.87[a]	16.64 ± 6.08[a]
MC	20.56 ± 9.62[a]	20.38 ± 7.56[a]	24.37 ± 6.96[a]	29.61 ± 7.39[a]
Non-Appressed Thylakoid Density (µm/µm^2)				
BSC	13.83 ± 3.31[a]	22.49 ± 3.33[a]	19.35 ± 6.90[a]	19.46 ± 6.45[a]
MC	31.73 ± 13.63[a]	40.36 ± 9.12[a]	25.77 ± 3.30[a]	31.28 ± 6.49[a]
Total Thylakoid Density (µm/µm^2)				
BSC	29.07 ± 5.01[a]	30.53 ± 4.71[a]	33.37 ± 10.55[a]	36.10 ± 10.80[a]
MC	52.29 ± 22.64[a]	60.73 ± 13.93[a]	50.14 ± 9.42[a]	60.90 ± 9.13[a]
Thylakoids/Granum				
BSC	9.17 ± 2.67[a]	4.08 ± 1.21[c]	6.52 ± 1.11[b]	6.29 ± 0.61[b]
MC	7.44 ± 2.22[a]	4.78 ± 0.56[c]	9.13 ± 1.74[a]	6.95 ± 1.39[b]
Appressed/Non-Appressed Thylakoids				
BSC	1.14 ± 0.28[a]	0.37 ± 0.03[c]	0.76 ± 0.27[b]	0.90 ± 0.27[b]
MC	0.67 ± 0.16[b]	0.51 ± 0.15[b]	0.94 ± 0.21[ab]	0.98 ± 0.30[a]

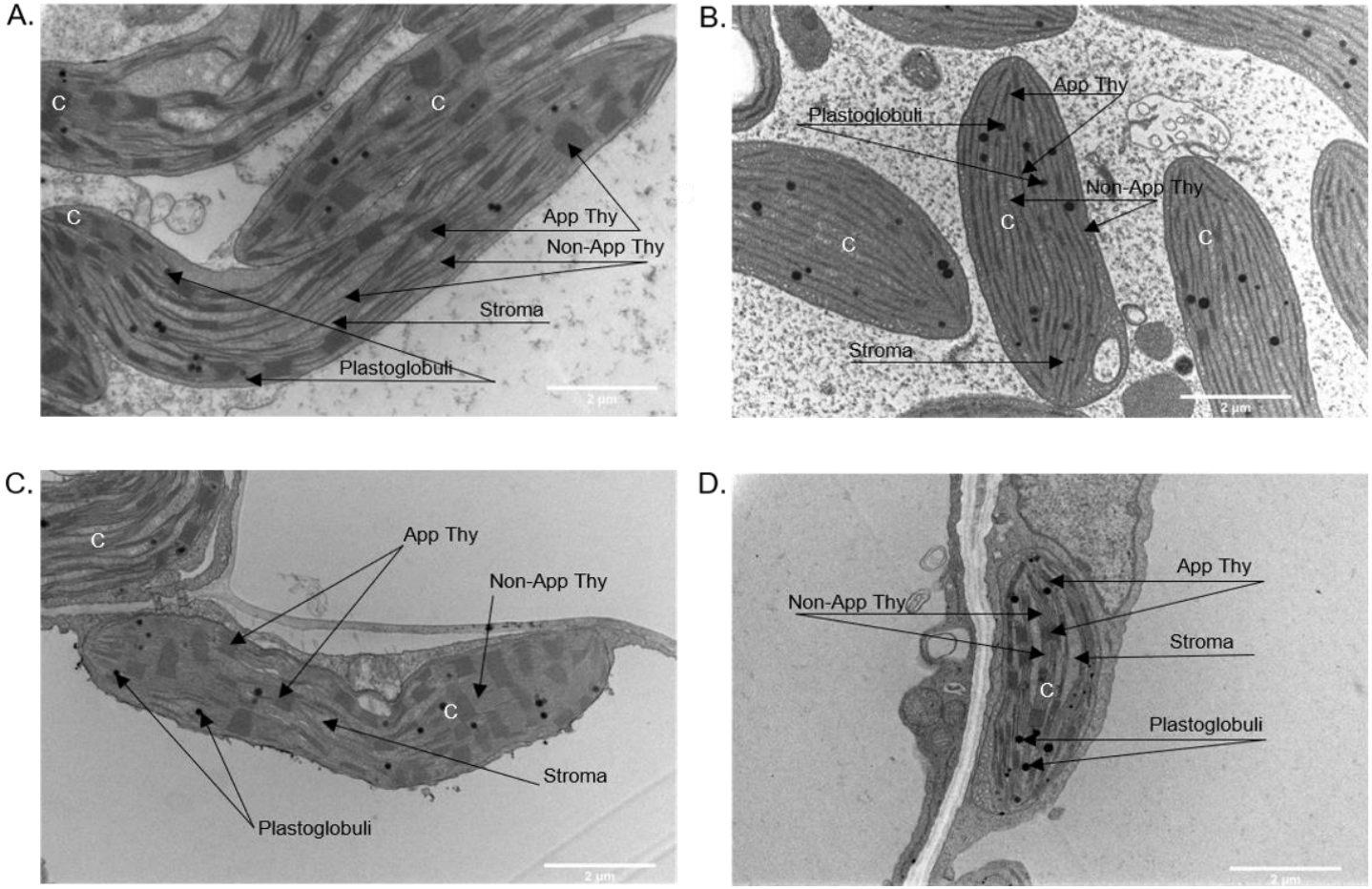

Figure 4.15 Chloroplast ultrastructure of cells in leaves of *Amaranthus* grown under HL. Sections from fourth leaves of the red (**A., C.**) and green (**B., D.**) varieties were analyzed from profiles of BSC (**A., B.**) and MC (**C., D.**). Scale bars indicate 2 µm. Representative images are shown. App Thy, appressed thylakoids; C, chloroplast; BSC, bundle sheath cell; HL, high light; LL, low light; MC, mesophyll cell; Non-App, non-appressed thylakoids. Results under LL growth irradiance are presented in Fig. A5.

4.6.2 Chloroplast Features

4.6.2.1 Peripheral Reticulum

The peripheral reticulum (PR) type I and type II was found only in the green variety in the chloroplasts of BSC, MC, VPC and CC under HL (Fig. 4.16) and LL growth irradiance (Fig. 4.17). The images from the MC under LL conditions illustrated that the PR type II was more expressed than the type I. However, there was no difference in the area of these features among the growth irradiance (Table A6).

4.6.2.2 Cytoplasmic Protrusions

It was also observed that the green variety possessed structures that are best described as CP under HL (Fig. 4.16) and LL conditions (Fig. 4.17). The area of these features is combined with the area of PR, as their areas are difficult to differentiate accurately based on the resolution of the micrographs. Overall, there was no difference in the area of these features either between the cell type neither between the growth irradiance (Table A6).

4.6.2.3 Crystalline Inclusions

Crystalline inclusions (CI) were observed in the chloroplasts of the green variety. Under HL, few CI were observed but only in the BSC. However, under LL growth irradiance, many CI were observed in the BSC, and fewer were observed in the MC (Fig. 4.18). However, the CI/chloroplast area ratio did not detect any significant difference with respect to the growth irradiance (Table 4.10).

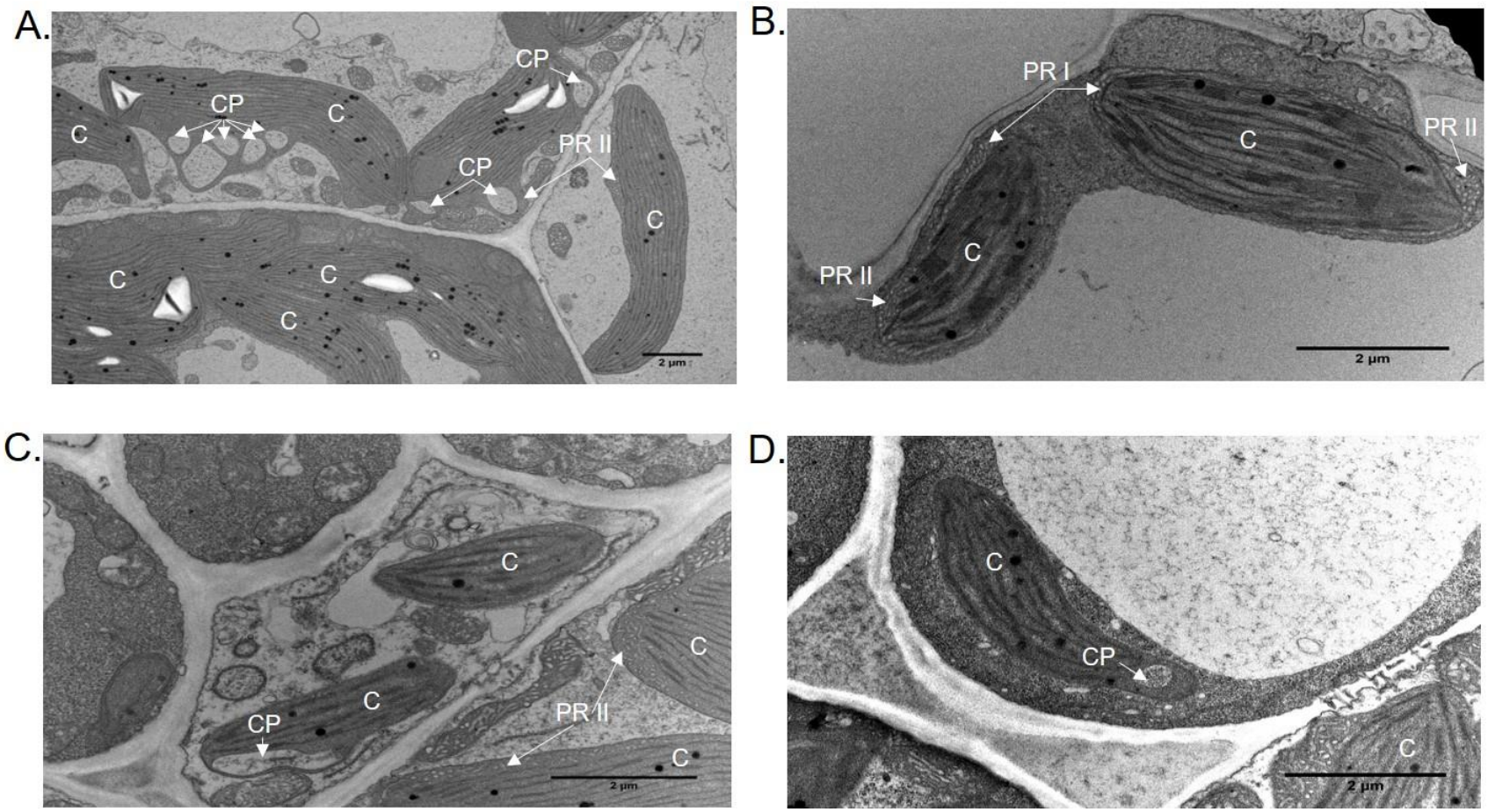

Figure 4.16 Peripheral reticulum type I (PRI) and type II (PR II) in chloroplasts and cytoplasmic protrusions (CP) of *Amaranthus* grown under HL. Chloroplasts were analyzed from profiles of BSC **(A.),** MC **(B.),** VPC **(C.)** and CC **(D.)** in sections from the fourth leaves of the green variety. Scale bars indicate 2 µm. Representative images are shown. C, chloroplast; BSC, bundle sheath cell; CC, companion cell; HL, high light; MC, mesophyll cell; VPC, vascular parenchyma cell.

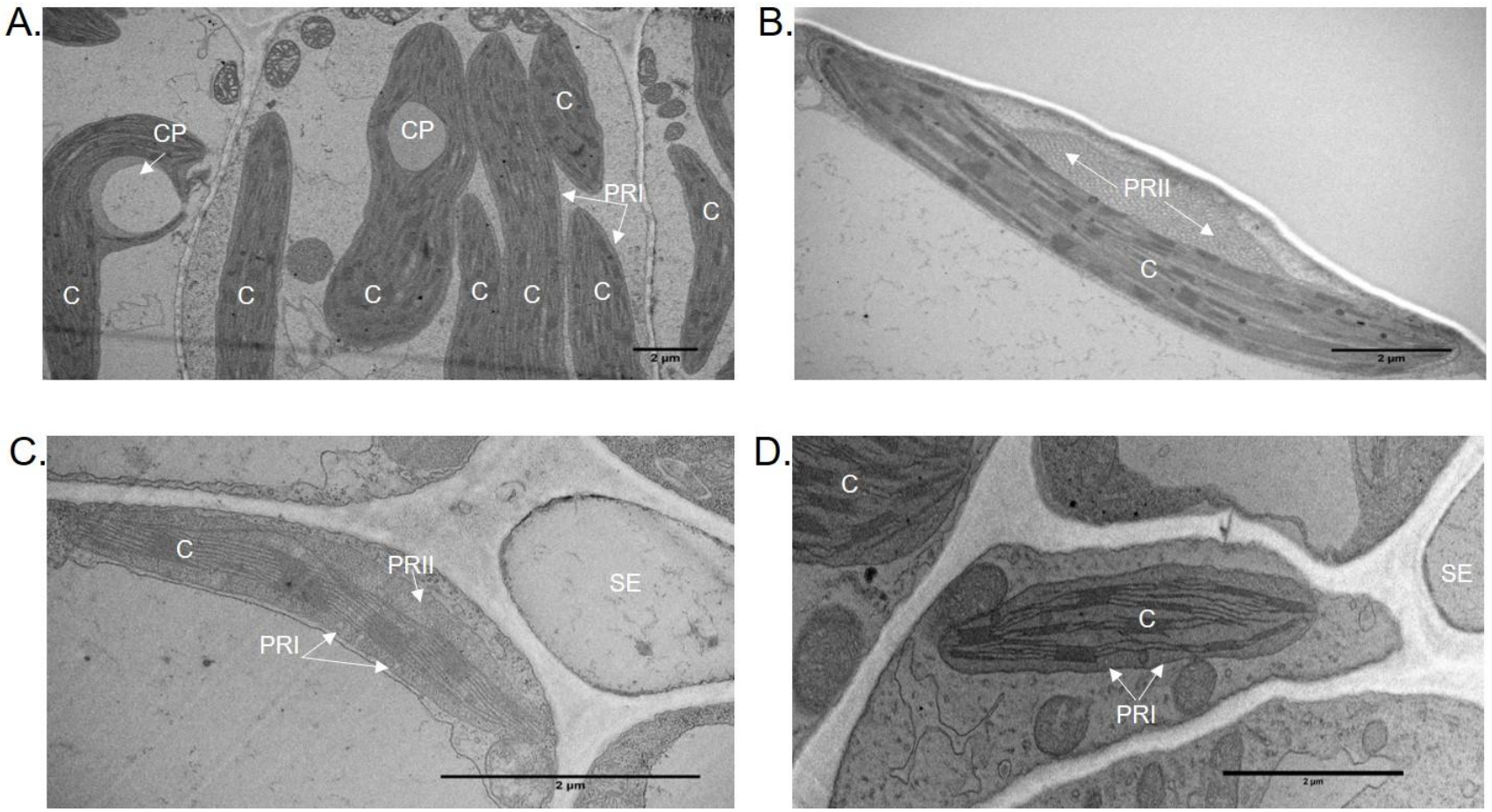

Figure 4.17 Peripheral reticulum type I (PRI) and type II (PR II) in chloroplasts and cytoplasmic protrusions (CP) of *Amaranthus* grown under LL. Chloroplasts were analyzed from profiles of BSC **(A.),** MC **(B.),** VPC **(C.)** and CC **(D.)** in sections from the fourth leaves of the green variety. Scale bars indicate 2 µm. Representative images are shown. C, chloroplast; BSC, bundle sheath cell; CC, companion cell; HL, high light; MC, mesophyll cell; VPC, vascular parenchyma cell.

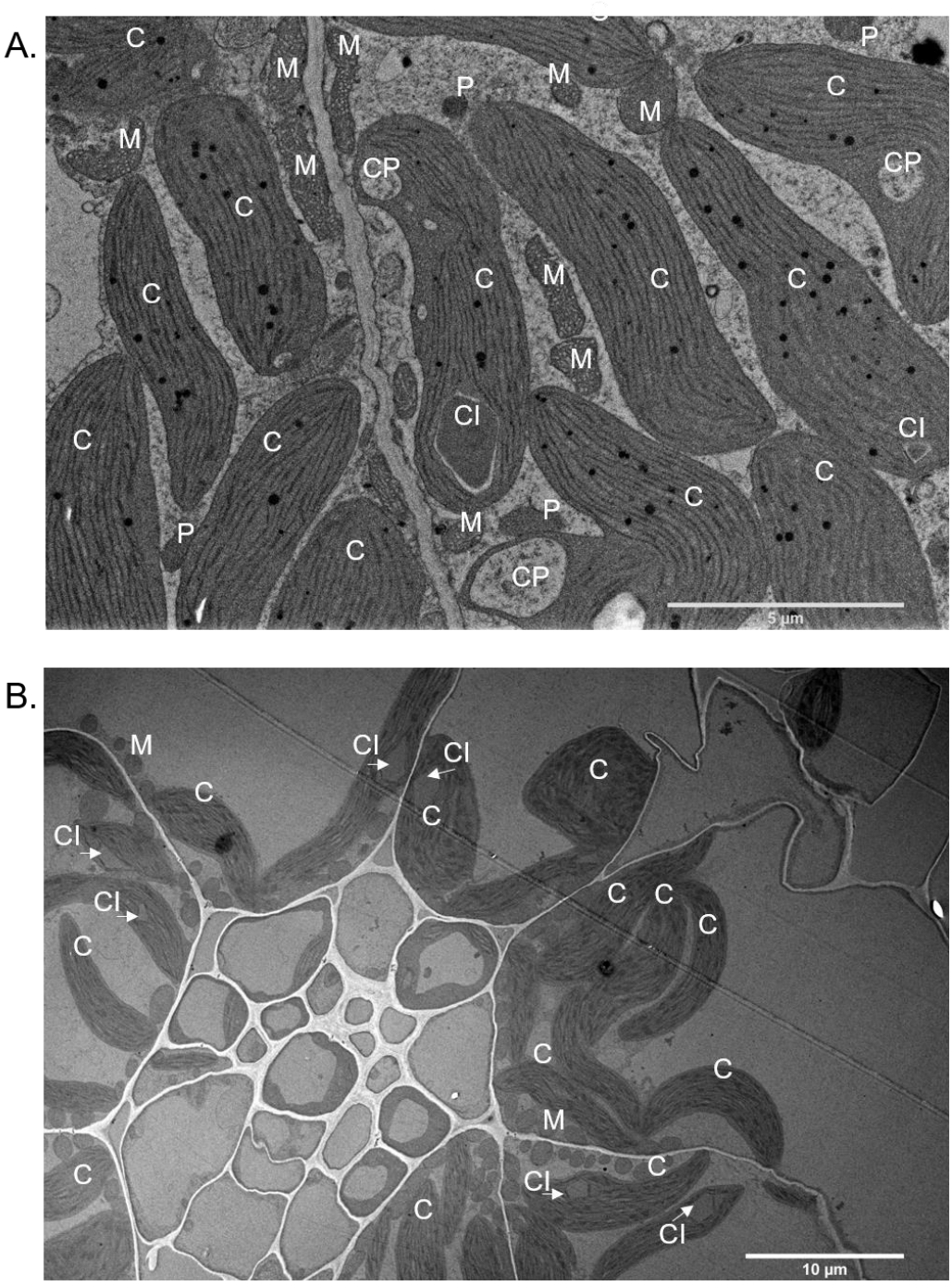

Figure 4.18 Distribution of crystalline inclusions (CI) from profiles of BSC. Sections were obtained from fourth leaves of the green variety of *Amaranthus* grown under HL (**A.**) and LL (**B.**). Scale bars indicate 5 µm at HL and 10 µm at LL. Representative images are shown. BSC, bundle sheath cell; C, chloroplast; CP, cytoplasmic protrusion; HL, high light; LL, low light; M, mitochondrion; P, peroxisome.

Table 4.10 Area of crystalline inclusions (CI) from profiles of BSC. Sections were obtained from the fourth leaves of the red and green varieties of *Amaranthus* grown under HL and LL. Values represent means ± SD (*n* = 3 to 7 chloroplasts). Values followed by different letters in each column indicate a significant difference at *P* = 0.05 using a Holm-Sidak post-hoc test. BSC, bundle sheath cell; C, chloroplasts; HL, high light; LL, low light; SD, standard deviation.

Growth Irradiance and Variety	Area C (μm^2)	Area CI (μm^2)	Area CI/C
HL Green BSC	22.24 ± 3.44[a]	1.70 ± 0.32[a]	0.08 ± 0.03[a]
LL Green BSC	31.18 ± 11.73[a]	2.21 ± 0.97[a]	0.07 ± 0.03[a]

CHAPTER 5

5.0 DISCUSSION

Excess irradiance has the potential to cause an imbalance between the light energy absorbed through photochemistry versus the energy utilized through metabolism. The balance of these processes is known as photostasis. Maintaining photostasis involves adjustments at the level of the source (energy supplied) and at the level of the sink (energy utilized) or both (Hüner *et al.*1998, 2003, Ensminger *et al.* 2006, Wilson *et al*. 2006, Biswal *et al.* 2011). The inability to restore photostasis will result in photoinhibition, defined as a light dependent decrease in quantum yield (Φ) and/or P_{max} (Krause 1988, Osmond 1994, Gray *et al.* 1996). The extent of photoinhibition is determined by the rate of photodamage of the PSII reaction center D1 protein and its repair (Takahashi and Badger 2011). Photoacclimation is the process in which plants respond to the prevailing environment to maximize photosynthesis under light-limiting conditions and photoprotection under conditions where light is excessive. Several regulatory and photoprotective strategies have evolved to ensure photoacclimation. A universal mechanism is that of NPQ, a complex process involving the dissipation of excitation energy as heat (Demming-Adams and Adams 1992, Horton and Ruban 2004). Changes at the morphological level are also involved in photoacclimation including increases in leaf area and thickness (Mishra *et al.* 2012), changes in cell tissue layers (epidermal, palisade mesophyll) (Kim *et al.* 2005) and SI and trichome density.

This thesis examines the photoacclimation responses to HL and LL growth irradiance in the red and green varieties of *Amaranthus blitum*. Important findings are grouped into three categories; photosynthetic responses to growth irradiance, a role for betalains in photoprotection, as well as anatomical and ultrastructural mechanisms of photoacclimation.

5.1. Photosynthetic Responses to Growth Irradiance

Growth and development of both red and green varieties under HL were markedly faster, resulting in a greater plant biomass accumulation than under LL growth

irradiance. This findinding has been reported previously for photoacclimation in many species (Boardman 1977, Givnish 1988). Under HL growth irradiance, the red variety grew faster, resulting in increased height and leaf count per plant than in the green variety; however, the fourth LA was greater in the green variety than in the red variety. Under LL growth irradiance, both varieties had a similar rate of growth.

In both varieties of *Amaranthus*, in plants grown under HL, the fourth leaf of the red and green varieties exhibited 2.2- and 4.1-fold greater LA, respectively than under LL. This was unexpected since it is generally recognized that the LA under LL are greater than in plants grown under HL growth irradiance (Björkman *et al.* 1981, Lichtenthaler 1981, Li *et al.* 2014). Leaf thickness (LT), as mentioned above are usually greater under HL growth irradiance (Björkman 1981). The red and green varieties exhibited significantly greater LT under HL compared to LL growth irradiance. Similar responses were illustrated in C4 grasses (Ward and Woolhouse 1986), *Phaseolus vulgaris* and *Zea maize* (Louwerse and Zweerde 1977). However, in *Amaranthus cruentus,* LT was not affected by the growth irradiance (Tazoe *et al.* 2006). The greater LT in the red and green varieties under HL was based on increased thickness (cells and intercellular air spaces) of the adaxial and abaxial mesophyll layer, as well as increased area of BSC, when compared to LL growth irradiance. Similar responses in several studies demonstrated that thicker HL leaves contain significantly more cells as compared to the thinner LL leaves (Louwerse and Zweerde 1977, Björkman 1981, Lichtenthaler 1981). This study suggests that under HL, the diffusion of CO_2 was increased and contributed to optimizing the rates of photosynthesis, a phenomenon well documented in other studies (Terashima *et al.* 2001, 2006, Evans *et al.* 2009, Niinemets *et al.* 2009).

Both red and green varieties under HL conditions exhibited higher $\Phi_{app}O_2$ than plants grown under LL. A similar trend of greater values of $\Phi_{app}CO_2$ under HL than under LL were previously reported in *Aeschynanthus longicaulis, Leptochloa fusca, Megathyrsus maximus, Panicum coloratum, Sorghum bicolor, Zea maize* (Li *et al.* 2014, Sonawane *et al.* 2018), with no differences observed in *Panax notoginseng* (Chen *et al.* 2016). In contrast, *Amaranthus cruenthus* had greater $\Phi_{app}CO_2$ values under LL (Tazoe *et al.* 2008), although it is generally accepted that C4 plants have less potential to

acclimate to low irradiance than C3 plants (Sage and McKown 2006). Similar to other studies, the $P_{max}O_2$ of photosynthesis was higher under HL with 81% (red variety) and 71% (green variety) when compared to LL growth irradiance. A similar trend for P_{max} under HL and LL were previously reported in *Spinacia oleracea* (Anderson and Osmond 1987), *Arabidopsis thaliana* (Walters and Horton 1994), *Amaranthus cruentus* (Tazoe *et al.* 2006), and *Flaveria bidentis* (Pengelly *et al*. 2010). In contrast, the opposite responses were reported in *Castanospermum australe* (Anderson and Osmond 1987) and in typical shade tolerant plants such as *Aeschynanthus longicaulis* (Li *et al.* 2014) and *Panax notoginseng* (Chen *et al.* 2016). Between varieties under HL, the red variety exhibited 35% and 52% greater values of $P_{max}O_2$ and R_{dark}, respectively, than the green variety.

The light response curves revealed the LSP in the HL green variety occurred much earlier than in HL red variety. The LSP in both varieties was higher under HL than under LL growth irradiance. The LSP between varieties was greater in the red than in the green variety under either growth irradiance. This result may indicate that the red variety possesses a larger spectral range to acclimate and restore photostasis than the green variety. Overall, in this study, the LSP was directly dependent on growth irradiance. However, this outcome was not found in *Aeschynanthus longicaulis,* were the LSP was greater under LL (Li *et al.* 2014), while *Panax notoginseng* had a similar LSP at either HL or LL growth irradiance (Chen *et al.* 2016).

Under HL growth irradiance, the red variety exhibited greater values of $\Phi_{app}O_2$ (16%) and $P_{max}O_2$ (35%) than the green variety. As expected, these responses were supported by increased R_{dark} (52%) and LCP (24%) in the red than the green variety. Only the red variety exhibited a 69% and 18% increase of R_{dark} and LCP under HL compared to LL. Similar values of R_{dark} and LCP in the green variety at either growth irradiance may suggest that the green variety had a reduced capacity to photoacclimate to HL than the red variety, as there were no differences among varieties under LL growth irradiance. Overall, these data may suggest that photoacclimation of both varieties to HL may be variety-specific. The lack of differential response between the red and green varieties under our LL conditions (70 µmol m^{-2} s^{-1} PPFD) may not reflect differences under other LL irradiance and a LL irradiance dose response should be

performed under a broader irradiance range or a wider range of genetics. Bailey *et al.* (2001, 2004) demonstrated by using 7 ranges of irradiance in *Arabidopsis thaliana* that only two ranges of irradiance, which many studies commonly use to reflect HL and LL acclimation, are not adequate to determine the multiple regulatory mechanisms that underlie photosynthetic acclimation. In this study, ETR in both varieties was about 4-fold higher under HL than under LL growth irradiance. The ETR between varieties under either growth irradiance were similar. However, a 10-fold difference in growth irradiance resulted in a 2-fold greater ETR in *Hordeum vulgare* (De la Torre and Burkey 1990) and 4-fold greater ETR in *Atriplex* (Boardman 1977). Conversely, a difference of 22-fold in growth irradiance resulted in only a 1.3-fold difference of ETR in *Chamaesyce herbstii* or 2.3-fold difference in *Claoxylon sandwicense* (Pearcy and Franceschi 1986), which reflects species-specific ETR adjustments in the photosynthetic apparatus to adapt to variations in irradiance. The results suggest that both varieties at the ETR level are not varietal different under either growth irradiance.

The red and green varieties exhibited an enhancement of Chl and increased Car content on a LA basis under HL compared to LL. Photoacclimation to HL typically includes increased Chl and Car content on a LA basis or decreased Chl and Car content on a FW basis (Lichtenthaler 1981). When expressed on a FW basis, Chl content was unexpectedly greater in the red under HL and similar in the green variety among the growth irradiance, which again may suggest that both varieties possessed restricted capacity to adjust the light harvesting pigments accumulation under LL growth irradiance. The increased values for Car content on a LA basis under HL growth irradiance was observed previously in other studies (Boardman 1977, Thayer and Björkman 1990, Lichtenthaler *et al.* 2007). Carotenoid pigments play a role preventing photooxidation and are involved in the dissipation of excess energy through NPQ (Demming-Adams and Adams 1992). Among red and green varieties, on a LA basis, the red variety showed an increased 60% and 62% Chl and Car accumulation under HL and 43% and 55% under LL conditions. The most striking response for both varieties at either growth irradiance were similar Chl *a/b* ratios. Changes in the Chl *a/b* ratio is one of the most frequent and most easily observed responses to different growth irradiance. The Chl *a/b* ratio reflects the proportion of Chl bound by the light harvesting complexes

and indirectly estimates antennae size (LHC protein accumulation; Leong and Anderson 1984a, Walters and Horton 1994, Bailey *et al.* 2001). Plants grown under LL growth irradiance frequently possess a low Chl *a/b* ratio (large antennae). For example, decreases in the Chl *a/b* under LL compared to HL have been reported for *Pisum sativum* (Leong and Anderson 1984a, 1984b), *Arabidopsis thaliana* (Walters and Horton 1994), *Spinacia oleracea* (Lindahl *et al.* 1995), *Amaranthus cruenthus* (Tazoe *et al.* 2006), and *Flaveria bidentis* (Pengelly *et al*. 2010). Similar Chl *a/b* results were not expected, as both varieties were anticipated to adjust the absorption cross section of their antennae to enhance maximal use of the irradiance (Lichtenhaler *et al.* 1981, Anderson and Osmond 1987, Givnish 1988). Nevertheless, similar results for Chl *a/b* under HL and LL were reported for *Tradescantia albiflora* (Chow *et al.* 1991), barley (Falbel *et al.* 1996), *Epilobium hirsutum, Lolium perenne, Hypericum perforatum, Urtica urens, Festuca ovina, Festuca rubra* (Murchie and Horton 1997), *Hordeum vulgare* (Król *et al.* 1999, Kurasova *et al.* 2003, Zivcak 2014) and *Aeschynanthus longicaulis* (Li *et al.* 2014). These data demonstrate the modulation of Chl *a/b* ratios may be dependent on plant species. The modulation of Chl *a/b* ratios in our study did not occur in either variety, which demonstrated that this mechanism was not varietal specific.

Overall, the photosynthetic parameters in response to growth irradiance illustrated that both varieties exhibited higher values of $\Phi_{app}O_2$, $P_{max}O_2$, ETR and NPQ under HL than under LL growth irradiance. The photosynthetic parameters described above were similar between varieties under LL growth irradiance, which may indicate that the differentiation of photoacclimatory mechanisms between red and green varieties may not have occurred as a consequence of low irradiance value (Leong and Anderson 1984a, 1984b, Bailey *et al*. 2001, 2004).

5.2 A Role for Betalains in Photoprotection

The tolerance to photoinhibition under either HL or LL growth irradiance was greater in the red variety compared to the green variety. The red variety also had higher levels of Car than the green variety. However, the red variety did not have a greater NPQ value than the green variety and thus NPQ does not appear to be a component of photoinhibitory tolerance between varieties under either growth irradiance.

However, among the varieties under HL growth irradiance, betalain accumulation was 79% greater in the red than in the green variety. Betalains consist of betacyanins and betaxanthins, which are non-photosynthetic red-violet and yellow-orange pigments, respectively, that replace anthocyanins in plants of the Order Caryophyllales, such as *Amaranthus* (Stafford 1994, Strack *et al.* 2003, Tanaka *et al.* 2008, Solovchenko and Merzlyak 2008). Betalains possess similar absorption spectra and antioxidant properties *in vivo* as anthocyanins, and as such, they are also considered to possess many of the other characteristics of anthocyanins (Nakashima *et al.* 2011, Mosco 2012).

Furthermore, the composition of the betalains were substantially different. In the red variety under HL growth irradiance, the total betalain content consisted of 52% betacyanins and 48% betaxanthins and in the green variety only 8% were attributable to betacyanins. The tolerance to photoinhibition after 4 h of exposure to a PPFD of 1450 µmol m^{-2} s^{-1} at 2°C under HL was 49% greater in the red than in the green variety, which suggested betalains attenuated incident light, thereby preventing photoinhibition. Among the varieties under LL growth irradiance, again the red variety showed a greater tolerance to photoinhibition. After 4 h of exposure to excess light, tolerance under LL conditions was 62% greater in the red variety than in the green variety, corresponding with a 71% increase in betalain content in the red variety. Additionally, the composition of betalains also differed; in the red variety the betacyanins were 93% and betaxanthins 56% greater than in the green variety under LL growth irradiance. Recent studies have reported the protective function of betalains under chilling-induced photoinhibition in leaves of *Suaeda salsa* (Wang and Liu 2007). Increased recovery after photoinhibition in *Amaranthus tricolor* (Shu *et al.* 2009), *Suaeda japonica* (Hayakawa and Agarie 2010) and *Amaranthus cruenthus* (Nakashima *et al.* 2011) was attributed to betalain content accumulation.

Solovchenko and Merzlyak (2008) have suggested photoprotective pigments should comply with certain criteria that pigments should absorb radiation in the spectral band(s) overlapping with the absorption band(s) of the photosynthetic pigments, the irradiation in the corresponding spectral range should trigger the synthesis of the pigment in the natural and model systems (e.g. cell or tissue culture), and the

accumulation of the compound in question should induce resistance to the radiation in the spectral range of the pigment absorption. Betalain pigments meet all three criteria which supports their photoprotective role (Strack *et al.* 2003, Takahashi *et al.* 2010, Nakashima *et al.* 2011, Takahashi and Badger 2011). Based on transverse and longitudinal sections, at either growth irradiance, both varieties revealed betalain preferentially accumulated in the LMC with lower contents in the UMC. Betalains were absent in EC and not observed in the BSC, VPC and CC. Accumulation of anthocyanins in UEC in *Pinus banksiana* (Król *et al.* 1995, Hüner *et al.* 1998), or in the UMC as in *Begonia heracleifolia* (Hughes *et al.* 2008) appear to confer photoprotection through attenuation and screening. However, the absence of betalain in the UEC and LEC in this study is contradictory to other studies which indicated betalain accumulated in either EC (Bianco-Colomas and Hugues 1990, Stafford 1994, Nakashima *et al.* 2011). It has also been demonstrated that in *Obregonia denegrii* betacyanins were present only in the hypodermis (layer of cells immediately below the epidermis), whereas in *Leuchtembergia principis,* betacyanins accumulated mostly in the hypodermis cells and in lesser amounts in some chlorenchyma (parenchyma cells that contain chloroplasts) cells. Furthermore, in *Mammillari sartorii,* betacyanins were present only in the outer chlorenchyma cells (Mosco 2012). The localization of betalain mainly in the LMC has been suggested to enhance photoprotection by shielding chloroplasts from green and yellow light. Several studies have demonstrated that green and yellow light can also cause photoinhibition (Hughes *et al.* 2005, Takahashi and Badger 2011). Additionally, Koizumi *et al.* (1998) and Vogelmann and Han (2000) found green light penetrated deeper into leaf tissue than blue and red light. Oguchi *et al.* (2011) more recently found green light also induced more photodamage than red light. Therefore, the accumulation of leaf betalains deeper in the leaf tissue may ameliorate photoinhibition by shielding chloroplasts from the green light. Overall these data suggest betalain accumulation, composition and localization may play a significant photoprotectory role in the red and green varieties of *Amaranthus blitum*.

5.3 Anatomical and Ultrastructural Mechanisms of Photoacclimation

Stomata are considered one of the main factors within the leaf allowing higher plants to adapt and photoacclimate to different environments by adjusting their size, density and distribution, which have a direct impact on CO_2 diffusion in leaves (Zarinkamar 2007). The examination of imprints of leaf surfaces revealed the red and green varieties of *Amaranthus* contain anomocytic stomata (absence of subsidiary cells, Esau 1977) on either the adaxial or the abaxial side of the leaf, a common condition in plants known as amphistomatous (Fricker and Wilmer 1996).

The red variety had a greater SI only on the abaxial side under HL than under LL growth irradiance. In contrast, the green variety showed greater SI on both adaxial and abaxial sides when compared to LL growth irradiance. Overall, both varieties had more stomata on the abaxial than on the adaxial side under HL conditions, and under LL conditions, only the green variety had more stomata on the abaxial than on the adaxial side. These results may suggest the SI may be associated with greater CO_2 diffusion in leaves and likely increased photosynthesis performance only under HL growth irradiance, where the red variety exhibited greater values of $\Phi_{app}O_2$, $P_{max}O_2$, R_{dark}, LCP than the green variety. Tsutsumi *et al.* (2017) when analyzing 12 species of *Amaranthus*, found that stomatal density was also greater on the abaxial than adaxial side but with no direct correlation between the net photosynthetic rate.

Both varieties had short and tall, multicellular and uniseriate glandular trichomes on either side of leaf. Trichome density was different between varieties when compared among the growth irradiance. Under HL, the red variety had greater trichome density on the abaxial side, and the green variety had greater numbers of trichomes on the adaxial side when compared to LL growth irradiance. The trichomes are distributed mainly on the veins and very rarely can be observed in the stomata-zone. This likely indicates their impact on the boundary layer and subsequently the effect on photosynthesis is not playing a significant role (Costea and DeMason 2001).

The transverse sections of the inner leaf structure in both varieties of *Amaranthus* exhibited features typical of NAD-ME type C4 dicot plants with BSC surrounding the vascular bundle (VB) (Gutierrez *et al.* 1974, Hatch *et al*. 1987). The BSC were filled with chloroplasts and mitochondria in the centripetal (radial) position

around the VB. The presence of mitochondria near the chloroplasts is in accordance with the finding that in the NAD-ME subtype, the decarboxylating malic enzyme is in the mitochondrion (Edwards and Walker 1983, Sage 2004). The transverse sections revealed that the UMC (adaxial mesophyll layer) and the LMC (abaxial mesophyll layer) were morphologically differentiated into an upper palisade and lower spongy layers. This contrasts with findings of mesophyll tissue in *Amaranthus tricolor* which was not differentiated (Hong *et al.* 2005). Upper mesophyll cells are elongated, cylindrical with the long axis perpendicular to the surface of the leaf, and the LMC are of irregular forms. The thickness of the abaxial mesophyll layer at HL growth irradiance was 17% greater in the red than in the green variety. Leaf thickness plays an important role in capturing photons when light is limited (Sun *et al.* 1998, Terashima *et al.* 2009). The LT has also been suggested to augment NPQ under photoinhibtory conditions (Gould *et al.* 2000).

Additionaly, the transverse sections in both varieties revealed that the number of BSC around the VB were greater under HL than under LL growth irradiance, which indicate that the growth irradiance affected not only the area of the cells, but also the number. This further supports that under HL growth irradiance, the increase of LT was not just a result of increasing the area of the cells, but also of changes in morphology and number of the cells. Increased number of BSC in profile view had a positive association with increased LT and photosynthetic performance. Furthemore, the number of chloroplasts per profile of a BSC in section was affected by growth irradiance. Both varieties possessed greater number under HL than under LL. Under HL, both varieties possessed a similar number of chloroplasts, but as the micrographs illustrated the chloroplasts were of different shapes. Longer chloroplasts and their distribution in the cell may facilitate light harvesting and/or may help to avoid the excess excitation by moving the chloroplasts to the periphery of the cell. The results suggest that the shape of chloroplasts may enhance the photosynthetic performance, as higher $\Phi_{app}O_2$ and/or $P_{max}O_2$ were greater in the red than in the green variety under HL.

Chloroplast ultrastructure and thylakoid architecture were significantly different among varieties and treatments. The ultrastructure of the chloroplast (granal and stromal lamellae, stroma, features in the stroma (PR), features in the thylakoid

membranes (CI), and CP, were different between varieties at either growth irradiance. Thylakoid architecture (structure of granal and stromal lamellae) among the growth irradiance were different between varieties. In general, plants grown under LL have more thylakoids per granum than those grown under HL (Lichtenthaler 1981, Anderson 1986). However, GI and thylakoids/granum under HL in profiles of the BSC of the red variety was increased when compared to LL growth irradiance. But the GI and thylakoids/granum under HL in profiles of the BSC of the green variety was decreased when compared to LL growth irradiance. These differences in thylakoid architecture contributed positively to modulate the capacity of red variety to use better the irradiance than the green variety under HL growth irradiance, by enhancing photosynthetic performance.

Under HL, the thylakoid architecture in BSC of the red variety consisted of granal lamellae which were well developed, with many thylakoids/granum. By contrast, the thylakoid architecture in BSC of the green variety showed a greater number of granal lamellae per chloroplast than the red variety, but with a reduced number of thylakoids/granum. This further resulted in an increased GI and thylakoids/granum in the BSC of the red variety than in the BSC of the green variety. In the MC, the GI was similar among varieties, but the thylakoids/granum was greater in the red than in the green variety.

Under LL, the thylakoid architecture in the BSC and MC in both varieties exhibited a similar GI. Although the thylakoids/granum in the BSC among varieties was similar, it was greater in the MC in the red than in the green variety.

Overall, it appears that the thylakoid architecture plays a crucial role in enhancing the photosynthetic performance under HL conditions in these varieties. The primary function of the stacked grana is still unclear but appears to enhance photosynthesis by increasing spatial separation of PSI and PSII between granal and stromal lamellae (Barber 1980), functionality of light harvesting complexes (Dekker and Boekema 2005), regulation of light harvesting (NPQ; Horton 1999) and delay of premature degradation of D1 protein (Anderson and Aro 1994, Lee *et al.* 2001). However, the stackness from other side may restrict photosynthesis by requiring long-range diffusion of electron carriers between PSII and PSI (Mullineaux 2008, Kirchhoff *et al.* 2011) and/or relocation

of PSII between the appressed and non-appressed regions during the PSII repair cycle (Mulo *et al.* 2008). According to the GI and thylakoids per granum results obtained in BSC under LL growth irradiance in both varieties, which were greater than in the green variety under HL growth irradiance, it appeared that they did not contribute as much to impact the photosynthesis performance from one side. From the other side, it appeared that they also did not restrict the photosynthesis, as the maximal photochemical efficiency of PSII (F_v/F_m) were similar with the plants grown under HL growth irradiance. In general, the stacking results from the interplay of physico-chemical forces of attraction and repulsion between adjacent membranes (Chow *et al.* 2005, Anderson *et al.* 2008). There are a multitude of factors that can influence stacking that include phosphorylation of thylakoid proteins, thylakoid lipid composition and lipid-protein interactions (Gounaris and Barber 1983, Anderson 1989, Webb and Green 1991, Navari-Izzo *et al.* 2000, Dekker and Boekema 2005, Fristedt *et al.* 2009). Overall, the greater GI and thylakoids per granum in the red variety under HL conditions appears to support the results of greater $\Phi_{app}O_2$, $P_{max}O_2$, and tolerance to photoinhibition, when compared to the green variety.

Only chloroplasts from the green variety had PRI and PRII. Under HL growth irradiance in BSC chloroplasts, the PR was more evident than in BSC under LL, however in MC, the PR was more evident under LL growth irradiance. Previous studies have suggested PR may play a role in photosynthetic performance by increasing the surface area of the chloroplast inner envelope membrane, thereby influencing metabolite exchange between the plastid and the cytoplasm (Held and Saur 1971, Westphal *et al.* 2003, Wise 2006, Brautigan and Weber 2011, Szczepanik and Sowinski 2014). However, its role in photosynthetic performance is not clear in our study since the red variety demonstrated greater $\Phi_{app}O_2$ and $P_{max}O_2$ in the absence of PR.

In addition to PR, chloroplasts of the green variety were distorted appearing as CP, which are hypothesized to increase chloroplast transport and further enhance photosynthesis (Larkin *et al.* 2016). The TEM micrographs showed CP in the BSC under HL growth irradiance were very dense and more diverse in shape than under LL conditions. The CP in MC, VPC and CC are less abundant at either growth irradiance. This may indicate that their prevalent presence in the BSC may be associated with the

mechanism to increase the metabolite exchange between chloroplast and cytoplasm and increase the CO_2 assimilation. However, similar to the PR, the presence of CP was only observed in the green variety which may suggest CP are not associated with photosynthesis, although this does not exclude a possible role in photorespiration.

Additionally, many peroxisomes in the green variety in the BSC were observed at either growth irradiance. Initially, based on TEM micrographs, it appeared that their distribution was more abundant under HL growth irradiance. However, there was no significant difference in area among the growth irradiance. While photorespiration rates were not measured in this study, these results may indicate that the increase peroxisomes presence is not directly associated with photorespiratory rates, since *Amaranthus* are C4 plants and should have only minimal rates of photorespiration. Their increased presence may be correlated with signaling molecules such as H_2O_2 (see Section 6.2) or presence of PR. Nevertheless, Hilliard *et al*. (1971) examined the correlation between photorespiration and the presence of PR. They demonstrated in the C3 plant *Dactylis glomerata,* photorespiration rates were not correlated with the presence of PR. Again, while photorespiration rates were not measured in this study, more PR abundance in the MC than in the BSC per area of chloroplast (data not shown) may suggest there is no association between the increased photorespiration and PR, as well of peroxisomes abundance and photorespiration.

Finally, the presence of CI were observed only in the green variety in BSC under HL and in BSC and MC under LL. They were more abundant under the LL growth irradiance but with no difference in area. Early reports in *Spinacia oleracea* chloroplasts suggested CI consist of Rubisco (Esau 1975, Sprey 1977, Sprey and Lambert 1977), however, a later study did not support that conclusion (Shojima *et al.* 1987). The presence of CI was reported in BSC, MC and EC of *Amaranthus viridis* (Ueno 2000). Whereas their function has not been experimentally determined, it is hypothesized they serve as a storage structure utilizable in the synthesis of thylakoid membranes or of stromal proteins (Ueno 2000). The absence of CI in the red variety indicates their photosynthetic role is questionable.

Overall the adjustments at anatomical and ultrastructural levels revealed that primarily the GI and thylakoids per granum plays a significant role in enhancing

photosynthetic performance. Secondarily, alterations in LT and increased SI may result in a greater CO_2 difusion. All these photosynthetic adjustments appeared to contribute to the increased $\Phi_{app}O_2$ and $P_{max}O_2$ values in the red variety than in the green variety under HL growth irradiance.

Lack of variation in adjustments between red and green varieties under LL suggests either that there are no differences or is possible that the 70 µmol m^{-2} s^{-1} PPFD irradiance level was too low to discern the differential adjustments in the photosynthetic apparatus in these varieties.

CHAPTER 6

6.0 CONCLUSIONS AND FUTURE STUDIES

6.1 Conclusions

Amaranthus blitum red and green varieties showed a greater ability to photoacclimate to HL than to LL growth irradiance. Growth and development under HL growth irradiance was faster, resulting in greater accumulation of biomass. Unexpectedly, the LA in both varieties was greater under HL than under LL. However, although the red variety had a higher number of leaves under HL, its individual LA was smaller than the green variety. Photosynthetically, both varieties performed better under HL than under LL growth irradiance due to a larger range of photosynthetic adjustments (higher accumulation of pigments, higher O_2 evolution parameters, higher tolerance to photoinhibition and a thicker leaf). Between the varieties grown under HL, the red variety exhibited greater values of $\Phi_{app}O_2$, $P_{max}O_2$, accumulation of Chl, accumulation of Car and betalain pigments and greater tolerance to photoinhibition than the green variety. However, the Chl *a/b* ratio was similar between varieties, indicating that the absorption cross section of light harvesting antenna per reaction center were similar between varieties. Greater values of $\Phi_{app}O_2$, $P_{max}O_2$ in the red variety than in the green variety under HL growth irradiance suggests that the red variety has a greater ability to adjust to different growth irradiance and use the excess irradiance. The greater tolerance to photoinhibition appears to be associated with increased content of betalains, as both varieties were showing similar NPQ capacity. Additionally, it appears that the major role of betalains in conferring photoprotection is primarily based on screening of excess light in the LMC, where betalains predominantly accumulates, and secondarily by screening the UMC.

At the anatomical level, both varieties exhibited greater LT, based on increased area of UEC, UMC, BSC, LMC, LEC and increased area of chloroplasts in BSC under HL than under LL growth irradiance. The red variety compared to the green variety also exhibited increased LT based on thicker LMC layer. Additionally, the area of chloroplasts in BSC and MC was greater in the red variety than the green variety. Among HL and LL growth irradiance SI was greater in both varieties and on both sides

than under LL conditions. However, between varieties under HL conditions the red variety manifested a greater SI on adaxial side. Both varieties possessed a different thylakoid architecture (granal and stromal lamellae thylakoid membranes), which likely have implications on lateral heterogeneity, which also impacts granal stacking. At HL growth irradiance, the red variety possessed an increased GI and thylakoids/granum in BSC compared to LL. The increased GI and thylakoids/granum in red variety BSC appears to play a crucial role in affecting the $\Phi_{app}O_2$ and $P_{max}O_2$ capacity at HL conditions. By contrast, the green variety had a decreased GI in BSC.

Under LL growth irradiance both varieties photoacclimated similarly. The growth kinetics parameters, leaf anatomy and thylakoid architecture were similar between varieties. The accumulation of light harvesting pigments was greater in the red variety, however that did not contribute to a greater photosynthetic performance. Neither variety was able to adjust the LA to be greater than under HL conditions. Unexpectedly and in contrast to many studies, the photoacclimation to LL in both varieties was not associated with major changes in absorption cross section of light harvesting antenna per reaction center, as indicated by the absence of changes in Chl *a/b* ratio. The main difference between varieties under LL growth irradiance was the red variety exhibited greater tolerance to photoinhibition, which may be related with increased betalain content, predominantly of betacyanin pigments.

Other novel findings of this thesis included the observation that only chloroplasts of the green variety possessed features such as PR, CI and the presence of CP regardless of growth irradiance. The role of these structures on photosynthetic performance appears to be questionable, as the red variety in the absence of these features exhibited greater rates of photosynthesis than the green variety. Overall, it can be concluded that PR, CP and CI are not required for higher rates of photosynthesis.

6.2 Future Studies

The interesting findings of this study suggest that additional experiments may further reveal how the red and green varieties of *Amaranthus blitum* adjust their photosynthetic apparatus to cope with HL and LL growth irradiance. In this research, it was found that neither variety demonstrated the ability to adjust the absorption cross

section of light harvesting complex antenna per reaction center or LT to cope with limited light conditions, which suggests that 70 µmol m^{-2} s^{-1} PPFD was too low to allow separation of photoacclimatory mechanisms under LL. An evaluation under a larger range of irradiance for LL photoacclimation may reveal the LL level of irradiance under which a distinguished differentiation of photoacclimatory mechanisms occur in *Amaranthus blitum* as were demonstrated in *Arabidopsis thaliana* (Leong and Anderson 1984a, 1984b, Bailey *et al.* 2001, 2004).

Evaluation of photosystems stoichiometry (PSII/PSI), is one well documented mechanism which plants evolved to cope with reduced light conditions (Chow and Hope 1987) and will reveal if this mechanism is characteristic for *Amaranthus blitum.* It may also be interesting to examine pigment (betalains) accumulation in other aerial portion of the plant, such as shoots and petioles.

The ultrastructure of chloroplast in BSC under HL conditions in this study appears to play the crucial role in enhancing the $\Phi_{app}O_2$, and $P_{max}O_2$ in the red compared to the green variety. Evaluation of proteins involved in the formation of granal lamellae such as, CURVATURE THYLAKOID (CURT; Ambruster *et al.* 2013) may reveal if the GI and thylakoids per granum can be attributed to CURT or other proteins. This can be accomplished by immunoblotting for proteins previously identified in this process.

The evaluation of NDH-mediated cyclic electron flow may reveal if the increased abundance of peroxisomes in the green variety were related with demand for H_2O_2 to induce cyclic electron flow as postulated by Takabayashi *et al.* (2005) and Livingston *et al.* (2010). In addition, cyclic electron flow is considered an important mechanism of how C4 plants can adjust their ATP/NADH ratio and maintain energy balance.

Finally, there is a need to evaluate how these varieties photoacclimate during short shifts in light quantity and subsequently balance energy between photosystems. This usually involves the phosphorylation dependent detachment of LCHII from PSII (in the granal lamellae) and its diffusion to PSI (in the stromal lamellae). Further, these experiments may reveal the relationship between thylakoid architecture (GI and thylakoids per granum) and phosphorylation/dephosphorylation mechanisms.

CHAPTER 7

7.0 REFERENCES

Abrahams JP, Leslie AG, Lutter R, Walker JE. (1994) Structure at 2.8 Å resolution of F1-ATPase from bovine heart mitochondria. *Nature* **370**, 621–628.

Ambruster U, Labs M, Pribil M, Viola S, Xu S, Scharfenberg M, Hertle AP, Rojahn U, Jensen PF, Pappaport F, Joliot P, Dörmann GW, Leister D. (2013) *Arabidopsis* curvature thylakoid1 proteins modify thylakoid architecture by inducing membrane curvature. *The Plant Cell* **25**, 2661–2678.

Allakhverdiev SI, Nishiyama Y, Miyairi S, Yamamoto H, Inagaki N, Lanesaki Y, Murata N. (2002) Salt stress inhibits the repair of photodamaged photosystem II by suppressing the transcription and translation of psbA genes in *Synechocystis*. *Plant Physiology* **130**, 1443–1453.

Allakhverdiev SI, Murata N. (2004) Environmental stress inhibits the synthesis de novo of proteins involved in the photodamage-repair cycle of photosystem II in *Synechocystis* sp PCC 6803. *Biochimica et Biophysica Acta* **1657**, 23–32.

Albertsson PÅ. (2001) A quantitative model of the domain structure of the photosynthetic membrane. *Trends in Plant Science* **6**, 349–354.

Allemann J, Vanderheever E, Viljoen A. (1996) Evaluation of *Amaranthus* as a possible vegetable crop. *Applications in Plant Sciences* **10**, 1–4.

Allen JF, Bennett J, Steinback KE, Arntzen CJ. (1981) Chloroplast protein-phosphorylation couples plastoquinone redox state to distribution of excitation-energy between photosystems. *Nature* **291**, 25–29.

Allen JF, Forsberg J. (2001) Molecular recognition in thylakoid structure and function. *Trends in Plant Science* **6**, 317–326.

Al-Mamun AA, Husna J. Khatun M, Hasan R, Kamruzzaman M, Hoque KMF, Reza MA, Ferdousi Z. (2016) Assessment of antioxidant, anticancer and antimicrobial activity of two vegetable species of *Amaranthus* in Bangladesh. *BMC Complementary and Alternative Medicine* **16**, 157.

Alvarez-Jubete L, Holse M, Hansen A, Arendt EK, Gallagher E. (2009). Impact of baking on the vitamin E content of the pseudocereals amaranth, quinoa and buckwheat. *Cereal Chemistry*, 86, 511–515.

Alvarez-Jubete L, Arendt EK, Gallagher E. (2010) Nutritive value of pseudocereals and their increasing use as functional gluten free ingredients. *Trends in Food Science and Techonology* **21**, 106–113.

Amin I, Norazaidah Y, Emmy Hainida KI. (2006) Antioxidant activity and phenolic content of raw and blanched *Amaranthus* species. *Food Chemistry* **94**, 47–52.

Amunts A, Drory O, Nelson N. (2007) The structure of a plant photosystem I supercomplex at 3.4 Å resolution. *Nature* **447**, 58–63.

Amunts A, Toporik H, Borovikova A, Nelson N. (2010) Structure determination and improved model of plant photosystem I. *Journal of Biochemical Chemistry* **285**, 3478–3486.

Andersson B, Andersson JM. (1980) Lateral heterogeneity in the distribution of chlorophyll-protein complexes of the thylakoid membranes of spinach chloroplasts. *Biochimica et Biophysica Acta* **593**, 427–440.

Anderson JM. (1986) Photoregulation of the composition, function, and structure of thylakoid membranes. *Annual Review of Plant Physiology* **37**, 93–136.

Anderson JM, Osmond CB. (1987) Shade-sun responses: comprimises between acclimation and photoinhibition. In: Kyle DJ, Osmond CB, Arntzen CJ. (eds) Photoinhibition, Amsterdam: Elsevier Science Publishers, pp. 1–38.

Anderson JM, Chow WS, Goodchild DJ. (1988) Thylakoid membrane organization in sun/shade acclimation. *Australian Journal of Plant Physiology* **15**, 11–26.

Anderson JM. (1989) The grana margins of plant thylakoid membranes. *Physiologia Plantarum* **76**, 243–248.

Anderson JM, Aro EM. (1994) Grana stacking and protection of Photosystem II in thylakoid membranes of higher plant leaves under sustained high irradiance: an hypot. hesis *Photosynthesis Research* **41**, 315–326.

Anderson JM, Chow WS, Park YI. (1995) The grand design of photosynthesis: acclimation of the photosynthetic apparatus to environmental cues. *Photosynthesis Research* **46**, 129–139.

Anderson JM, Park YI, Chow WS. (1998) Unifying model for the photoinactivation of photosystem II in vivo under steady-state photosynthesis. *Photosynthesis Research* **56**, 1–13.

Anderson JM. (1999) Insights into the consequences of grana stacking of thylakoid membranes in vascular plants: a personal perspective. *Australian Journal of Plant Physiology* **26**, 625–639.

Anderson JM, Chow WS, De La Rivas J. (2008) Dynamic flexibility in the structure and function of photosystem II in higher plant thylakoid membranes: the grana enigma. *Photosynthesis Research* **98**, 575–587.

Arganda-Caeewras I, Kaynig V, Rueden C, Eliceiri KW, Schindelin J, Cardona A, Seung HS. (2017) Trainable Weka Segmentation: a machine learning tool for microscopy pixel classification. *Bioinformatics* **33**, 2424–2426.

Aro EM, Virgin I, Andersson B. (1993) Photoinhibition of photosystem II. Inactivation, protein damage and turnover. *Biochimica et Biophysica Acta* **1143**, 113–134.

Aro EM, Suorsa M, Rokka A, Allahverdiyeva Y, Paakkarinen V, Saleem A, Battchikova N, Rintamäki E. (2005) Dynamics of photosystem II: a proteomic approach to thylakoid protein complexes. *Journal of Experimental Botany* **56**, 347–356.

Augspurger CK. (1984) Light requirements of neotropical tree seedlings: a comparative study of growth and survival. *Journal of Ecology* **72**, 777–795.

Azeredo HMC. (2009) Betalains: properties, sources, applications, and stability. *International Journal of Food Science and Technology* **44**, 2365–2376.

Baerr JN, Thomas JD, Taylor BG, Rodermel SR, Gray GR. (2005) Differential photosynthetic compensatory mechanisms exist in the i*mmutans* mutant of *Arabidopsis thaliana*. *Physiologia Plantarum* **124**, 390–402.

Bailey S, Walters RG, Jansson S, Horton P. (2001) Acclimation of *Arabidopsis thaliana* to the light environment: the existence of separate low light and high light responses. *Planta* **213**, 794–801.

Bailey S, Horton P, Walters RG. (2004) Acclimation of *Arabodopsis thaliana* to the light environment: the relationship between photosynthetic function and chloroplast composition. *Planta* **218**, 793-802.

Baker NR, Rosenqvist E. (2004) Applications of chlorophyll fluorescence can improve crop production strategies: an examination of future possibilities. *Journal of Experimental Botany* **55**, 1607–1621.

Baker NR. (2008) Chlorophyll fluorescence: a probe of photosynthesis in vivo. *Annual Review of Plant Biology* **59**, 89–113.

Ballottari M, Dall'Osto L, Morosinotto T, Bassi R. (2007) Contrasting behavior of higher plant photosystem I and II antenna systems during acclimation. *Journal of Biological Chemistry* **282**, 8947–8958.

Baránková B, Lazár D, Nauš J. (2016) Analysis of the effect of chloroplast arrangement on optical properties of green tobacco leaves. *Remote Sensing of Environment* **174**, 181–196.

Barber J. (1980) Membrane surface charges and potentials in relation to photosynthesis. *Biochimica et Biophysica Acta* **594**, 253–308.

Bazzaz FA. (1979) The physiological ecology of plant succession. *Annual Review of Ecology and Systematics* **10**, 351–371.

Beaudoin GAW, Facchini PJ. (2014) Benzylisoquinoline alkaloid biosynthesis in opium poppy. *Planta* **240**, 19–32.

Becker R, Wheeler EL, Lorenz K, Stafford AE, Grosjean OK, Betschart AA, Sauners RM. (1981) A compositional study of Amaranth grain. *Journal of Food Science* **46**, 1175–1180.

Bejosano FP, Corke H. (1998) Protein quality evaluation of *Amaranthus* whole meal flours and protein concentrates. *Journal of the Science of Food and Agriculture* **76**, 100–106.

Bellafiore S, Barneche F, Peltier G, Rochaix JD. (2005) State transitions and light adaptation require chloroplast thylakoid protein kinase STN7. *Nature* **433**, 892–895.

Bendall DS, Manasse RS. (1995) Cyclic photophosphorylation and electron transport. *Biochimica et Biophysica Acta* **1229**, 23–38.

Bianco-ColomasJ, Hugues M. (1990) Establishment and characterization of betacyanin producing cell line of amaranth tricolor: inductive effects of light and cytokinin. *Journal of Plant Physiology* **136**, 734–739.

Bilger W, Schreiber U. (1986) Energy-dependent quenching of dark-level chlorophyll fluorescence in intact leaves. *Photosynthesis Research* **10**, 303–308.

Biswal B, Joshi PN, Raval MK, Biswal UC. (2011) Photosynthesis, a global sensor of environmental stress in green plants: stress signaling and adaptation. *Current Science* **101**, 47–56.

Björkman O. (1981) Responses to different quantum flux densities. In: Lange OL, Nobel PS, Osmond CB, Ziegler H. (eds) Physiological Plant Ecology. I. Responses to the Physical Environment. Vol. 12A. Berlin: Springer-Verlag, pp. 57–107.

Boardman NK. (1977) Comparative photosynthesis of sun and shade plants. *Annual Review of Plant Physiology* **28**, 355–377.

Bonardi V, Pesaresi P, Becker T, Schleiff E, Wagner R, Pfannschmidt T, Jahns P, Leister D. (2005) Photosystem II core phosphorylation and photosynthetic acclimation require two different protein kinases. *Nature* **437**, 1179–1182.

Bowman WD, Hacker SD, Cain ML. (2017) Coping with environmental variation energy. In: Ecology. Sunderland: Sinauer Associates, Inc., pp. 109–134.

Brautigan A, Weber APM. (2011) Transport processes: connecting the reactions of C4

photosynthesis. In: Raghavendra AS, Sage RE. (eds) C4 Photosynthesis and Related CO_2 Concentrating Mechanisms. Dordrecht: Springer, pp. 199–219.

Bressani R. (2003) Amaranth. In: Caballero (ed) Encyclopedia of Food Sciences and Nutrition. Oxford: Academic Press, pp. 166–173.

Bricker TM, Roose JL, Fagerlund RD, Frankel LK, Eaton-Rye JJ. (2012) The extrinsic proteins of photosystem II. *Biochimica et Biophysica Acta* **1817**, 121–142.

Brockington SF, Walker RH, Glover BJ, Soltis PS, Soltis DE. (2011) Complex pigment evolution in the Caryophyllales. *New Phytologist* **190**, 854–864.

Brown WV. (1997) The Kranz syndrome and its sub-types in grass systematics. *Memoirs of the Torrey Botanical Club* **23**, 1–97.

Butera D, Tesoriere L, Di Gaudio F, Bongiorno A, Allegra M, Pintaudi AM. (2002) Antioxidant activities of sicilian prickly pear (*Opuntia ficus-indica*) fruit extracts and reducing properties of its betalains: betanin and indicaxanthin. *Journal of Agricultural and Food Chemistry* **50**, 6895–6901.

Cabanes J, Gandía-Herrero F, Escribano J, García-Carmona F, Jiménez-Atiénzar M. (2016) Fluorescent bioinspired protein labeling with betalamic acid. Derivatization and characterization of novel protein-betaxanthins. *Dyes and Pigments* **133**, 458–466.

Cai Y Z, Sun M, Corke H. (1998a) Colorant properties and stability of *Amaranthus* betacyanin pigments. *Journal of Agricultural and Food Chemistry* **46**, 4491–4495.

Cai YZ, Sun M, Wu HX, Huang R, Corke H. (1998b) Characterization and quantification of betacyanin pigments from diverse *Amaranthus* species. *Journal of Agricultural and Food Chemistry* **46**, 2063–2070.

Cai Y, Sun M, Wu H, Huang R, Corke H. (1998c) Characterization and quantification of betacyanin pigments from diverse *Amaranthus* species. *Journal of Agricultural and Food Chemistry* **51**, 2288–2294.

Cai YZ, Sun M, Corke H. (2001) Identification and distribution of simple and acylated betacyanin pigments in the Amaranthaceae. *Journal of Agricultural and Food Chemistry* **49**, 1971–1978.

Cai YZ, Sun M, Corke H. (2003) Antioxidant activity of betalains from plants of the Amaranthaceae. *Journal of Agricultural and Food Chemistry* **51**, 2288–2294.

Cai YZ, Sun M, Wu HX, Huang RH, Corke H. (2005) Characterization and application of betalain pigments from plants of the Amaranthaceae. *Trends in Food Science and Technology* **16**, 370–376.

Calogero G, Yum JH, Sinopoli A, Di Marco G, Gratzel M, Nazeeruddin MK. (2012) Anthocyanins and betalains as light harvesting pigments for dye-sensitized solar cells. *Solar Energy* **86**, 1563–1575.

Ceccato P, Flasse S, Tarantola S, Jacquemoud S, Gregoire JM. (2001) Detecting vegetation leaf water content using reflectance in the optical domain. *Remote Sensing of Environment* **77**, 22–33.

Chen C, Huang M, Lin KHK, Wong K, Huang S, Yang WD. (2014) Effects of light quality on the growth, development and metabolism of rice seedlings (*Oryza sativa* L.). *Research Journal of Biotechnology* **9**, 15–24.

Chen JW, Kuang SB, Long GQ, Yang SC, Meng ZG, Li LG, Chen ZJ, Zhang GH. (2016) Photosynthesis, light energy partitioning, and photoprotection in the shade-demanding species *Panax notoginseng* under high and low level of growth irradiance. *Functional Plant Biology* **43**, 479–491.

Chow WS, Hope AB. (1987) The stoichiometries of supramolecular complexes in thylakoid membranes from spinach chloroplasts. *Australian Journal of Plant Physiology* **14**, 21–28.

Chow WS, Adamson HY, Anderson JM. (1991) Photosynthetic acclimation of *Tradescantia albiflora* to growth irradiance: lack of adjustment of light harvesting-components and its consequences. *Physiologia Plantarum* **81**, 175–182.

Chow WS, Kim EH, Horton P, Anderson JM. (2005) Granal stacking of thylakoid membranes in higher plant chloroplasts: the physicochemical forces at work and the functional consequences that ensue. *Photochemical & Photobiological* Sciences **4**, 1081–1090.

Christinet L, Burdet F, Zaiko M, Hinz U, Zrÿd JP. (2004) Characterization and functional identification of a novel plant 4,5-extradiol dioxygenase involved in betalain pigment biosynthesis in *Portulaca grandiflora*. *Plant Physiology* **134**, 265–274.

Costea M, DeMason D. (2001) Stem morphology and anatomy in *Amaranthus* L. (Amaranthaceae), taxonomic significance. *Journal of the Torrey Botanical Society* **128**, 254–281.

Das S, Iamonico D. (2014) *Amaranthus bengalense* (Amaranthaceae) a new species from India, with taxonomical notes on *A. blitum* aggregate. *Phytotaxa* **181**, 293–300.

De la Torre WR, Burkey KO. (1990) Acclimation of barley to changes in light intensity: chlorophyll organization. *Photosynthesis Research* **24**, 117–125.

Debus RJ. (1992) The manganese and calcium ions of photosynthetic oxygen evolution. *Biochimica et Biophysica Acta* **1102**, 269–352.

Dekker JP, Boekema EJ. (2005) Supramolecular organization of thylakoid membrane proteins in green plants. *Biochimica et Biophysica Acta* **1706**, 12–39.

DeLoache WC, Russ ZN, Narcross L, Gonzales AM, Martin VJ, Dueber JE. (2015) An enzyme-coupled biosensor enables (S)-reticuline production in yeast from glucose. *Nature Chemical Biology* **11**, 465–471.

de Lucena CC, de Sequeira DL, Martinez HEP, Cecon PR. (2012) Salt stress change chlorophyll fluorescence in mango. *Revista Brasileira de Fructicultura* **34**, 1245–1255.

Demming-Adams B, Adams III WW. (1992) Photoprotection and other responses of plants to high stress. *Annual Review of Plant Physiology and Plant Molecular Biology* **43**, 599-626.

Demming-Adams B, Adams III WW. (2000) Harvesting sunlight safely. *Nature* **403**, 371–374.

Dengler NG, Nelson T. (1999) Leaf structure and development in C4 plants. In: Sage RF and Monson RK. (eds) C4 Plant Biology. San Diego: Academic Press, pp. 133–172.

Durães FOM, Gama EEG, Magalhães PC, Marriel IE, Casela CR, Oliveira AC, Junior AL, Shanahan JF. (2001) The usefulness of chlorophyll fluorescence in screening for disease resistance, water stress tolerance, aluminium toxicity tolerance, and N use efficiency in maize. In: Proceedings of the Seventh Eastern and Southern Africa Regional Maize Conference, pp. 356–360.

Edwards GE, Walker DA. (1983) C3, C4: Mechanisms, and Cellular and Environmental Regulation of Photosynthesis. Berkeley: University of California Press, pp. 543.

Ehrenworth AM, Peralta-Yahya P. (2017) Accelerating the semi-synthesis of alkaloid-based drugs through metabolic engineering. *Nature Chemical Biology* **13**, 249–258.

Ensminger I, Busch F, Hüner NPA. (2006) Photostasis and cold acclimation: sensing low temperature through photosynthesis. *Physiologia Plantarum* **126**, 28–44.

Esau K. (1975) Crystalline inclusion in thylakoids of spinach chloroplasts. *Journal of Ultrastructure Research* **53**, 235–243.

Esau K. (1977) Anatomy of Seed Plants. New York: John Wiley and Sons, pp. 576.

Escribano J, Pedreño MA, Garcia-Carmona F, Muñoz R. (1998) Characterization of the antiradical activity of betalains from *Beta vulgaris* L. roots. *Phytochemical Analysis* **9**, 124–127.

Evans JR, Kaldenhoff R, Genty B, Terashima I. (2009) Resistances along the CO_2 diffusion pathway inside leaves. *Journal of Experimental Botany* **60**, 2235–2248.

Falbel TG, Meehl JB, Staehelin LA. (1996) Severity of mutant phenotype in a series of chlorophyll-deficient wheat mutants depends on light intensity and the severity of the block in chlorophyll synthesis. *Plant Physiology* **112**, 821–832.

Falkowski PG, Chen YB. (2003) Photoacclimation of light harvesting systems in eukaryotic algae. In: Green BR, Parson WW. (eds) Light Harvesting Antennas in Photosynthesis. Dorfrecht: Kluwer Academic Publishers, pp. 423–447.

Foyer CH, Noctor G. (2009) Redox regulation in photosynthetic organisms: signaling, acclimation, and practical implications. *Antioxidants and Redox Signaling* **11**, 861–905.

Frederic SE, Newcomb EH. (1969) Cytochemical localization of catalase in leaf microbodies (peroxisomes). *Journal of Cell Biology* **43**, 34–353.

Fricker MD, Willmer CM. (1996) Stomata. Dordrecht: Springer, pp. 375.

Fristedt R, Willig A, Granath P, Crevecoeur M, Rochaix JD, Vener AV. (2009) Phosphorylation of photosystem II controls functional macroscopic folding of photosynthetic membranes in *Arabidopsis*. *The Plant Cell* **21**, 3950–3964.

Gandia-Herrero F, Garcia-Carmona F. (2013) Biosynthesis of betalains: yellow and violet plant pigments. *Trends in Plant Science* **18**, 334–343.

Gandia-Herrero F, Escribano J, Garcia-Carmona F. (2016) Biological activities of plant pigments betalains. *Critical Reviews in Food Science and Nutrition* **56**, 937–945.

Gannesan P, Karthik T. (2017) Analysis of color strength, color fastness and antimicrobial properties of silk fabric dyed with natural dye from red picky pear fruit. *Journal of the Textile Institute* **108**, 1173–1179.

Gengatharan A, Dykes GA, Choo WS. (2015) Betalains: natural plant pigments with potential application in functional foods. *Food Science and Technology* **64**, 645–649.

Genty B, Briantais JM, Baker NR. (1989) The relationship between the quantum yield of photosynthetic electron transport and quenching of chlorophyll fluorescence. *Biochimica et Biophysica Acta* **990**, 87–92.

Georgiev VG, Weber J, Kneschke EM, Denev PN, Bley T, Pavlov AI. (2010) Antioxidant activity and phenolic content of betalain extracts from intact plants and hairy root cultures of the red beetroot *Beta vulgaris* cv. Detroit dark red. *Plant Foods for Human Nutrition* **65**, 105–111.

Germ M, Bercic OU, Acko DK. (2005) The response of sunflower to acute disturbance in water availability. *Acta Agriculturae Slovenica* **85**.

Givnish TJ. (1988) Adaptation to sun and shade: a whole-plant perspective. *Australian*

Journal of Plant Physiology **15**, 63–92.

Glas JJ, Schimmel BC, Alba JM, Escobar-Bravo R, Schuurink RC, Kant MR. (2012) Plant glandular trichomes as targets for breeding or engineering of resistance to herbivores. *International Journal of Molecular Sciences* **13**, 17077–17103.

Gombos Z, Wada H, Murata N. (1994) The recovery of photosynthesis from low-temperature photoinhibition is accelerated by the unsaturation of membrane lipids: a mechanism of chilling tolerance. *Plant Biology* **91**, 8787–8791.

Gould KS, Kuhn DN, Lee DW, Oberbauer SF. (1995) Why leaves are sometimes red. *Nature* **378**, 241–242.

Gould KS, Markham KR, Smith RH, Goris JJ. (2000) Functional role of anthocyanins in the leaves of *Quintinia serrata* A. Cunn. *Journal of Experimental Botany* **51**, 1107–1115.

Guesmi A, Ladhari N, Hamadi B, Sakli F. (2012) Isolation, identification and dyeing studies of betanin on mofified acrylic fabrics. *Industrial Crops and Products* **37**, 342–346.

Gounaris K, Barber J. (1983) Monogalactosyldiacylglycerol: the most abundant polar lipid in nature. *Trends in Biochemical Sciences* **8**, 378-381.

Gutierrez M, Gracen VE, Edwards GE. (1974). Biochemical and cytological relationships in C4 plants. *Planta* **119**, 279–300.

Gray GR, Boese SR, Hüner NPA. (1994) A comparison of low temperature growth versus low temperature shifts to induce resistance to photoinhibition in spinach (*Spinacia oleracea*). *Physiologia Plantarum* **90**, 560–566.

Gray GR, Savitch LV, Ivanov AG, Huner NPA. (1996) Photosystem II excitation pressure and development of resistance to photoinhibition. (II. Adjustment of photosynthetic capacity in winter wheat and winter rye). *Plant Physiology* **10**, 61–71.

Gray GR, Hope BJ, Qin X, Taylor BG, Whitehead CL. (2003) The characterization of photoinhibition and recovery during cold acclimation in *Arabidopsis thaliana* using chlorophyll fluorescence imaging. *Physiologia Plantarum* **119**, 365–375.

Grieco M, Suorsa M, Jajoo A, Tikkanen M, Aro EM. (2015) Light-harvesting II antenna trimers connect energetically the entire photosynthetic machinery - including both photosystems II and I. *Biochimica et Biophysica Acta* **1847**, 607–619.

Grieco M, Tikkanen M, Paakkarinen V, Kangasjarvi S, Aro EM. (2012) Steady-state phosphorylation of light-harvesting complex II proteins preserves photosystem I under fluctuating white light. *Plant Physiology* **160**, 1896–1910.

Grubben GJH. (2004) *Amaranthus blitum* L. In: Grubben GJH, Denton OA. Plant Resources of Tropical Africa Vol. II. Vegetables (eds) Netherlands: PROTA Foundation, pp. 63–67.

Guesmi A, Ladhari N, Hamadi BN, Sakli F. (2012) Isolation, identification and dyeing studies of betanin on modified acrylic fabrics. *Industrial Crops and Products* **37**, 342–346.

Hansatech Intruments LTD. (2006) Operations manual. Norfolk: King's Lynn, pp. 64.

Hakala M, Tuominen I, Keranen M, Tyystjarvi T, Tyystjarvi E. (2005) Evidence for the role of the oxygen-evolving manganese complex in photoinhibition of photosystem II. *Biochimica et Biophysica Acta* **1706**, 68–80.

Harris NN, Javellana J, Davies KM, Lewis DH, Jameson PE, Deroles SC, Calcott KE, Gould KS, Schwinn KE. (2012) Betalain production is possible in anthocyanin-producing plant species given the presence of DOPA-dioxygenase and L-DOPA. *BMC Plant Biology* **12**, 34–46.

Hatch MD. (1987) C4 photosynthesis: a unique blend of modified biochemistry, anatomy and ultrastructure. *Biochemica et Biophysica Acta* **895,** 81–106.

Hatch MD, Slack CR. (1970) Photosynthetic CO_2-fixation pathways. *Annual Review of Plant Physiology* **21**, 141–162.

Hatch MD, Kagawa T, Craig S. (1987) Subdivision of C4-pathway species based on differing C4 acid decarboxylating systems and ultrastructural features. *Australian Journal of Plant Physiology* **2**, 11–128.

Hayakawa K, Agarie S. (2010) Physiological roles of betacyanin in a halophyte, *Suaeda japonica* Makino. *Plant Production Science* **13**, 351–359.

He HP, Cai Y, Sun M, Corke H. (2002) Extraction and purification of squalene from Amaranthus grain. *Journal of Agricultural and Food Chemistry* **50**, 368–372.

Heckmann D. (2016) C4 photosynthesis evolution: the conditional Mt. Fuji. *Current Opinion in Plant Biology* **31**, 149–154.

Held HW, Saur F. (1971) The inner membrane of the chloroplast envelope as a side of specific metabolite transport. *Biochemica et Biophysica Acta* **243**, 83–91.

Herbach KM, Stintzing FC, Carle R. (2006) Betalain stability and degradation-structural and chromatic aspects. *Journal of Food Science* **71**, R41–R50.

Herrmann KM. (1995) The shikimate pathway–early steps in the biosynthesis of aromatic-compounds. *The Plant Cell* **7**, 907–919.

Hilliard JH, Grasen VE, West SH. (1971) Leaf microbodies (peroxisomes) and catalase localization in plants differing in their photosynthetic carbon pathways. *Planta* **97**, 93-105.

Hocking PJ, Meyer CP. (1991) Effects of CO_2 enrichment and nitrogen stress on growth and partitioning of dry matter and nitrogen in wheat and maize. *Functional Plant Biology* **18**, 339–396.

Hoffmann WA, Poorter H. (2002) Avoiding bias in calculations of relative growth rate. *Annals of Botany* **80**, 37–42.

Hong J, Jiang DA, Weng XY, Wang WB, Hu DW. (2005) Leaf anatomy, chloroplast ultrastructure, and cellular localisation of ribulose-1,5-biphosphate carboxylase/oxygenase (Rubisco) and Rubisco activase in *Amaranthus tricolor* L*. Photosynthetica* **43**, 519–528.

Hopkins WG, Hüner NPA. (2008) Introduction to Plant Physiology. New York: John Wiley, pp. 523.

Horton P. (1999) Are grana necessary for regulation of light harvesting? *Australian Journal of Plant Physiology* **26**, 659–699.

Horton P, Ruban A. (2004) Molecular design of the photosystem II light-harvesting antenna: photosynthesis and photoprotection. *Journal of Experimental Botany* **56**, 365–373.

Hughes NM, Neufeld HS, Burkey KO. (2005) Functional role of anthocyanins in high-light winter leaves of the evergreen herb *Galax urceolata*. *New Phytologist* **168**, 575–587.

Hughes NM, Vogelmmann TC, Smith WK. (2008) Optical effects of abaxial anthocyanin on absorption of red wavelengths by understorey species: revisiting the back-scatter hyphothesis. *Journal of Experimental Botany* **59**, 3435–3442.

Hüner NPA, Öquist G, Hurry VM, Król M, Falk S, Griffith M. (1993) Photosynthesis, photoinhibition and low temperature acclimation in cold tolerant plants. *Photosynthesis Research* **37**, 19–39.

Hüner NPA, Öquist G, Sarhan F. (1998) Energy balance and acclimation to light and cold. *Trends in Plant Science* **3**, 224–230.

Hüner NPA, Öquist G, Melis A. (2003) Photostasis in plants, green algae and cyanobacteria: the role of light harvesting complexes. In Green BR, Parson WW. (eds) Light Harvesting Antennas in Photosynthesis. Dordrecht: Springer, pp. 404–421.

Iamonico D. (2014a) *Amarathus gangeticus* (Amaranthaceae), a name *incertae sedis*.

Phytotaxa **162**, 299–300.

Iamonico D. (2014b) Lectotypification of Linnaean names in the genus *Amaranthus* L. (Amaranthaceae). *Taxon* **63**, 146–150.

Iamonico D. (2016a) Nomenclature survey of the genus *Amaranthus* (Amaranthaceae). 4. Detailed questions arising around the name *Amaranthus gracilis*. *Botanica Serbica* **40**, 61–68.

Iamonico D. (2016b) Nomenclature survey of the genus *Amaranthus* (Amaranthaceae). 5. Moquin-Tandon's names. *Phytotaxa* **273**, 81–114.

Ibdah M, Krins A, Seidlitz H. (2002) Spectral dependence of flavonol and betacyanin accumulation in *Mesembryanthemum crystallinum* under enhanced ultraviolet radiation. *Plant, Cell & Environment* **25**, 1145–1154.

Jang C, Seo EY, Nam J, Bae H, Gim YG, Kim HG, Cho IS, Lee ZW, Bauchan GR, Hammond J, Lim HS. (2013) Insights into *Alternanthera mosaic virus* TGB3 functions: interactions with *Nicotiana benthamiana* PcbO correlate with chloroplast vesiculation and veinal necrosis caused by TGB3 over-expression. *Frontiers in Plant Science* **4**.

Jansson S. (1999) A guide to the Lhc genes and their relatives in *Arabidopsis*. *Trends in Plant Science* **4**, 236–240.

Järvi S, Suorsa M, Aro EM. (2015) Photosystem II repair and plant chloroplasts-regulation, assisting proteins and shared components with photosystem II biogenesis. *Biochimica et Biophysica Acta* **1847**, 900–909.

Järvi S, Isojärvi J, Kangasjärvi S, Saljärvi J, Mamedov F, Suorsa M, Aro EM. (2016) Photosystem II repair and plant immunity: lessons learned from *Arabidopsis* mutant lacking the THYLAKOID LUMEN PROTEIN 18.3. *Frontiers in Plant Science* **7**, 405.

Johnson MP, Vasilev C, Olsen JD, Hunter CN. (2014) Nanodomains of cytochrome b6f and photosystem II complexes in spinach grana thylakoid membranes. *The Plant Cell*, **26**, 3051–3061.

Kadoshnikov SI, Kadoshnikova IG, Kulikov YA, Martirosyan DM. (2008) Researches of fractional composition of protein of amaranth. *Current Nutrition & Food Science* **4**:196–205.

Kalaji HM, Oukarroum A, Alexandrov V, Kouzmanova M, Brestic M, Zivck M, Sanborska IA, Cetner MD, Allakherdiev SI, Goltsev V. (2014) Identification of nutrient deficiency in maize and tomato plants by in vivo chlorophyll *a* fluorescence measurements. *Plant Physiology and Biochemistry* **81**, 16–25.

Khan MI. (2016) Plant betalains: safety, antioxidant activity, clinical efficacy, and

bioavailability. *Comprehensive Reviews in Food Science and Food Safety* **15**, 316–330.

Kim GT, Yano S, Kozuka T, Tsukaya H. (2005) Photomorphogenesis of leaves: shade-avoidance and differentiation of sun and shade leaves. *Photochemical and Sciences* **4**, 770–774.

Kirchhoff H, Mukherjee U, Galla HJ. (2002) Molecular architecture of the thylakoid membrane: lipid diffusion space for plastoquinone. *Biochemistry* **41**, 4872–4882.

Kirchhoff H, Lenhert S, Buchel C, Chi L, Nield J. (2008) Probing the organization of photosystem II in photosynthetic membranes by atomic force microscopy. *Biochemistry* **47**, 431–440.

Kirchhoff H, Hall C, Wood M, Herbstovà M, Tsabari O, Nevo R, Charuvi D, Shimoni E, Reich Z. (2011) Dynamic control of protein diffusion within the granal thylakoid lumen. *Proceedings of the National Academy of Sciences of the United States of America* **108**, 20248–20253.

Kirchhoff H. (2014) Diffusion of molecules and macromolecules in thylakoid membranes. *Biochimica et Biophysica Acta* **1837**, 495–502.

Klimczak I, Malecka M, Pacholek B. (2002) Antioxidant activity of ethanolic extracts of Amaranth seeds. *Food* **46**, 184–186.

Koivuniemi A, Aro EM, Andersson B. (1995) Degradation of the D1- and D2-proteins of photosystem II in higher plants is regulated by reversible phosphorylation. *Biochemistry* **34**, 16022–16029.

Koizumi M, Takahashi K, Mineuchi K, Nakamura T, Kano H. (1998) Light gradients and the transverse distribution of chlorophyll fluorescence in mangrove and *Camellia* leaves. *Annals of Botany* **81**, 527–533.

Kong SG, Wada M. (2014) Recent advances in understanding the molecular mechanism of chloroplast photorelocation movement. *Biochimica et Biophysica Acta* **1837**, 522–530.

Korres NE, Frowd-Williams RJ, Moss SR. (2003) Chlorophyll fluorescence technique as a rapid diagnostic test of the effects of the photosynthetic inhibitor chlorotoluron on two winter wheat cultivars. *Annals of Applied Biology* **143**, 53–56.

Kościelniak J, Janowiak F, Kurczych Z. (2005) Increase in photosynthesis of maize hybrids (*Zea mays* L.) at suboptimal temperature (15°C) by selection of parental lines on the basis of chlorophyll *a* fluorescence measurements. *Photosynthetica* **43**, 125–134.

Kramer DM, Johnson G, Kiirats O, Edwards GE. (2004) New fluorescence parameters for determination of Q_A redox state and excitation energy fluxes. *Photosynthesis Research* **79**, 209–218.

Krause GH. (1988) Photoinhibition of photosynthesis. An evaluation of damaging and protective mechanisms. *Physiologia Plantarum* **41**, 1044–1049.

Krause GH, Weis E. (1991) Chlorophyll fluorescence and photosynthesis: the basics. *Annual Review of Plant Physiology and Plant Molecular Biology* **42**, 313–349.

Krause GH. (1994a) Photoinhibition induced by low temperatures. In: Baker NR, Bowyer JR. (eds) Photoinhibition of Photosynthesis. From Molecular Mechanisms to the Field. Oxford: BIOS Scientific Publishers, pp. 331–348.

Krause GH. (1994b) The role of oxygen in photoinhibition of photosynthesis. In: Foyer CF, Mullineaux CW. (eds) Causes of Photooxidative Stress and Amelioration of Defense Systems in Plants. Boca Raton: Chemical Rubber Company Press, pp. 43–76.

Król M, Gray GR, Hurry VM, Öquist G, Malek L, Hüner NPA. (1995) Low-temperature stress and photoperiod affect an increased tolerance to photoinhibition in *Pinus banksiana* seedlings. *Canadian Journal of Botany* **73**, 1119–1127.

Król M, Ivanov AG, Jansson S, Kloppstech K, Hüner NPA. (1999) Greening under high light or cold temperature affects the level of xanthophyll-cycle pigments, early light-inducible proteins, and light-harvesting polypeptides in the wild-type barley and the chlorina f2 mutant. *Plant Physiology* **120**, 193–204.

Kugler F, Stintzing FC, Carle R. (2004) Identification of betalains from petioles of differently colored swiss chard (*Beta vulgaris L. ssp. cicla* [L.] Alef. Cv. Bright Lights) by high-performance liquid chromatography−electrospray ionization mass spectrometry. *Journal of Agricultural and Food Chemistry* **52**, 2975–2981.

Kugler F, Stintzing FC, Carle R. (2007) Characterisation of betalain patterns of differently coloured inflorescences from *Gomphrena globosa* L. and *Bougainvillea* sp. by HPLC–DAD–ESI–MSn. *Analytical and Bioanalytical Chemistry* **387**, 637–648.

Kulma A, Szopa J. (2007) Catecholamines are active compounds in plants. *Plant Science* **172**, 433–440.

Kuklin AI, Conger BV. (1995) Catecholamines in plants. *Journal of Plant Growth Regulation* **14**, 91–97.

Kurasova I, Kalina J, Štroch M, Urban O, Špunda V. (2003) Response of photosynthetic apparatus of spring barley (*Hordeum vulgare* L.) to combined effect of elevated CO_2 concentration and different growth irradiance. *Photosynthetica* **41**, 209–219.

Lambers H, Chapin III FS, Pons TL. (1998) Response of photosynthesis to light. In: Plant Physiological Ecology. New York: Springer, pp. 26–47.

Larcher W. (1994) Photosynthesis as a tool for indicating temperature stress events. In: Schulze ED, Caldwell MM. (eds) Ecophysiology of Photosynthesis. Berlin: Springer-Verlag, pp. 261–277.

Larkcom J. (1991) Oriental vegetables: the complete guide for garden and kitchen. London: John Murray, pp. 232.

Larkin RM, Stefano G, Ruckle ME, Stavoe AK, Sinkler CA, Brandizzi F, Malmstrom CM, Osteryoung KW. (2016) Reduced chloroplast coverage genes from *Arabidopsis thaliana* help to establish the size of the chloroplast compartment. *Proceedings of the National Academy of Sciences of the United States of America* **113**, E1116–E1125.

Lee HY, Hong YN, Chow WD. (2001) Photoinactivation of photosystem II complexes and photoprotection by non-functional neighbors in *Capsicum annuum* L. *Planta* **212**, 232–242.

Leong TY, Anderson JM. (1984a) Adaptation of the thylakoid membranes of pea chloroplasts to light intensities.1. Study on the distribution of chlorophyll-protein complexes. *Photosynthesis Research* **5**, 105–115.

Leong TY, Anderson JM. (1984b) Adaptation of the thylakoid membranes of pea chloroplasts to light intensities II. Regulation of electron transport capacities, electron transport carriers, coupling factor (CF1) activity and rates of photosynthesis. *Photosynthesis Research* **5**, 117–128.

Li Q, Deng M, Xiong Y, Coombes A, Zhao W. (2014) Morphological and photosynthetic response to high and low irradiance of *Aeschynanthus longicaulis. The Scientific World Journa*l **2014**, Article ID 347461.

Li XP, Björkman O, Connie S, Grossman AR, Rosenquist M, Jansson S, Niyogi KK. (2000) A pigment -binding protein essential for regulation of photosynthetic light harvesting. *Nature* **403**, 391-395.

Liakopoulos G, Stavrianakou S, Karabourniotis G. (2006) Trichome layers versus dehaired lamina of *Olea europaea* leaves: differences in flavonoid distribution, UV-absorbing capacity, and wax yield. *Environmental and Experimental Botany* **55**, 294–304.

Lichtenthaler HK. (1981) Adaptation of leaves and chloroplasts to high quanta fluence rates. In: Akoyunoglou G. (ed) Photosynthesis. VI. Photosynthesis and Productivity. Philadelphia: Balaban International Science Service, 273–287.

Lichtenthaler HK, Buschmann C, Döli M, Fietz HJ, Bach T, Kozel U, Meier D,

Rahmsdorf U. (1981) Photosynthetic activity, chloroplast ultrastructure, and leaf characteristics of high-light and low-light plants and of sun and shade leaves. *Photosynthesis Research* **2**, 115-141.

Lichtenthaler HK, Welburn AR. (1983) Determination of total carotenoids and chlorophylls *a* and *b* of leaf extracts in different solvents. *Biochemical Society Transactions* **11**, 591–592.

Lichtenthaler HK, Ač A, Marek MV, Kalina J, Urban O. (2007). Differences in pigment composition, photosynthetic rates and chlorophyll fluorescence images of sun and shade leaves of four tree species. *Plant Physiology and Biochemistry* **45**, 577–588.

Lindahl M, Yang DH, Andersson B. (1995) Regulatory proteolysis of the major light-harvesting chlorophyll *a/b* protein of photosystem II by a light-induced membrane-associated enzymic system. *European Journal of Biochemistry* **231**, 503–509.

Lindeboom N, Chang P, Tyler R. (2004) Analytical, biochemical and physicochemical aspects of starch granule size, with emphasis on small granule starches. *Starch* **56**, 89–99.

Livingston AK, Cruz JA, Kohzuma K, Dhindra A, Kramer DM. (2010) An *Arabidopsis* mutant with high cyclic electron flow around photosystem I (hcef) involving the NADPH dehydrogenase complex. *The Plant Cell* **22**, 221–233.

Long SP. (1999) Environmental responses. In: Sage RF and Monson RK. C4 Plant Biology. (eds) San Diego: Academic Press, pp. 215–249.

Louwerse W, Zweerde WVD. (1977) Photosynthesis, transpiration and leaf morphology of *Phaseolus* and *Zea mays* frown at different irradiance in artificial and sunlight. *Photosynthetica* **11**, 11–21.

Malkin R, Niyogi K. (2000) Photosynthesis. In: Buchanan BB, Gruissem W, Jones RL. (eds) Biochemistry & Molecular Biology of Plants. Rockville: American Society of Plant Physiologists, pp. 568–628.

Mauricio R, Rausher MD. (1997) Experimental manipulation of putative selective agents provides evidence for the role of natural enemies in the evolution of plant defense. *Evolution* **51**, 1435–1444.

Marx JL. (1977) Amaranth: A comeback of the food of the Aztecs? *Science* **198**, 40.

Maxwell K, Johnson GN. (2000) Chlorophyll fluorescence - a practical guide. *Journal of Experimental Botany* **51**, 659–668.

Melis A. (1999) Photosystem II damage and repair cycle in chloroplasts: what modulates the rate of photodamage in vivo? *Trends in Plant Science* **4**, 130–135.

Metcalfe CR, Chalk L. (1950) Anatomy of the dicotyledons.Vol. I and II. Oxford: Clarendon Press, pp. 1500.

Mishra Y, Yankanpaa HJ, Kiss AZ, Funk C, Schroder WP, Jansson S. (2012) A*rabidopsis* plants grown in the field and climate chambers significantly differ in leaf morphology and photosystem components. *BMC Plant Biology* **12**, 6.

Mosco A. (2012) Tissue localization of betacyanins in cactus stems. *Revista Mexicana de Biodiversidad* **83**, 413–420.

Mullineaux CW. (2008) Factors controlling the mobility of photosynthetic proteins. *Photochemistry and Photobiology* **84**, 1310–1316.

Müller P, Li XP, Niyogi KK. (2001) Nonphotochemical quenching. A response to excess light energy. *Plant Physiology* **125**, 1558–1566.

Mulo P, Sirpiö S, Suorsa M, Aro EM. (2008) Auxiliary proteins involved in the assembly and sustenance of photosystem II. *Photosynthesis Research* **98**, 489–501.

Murchie EH, Horton P. (1997) Acclimation of photosynthesis to irradiance and spectral quality in British plant species: chlorophyll content, photosynthetic capacity and habitat preference. *Plant, Cell & Envoronment* **20**, 438–448.

Myers DA, Vogelmann TC, Bornman JF. (1994) Epidermal focusing and effects on light utilization in *Oxalis acetosella. Physiologia Plantarum* **91**, 651–656.

Nagatsu T, Sawada M. (2009) L-dopa therapy for Parkinson's disease: past, present, and future. *Parkinsonism & Related Disorders* **15**, S3–S8.

Nakashima T, Araki T, Ueno O. (2011) Photoprotective function of betacyanin in leaves of *Amaranthus cruentus* L. under water stress. *Photosynthetica* **49**, 497–506.

National Research Council. (1984) Amaranth: Modern Prospects for an Ancient Crop. (eds) Washington D.C.: National Academy Press, pp. 81.

Natural Resources Conservation Service PLANTS Database, USDA. (2018) The PLANTS Database (http://plants.usda.gov, 5 June 2018). National Plant Data Team, Greensboro, NC 27401-4901 USA.

Navari-Izzo F, Quartacci MF, Pinzino C, Rascio N, Vazzana C, Sgherii CLM. (2000) Protein dynamics in thylakoids of the desiccation-tolerant plant *Boea hygrscopica* during dehydration and rehydration. *Plant Physiology* **124**, 1427–1436.

Neill SO, Gould KS. (2003) Anthocyanins in leaves: light attenuators or antioxidants? *Functional Plant Biology* **30**, 865–873.

Nelson N, Yocum CF. (2006) Structure and function of photosystems I and II. *Annual Review of Plant Biology* **57**, 521–565.

Nelson N, Junge W. (2015) Structure and energy transfer in photosystems of oxygenic photosynthesis. *Annual Review of Biochemistry* **84**, 659–683.

Nickelsen J, Rengstl B. (2013) Photosystem II assembly: from cyanobacteria to plants. *Annual Review of Plant Biology* **64**, 609–635.

Niinemets Ü, Dìaz-Espejo A, Flexas J, Galmès J, Warren CR. (2009) Role of mesophyll diffusion conductance in constraining potential photosynthetic productivity in the field. *Journal of Experimental Botany* **60**, 2249–2270.

Nishiyama Y, Yamamoto H, Allakhverdiev SI, Inaba M, Yokota A, Murata N. (2001) Oxidative stress inhibits the repair of photodamage to the photosynthetic machinery. *EMBO Journal* **20**, 5587–5594.

Nixon PJ, Michoux F, Yu J, Boehm M, Komenda J. (2010) Recent advances in understanding the assembly and repair of photosystem II. *Annals of Botany* **106**,1–16.

Niyogi KK. (1999) Photoprotection revisited: genetic and molecular approaches. *Annual Review of Plant Physiology and Plant Molecular Biology* **50**, 333–359.

Nomura T, Kutchan TM. (2010) Three new O-methyltransferases are sufficient for all O-methylation reactions of ipecac alkaloid biosynthesis in root culture of *Psychotria ipecacuanha*. *Journal of Biological Chemistry* **285**, 7722–7738.

Oaks A. (1994) Efficiency of nitrogen utilization in C3 and C4 cereals. *Plant Physiology* **106**, 407–414.

Oguchi R, Hikosaka K, Hirose T. (2005) Leaf anatomy as a constraint for photosynthetic acclimation: differential responses in leaf anatomy to increasing growth irradiance among three deciduous trees. *Plant, Cell & Environment* **28**, 916–927.

Oguchi R, Douwstra P, Fujita T, Chow WS, Terashima I. (2011) Intra-leaf gradients of photoinhibition induced by different color lights: implications for the dual mechanisms of photoinhibition and for the application of conventional chlorophyll fluorometers. *New Phytologist* **191**, 146–159.

Ohnishi N, Allkhverdiev SI, Takahashi S, Higashi S, Watanabe M, Nishiyama Y, Murata N. (2005) Two-step mechanisms of photodamage to photosystem II: step 1 occurs at the oxygen-evolving complex and step 2 occurs at the photochemical reaction center. *Biochemistry* **44**, 8494–8499.

Osmond CB. (1994) What is photoinhibition? Some insights from comparisons of sun and shade plants. In: Baker NR and Bowyer JR. (eds) Photoinhibition of

Photosynthesis: from Molecular Mechanisms to the Field. Oxford: Bios Scientific Publishers, pp. 1–24.

Ozsoy N, Yilmaz T, Kurt O, Can A, Yanardag R. (2009) In vitro antioxidant activity of *Amaranthus lividus* L. *Food Chemistry* **116**, 867–872.

Pagliano C, Nield J, Marsano F, Pape T, Barera S, Saracco G, Barber J. (2014) Proteomic characterization and three-dimensional electron microscopy study of PSII-LHCII supercomplexes from higher plants. *Biochimica et Biophysica Acta* **1837**, 1454–1462.

Pearcy RW, Calkin HW. (1993) Carbon dioxide exchange of C3 and C4 tree species in the understory of a Hawaiian forest. *Oecologia* **58**, 26–32.

Pearcy RW, Franceschi VR. (1986) Photosynthetic characteristics and chloroplast ultrastructure of C3 and C4 tree species grown in high- and low-light environments. *Photosynthesis Research* **9**, 317–331.

Pengelly JJL, Xavier RR, Sirault YT, John R E, Robert TF, von Caemmerer S. (2010) Growth of the C4 dicot *Flaveria bidentis*: photosynthetic acclimation to low light through shifts in leaf anatomy and biochemistry. *Journal of Experimental Botany* **61**, 4109–4122.

Petit-Paly G, Andreu F, Chénieux JC, Rideau M. (1994) *Phytolacca americana* L. (Pokeweed): in vitro production of betacyanins and medicinal compounds. In: Bajaj YPS. (ed) Medicinal and Aromatic Plants. Vol. 7. Berlin: Springer, pp. 366–385.

Petr J, Michalik I, Tlaskalova H, Capouchova I, Famera O, Urminska D, Tukova L, Knoblochova H. (2003) Extension of the spectra of plant products for the diet in celiac disease. *Czech Journal of Food Sciences* **21**, 59–70.

Polturak G, Breitel D, Grossman N, Sarrion-Perdigones A, Weithorn E, Pliner M, Orzaez D, Granell A, Rogachev I, Aharoni A. (2016) Elucidation of the first committed step in betalain biosynthesis enables the heterologous engineering of betalain pigments in plants. *New Phytologist* **210**, 269–283.

Polturak G, Aharoni A. (2018) “La vie en Rose”: biosynthesis, sources, and applications of betalains pigments. *Molecular Plant* **11**, 7–22.

Polturak G, Grossman N, Vela-Corcia D, Dong Y, Nudel A, Pliner M, Levy M, Rogachev I, Aharoni A. (2017) Engineered gray mold resistance, antioxidant capacity, and pigmentation in betalain-producing crops and ornamentals. *Proceedings of the National Academy of Sciences of the United States of America* **114**, 9062–9067.

Powles SB. (1984) Photoinhibition of photosynthesis induced by visible light. *Annual Review of Plant Physiology* **35**, 15–44.

Pribil M, Pesaresi P, Hertle A, Barbato R, Leister D. (2010) Role of plastid protein phosphatase TAP38 in LHCII dephosphorylation and thylakoid electron flow. *PLoS Biology*, **8**, e1000288.

Pribil M, Labs M, Leister D. (2014) Structure of thylakoids in land plants. *Journal of Experimental Botany* **65**, 1955–1972.

Puterka GJ, Farone W, Palmer T, Barrington A. (2003) Structure-function relationships affecting the insecticidal and miticidal activity of sugar esters. *Journal of Economic Entomology* **96**, 636–644.

Reece JB, Urry LA, Cain ML, Wasserman SA, Minorsky PV, Jackson RB. (2010) The cell. In: Campbell Biology. Chapter 10. San Francisco: Pearson Education Inc., pp. 92–246.

Reynolds ES. (1963) The use of lead citrate at high pH as an electron-opaque stain in electron microscopy. *Journal of Cell Biology* **17**, 208–212.

Rintamäki E, Martinsuo P, Pursiheimo S, Aro EM. (2000) Cooperative regulation of light-harvesting complex II phosphorylation via the plastoquinol and ferredoxin- *the* thioredoxin system in chloroplasts. *Proceedings of the National Academy of Sciences of the United States of America* **97**, 11644–11649.

Rintamäki E, Salonen M, Suoranta UM, Carlberg I, Andersson B, Aro EM. (1997) Phosphorylation of light-harvesting complex II and photosystem II core proteins shows different irradiance-dependent regulation in vivo: application of phosphothreonine antibodies to analysis of thylakoid phosphoproteins. *Journal of Biological Chemistry* **272**, 30476–30482.

Royer DL. (2001) Stomatal density and stomatal index as indicators of paleoatmospheric CO_2 concentration. *Review of Palaeobotany and Palynology* **114**, 1–28.

Ruban AV. (2009) Plants in light. *Communicative and Integrative Biology* **2**, 50–55.

Ruban AV, Johnson MP, Duffy CD. (2012) The photoprotective molecular switch in the Photosystem II antenna. *Biochimica et Biophysica Acta* **1817**, 167–181.

Rueden CT, Schindelin J, Hiner MC, DeZonia BE, Walter AE, Arena ET, Eliceiri KW. (2017) ImageJ2: ImageJ for the next generation of scientific data. *BMC Bioinformatics* **18**, 529.

Sage RF. (1999) Why C4 photosynthesis? In: Sage RF and Monson RK. (eds) C4 Plant Biology. San Diego: Academic Press, pp. 473–507.
Sage RF. (2004) The evolution of C4 photosynthesis. *New Phytologist* **161**, 341–370.

Sage RF, McKown AD. (2006) Is C4 photosynthesis less phenotypically plastic than C3 photosynthesis? *Journal of Experimental Botany* **57**, 303–317.

Sage RF, Monson RK. (1999) C4 Plant Biology. San Diego: Academic Press, pp. 616.

Salisbury EJ. (1928) On the causes and ecological significance of stomatal frequency, with special reference to the woodland flora. *Physiological Transactions of the Royal Society B: Biological Sciences* **216**, 1–65.

Sani HA, Rahmat A, Ismail M, Rosli R, Endrini S. (2004) Potential anticancer effect of red spinach (*Amaranthus gangeticus*) extract. *Asia Pacific Journal of Clinical Nutrition*, **13**, 396–400.

Sauer JD. (1967) The grain amaranths and their relatives: a revised taxonomic and geographic survey. *Annals of the Missouri Botanical Garden* **54**, 102–137.

Sauer JD. (1976) Grain amaranths, *Amaranthus* spp. (Amaranthaceae). In: Simmonds NW. (ed) Evolution of Crop Plants, London: Longman, pp. 4–7.

Sauer JD. (1993) Historical Geography of Crop Plants: A Select Roster. Boca Raton: Chemical Rubber Company Press, pp. 320.

Saunders RM, Becker R. (1984) Amaranthus- a potential food and feed resource. *Advances in Cereals Science and Technology* **6**, 357–396.

Schilmiller AL, Last RL, Pichersky E. (2008) Harnessing plant trichome biochemistry for the production of useful compounds. *The Plant Journal* **54**, 702–711.

Schindelin J, Arganda-Carreras I, Frise E, Kaynig V, Longair M, Pietzsch T, Preibisch S, Rueden C, Saalfeld S, Schmid B, Tinevez JY, White DJ, Hartenstein V, Eliceiri K, Tomancak P, Cardona A. (2012) Fiji: an open-source platform for biological-image analysis. *Nature Methods* **9**, 676–682.

Samol I, Shapiguzov A, Ingelsson B, Fucile G, Crèvecoeur M, Vener AV, Rochaix JD, Goldschmidt-Cllermont M. (2012) Identification of a photosystem II phospahatase involved in light acclimation in *Arabidopsis*. *The Plant Cell* **24**, 2596–2609.

Schreiber U, Bilger W, Neubauer C. (1994) Chlorophyll fluorescence as a non-intrusive indicator for rapid assessment of in vivo photosynthesis. In: Schulze ED, Caldwell MM. (eds) Ecophysiology of Photosynthesis. Berlin: Springer, pp. 49–70.

Shapiguzov A, Ingelsson B, Samol I, Andres C, Kessler F, Rochaix JD, Vener AV, Goldschmidt-Clermont M. (2010) The PPH1 phosphatase is specifically involved in LHCII dephosphorylation and state transitions in *Arabidopsis*. *Proceedings of the National Academy of Sciences of the United States of America* **107**, 4782–4787.

Shikanai T. (2007) Cyclic electron transport around photosystem I: genetic approaches. *Annual Review of Plant Biology* **58**, 199–217.

Shimoni E, Rav-Hon O, Ohad I, Brumfeld V, Reich Z. (2005) Three-dimensional organization of higher-plant chloroplast thylakoid membranes revealed by electron tomography. *The Plant Cell* **17**, 2580–2586.

Shojima S, Nishizawa NK, Mori S. (1987) Do intrathylakoidal inclusions really contain RuBPCase? *Protoplasma* **140**, 187–189.

Shu Z, Shao L, Huang HY, Zeng XQ, Lin ZF, Chen GY, Peng CL. (2009) Comparison of thermostability of PSII between the chromatic and green leaf cultivars of *Amaranthus tricolor* L. *Photosynthetica* **47**, 548–558.

Shukla S, Pandey V, Pachauri G, Dixit BS, Banerji R, Singh SP. (2003) Nutritional contents of different foliage cuttings oof vegetable amaranth. *Plant Foods for Human Nutrition* **58**, 1–8.

Shukla S, Bhargava A, Chatterjee A, Srivastava J, Singh N, Singh SP. (2006) Mineral profile and variability in vegetable amaranth (*Amaranthus tricolor*). *Plant Foods for Human Nutrition* **61**, 23–28.

Shukla A, Srivastava N, Suneja P, Yadav SK, Hussain Z, Rana JC, Yadav A. (2017) Untapped amaranth (*Amaranthus* spp.) genetic diversity with potential for nutritional enhancement. *Genetic Resources and Crop Evolution*.

Sivakumar V, Anna JL, Vijayeeswarri J, Swaminathan G. (2009) Ultrasound assisted enhancement in natural dye extraction from beetroot for industrial applications and natural dyeing of leather. *Ultrasonics Sonochemistry* **16**, 782–789.

Skillman JB, Garcia M, Virgo A, Winter K. (2005) Growth irradiance effects on photosynthetic and growth in two co-occuring shade-tolerant neotropical perennials of contrasting photosynthetic pathways. *American Journal of Botany* **92**, 1811–1819.

Solomon EI, Sundaram UM, Machonkin TE. (1996) Multicopper oxidases and oxygenases. *Chemical Reviews* **96**, 2563–2605.

Solovchenko AE, Merzlyak MN. (2008) Screening of visible and UV radiation as a photoprotective mechanism in plants. *Russian Journal of Plant Physiology* **55**, 719–737.

Sommer M, Brautigam A, Weber AP. (2012) The dicotyledonous NAD malic enzyme C4 plant *Cleome gynandra* displays age-dependent plasticity of C4 decarboxylation biochemistry. *Plant Biology* **14**, 621–629.

Sonawane BV, Sharwood RE, Whitney S, Ghannoum O. (2018) Shade compromises the photosynthetic efficiency of NADP-ME less than that of PEP-CK and NAD-ME

grasses. *The Journal of Experimental Botany,* **69**, 3053-3068.

Sprey B. (1977) Lamellae-bound inclusions in isolated spinach chloroplasts.1. Ultrastructure and isolation. *Zeitschrift für Pflanzenphysiologie* **83**, 159–179.

Sprey B, Lambert C. (1977) Lamellae-bound inclusions in isolated spinach chloroplasts. 2. Identification and composition. *Zeitschrift für Pflanzenphysiologie* **83**, 227–247.

Spring O, Pfannstiel J, Klaiber I, Conrad J, Beifuß U, Apel L, Aschenbrenner AK, Zipper R. (2015) The non-volatile metabolome of sunflower linear glandular trichomes. *Phytochemistry* **119**, 83–89.

Srinivasan A, Takeda H, Senboku T. (1996) Heat tolerance in food legumes as evaluated by cell membrane thermostability and chlorophyll fluorescence techniques. *Euphytica* **88**, 35–45.

Stafford HA. (1994). Anthocyanins and betalains: evolution of the mutually exclusive pathways. *Plant Science* **101**, 91–98.

Stintzing FC, Carle R. (2004) Functional properties of anthocyanins and betalains in plants, food, and in human nutrition. *Trends in Food Science and Technology* **15**, 19–38.

Stintzing F, Carle R. (2007) Betalains–emerging prospects for food scientists. *Trends in Food Science and Technology* **18**, 514–525.

Strack D, Vogt T, Schliemann W. (2003) Recent advances in betalains research. *Phytochemistry* **62**, 247–69.

Sun J, Nishio JN, Vogelmann TC. (1998). Green light drives CO_2 fixation deep within leaves. *Plant & Cell Physiology* **39**, 1020-1026.

Szczepanik J, Sowinski P. (2014) The occurrence of chloroplast peripheral reticulum in grasses: a matter of phylogeny or a matter of function? *Acta Physiologiae Plantarum* **36**, 1133–1142.

Taiz L, Zeiger E, Møller IM, Murphy A. (2015) Plant Physiology and Development. Sunderland: Sinauer Associates, pp. 761.

Takahashi S, Milward SE, Yamori W, Evans JR, Hillier W, Badger MR. (2010) The solar action spectrum of photosystem II damage. *Plant Physiology* **153**, 988–993.

Takahashi S, Badger MR. (2011) Photoprotection in plants: a new light on photosystem II damage. *Trends in Plant Science* **16**, 53–60.

Takabayashi A, Kishine M, Asada K, Endo T, Sato F. (2005) Differential use of two

cyclic electron flows around photosystem I for driving CO_2-concentration mechanism in C4 photosynthesis. *Proceedings of the National Academy of Sciences of the United States of America* **102**, 16898–16903.

Tanaka Y, Sasaki N, Ohmiya A. (2008) Biosynthesis of plant pigments: anthocyanins, betalains and carotenoids. *The Plant Journal* **54**, 733–749.

Tanino KK, Taylor M, Imai H, Jessa H. (2014) Novel low light tolerant edible crops. Progress Report for ADF Project #20140124, Saskatchewan Ministry of Agriculture Department of Plant Sciences, College of Agriculture and Bioresources, University of Saskatchewan.

Tattini M, Gravano E, Pinelli P, Mulinacci N, Romani A. (2000) Flavonoids accumulate in leaves and glandular trichomes of *Phillyrea latifolia* exposed to excess solar radiation. *New Phytologist* **148**, 69–77.

Tazoe Y, Noguchi K, Terashima I. (2006) Effects of growth light and nitrogen nutrition on the organization of the photosynthetic apparatus in leaves of a C4 plant, *Amaranthus cruentus*. *Plant, Cell & Environment* **29**, 691–700.

Tazoe Y, Hanba YT, Furamoto T, Noguchi K, Terashima I. (2008) Relationships between quantum yield for CO_2 assimilation, activity of key enzymes and CO_2 leakiness in *Amaranthus cruenthus*, a C4 dicot, growth in high or low light. *Plant & Cell Physiology* **49**,19–29.

Tenore GC, Novellino E, Basile A. (2012) Nutraceutical potential and antioxidant benefits of red pitaya (*Hylocereus polyrhizus*) extracts. *Journal of Functional Foods* **4**, 129–136.

Terashima I, Miyazawa S, Hanba Y. (2001) Why are sun leaves thicker than shade leaves? –Consideration based on analyses of CO_2 diffusion in the leaf. *Journal of Plant Research* **114**, 93–105.

Terashima I, Hanba YT, Tazoe Y, Vyas P, Yano S. (2006) Irradiance and phenotype: comparative eco-development of sun and shade leaves in relation to photosynthetic CO_2 diffusion. *Journal of Experimental Botany* **57**, 343–354.

Terashima I, Fujita T, Inoue T, Chow WS, Oguchi R. (2009) Green light drives leaf photosynthesis more efficiently than red light in strong white light: revisiting the enigmatic question of why leaves are green. *Plant & Cell Physiology* **39**, 1020–1026.

Thayer SS, Björkman O. (1990) Leaf xanthophyll content and composition in sun and shade leaves. *Photosynthesis Research* **23**, 331–343.

The Plant List (2013). Version 1.1. Published on the Internet; http://www.theplantlist.org/ (accessed 1st January).

Tikkanen M, Piippo M, Suorsa M, Sirpiö S, Mulo P, Vainonen J, Vener AV, Allahverdiyeva Y, Aro EM. (2006) State transitions revisited: a buffering system for dynamic low light acclimation of *Arabidopsis. Plant Molecular Biology* **62**, 779–793.

Tikkanen M, Nurmi M, Kangasjärvi S, Aro EM. (2008a) Core protein phosphorylation facilitates the repair of photodamaged photosystem II at high light. *Biochimica et Biophysica Acta* **1777**, 1432–1437.

Tikkanen M, Nurmi M, Suorsa M, Danielsson R, Mamedov F, Styring S, Aro EM. (2008b) Phosphorylation-dependent regulation of excitation energy distribution between the two photosystems in higher plants. *Biochimica et Biophysica Acta* **1777**, 425–432.

Tikkanen M, Grieco M, Kangasjärvi S, Aro EM. (2010) Thylakod protein phosphorylation in higher plant chloroplasts optimizes electron transfer under fluctuating light. *Plant Physiology* **152**, 723–735.

Tomizioli M. (2014) Proteomic and functional analysis of chloroplast and thylacoids sub-compartments. Molecular biology, Universite de Grenoble (online), pp. 237.

Trissl HW, Wilhelm C. (1993) Why do thylakoid membranes from higher plants form grana stacks? *Trends in Biochemical Sciences* **18**, 415–419.

Tsutsumi N, Tohya M, Nakashima T, Ueno O. (2017) Variations in structural, biochemical, and physiological traits of photosynthesis and resource use efficiency in *Amaranthus* species (NAD-ME-type C4). *Plant Production Science* **20**, 300–312.

Tyszka-Czochara M, Pasko P, Zagrodzki P, Gajdzik E, Wietecha-Posluszny R, Gorinstein S. (2016) Selenium supplementation of amaranth sprouts influences betacyanin content and improves anti-inflammatory properties via NFkB in Murine RAW 264.7 Macrophages. *Biological Trace Element Research*, **169**, 320–30.

Tyystjärvi E, Aro EM. (1996) The rate constant of photoinhibition, measured in lincomycin-treated leaves, is directly proportional to light intensity. *Proceedings of the National Academy of Sciences of the United States of America* **93**, 2213–2218.

Ueno O. (2001). Ultrastructural localization of photosynthetic and photorespiratory enzymes in epidermal, mesophyll, bundle sheath, and vascular bundle cells of the C_4 dicot *Amaranthus viridis. Journal of Experimental Botany* **52**, 1003–1013.

Ushiyama R, Matthews RE. (1970) The significance of chloroplast abnormalities associated with infection by turnip yellow mosaic virus. *Virology* **42**, 293–303.

Vainonen JP, Hansson M, Vener AV. (2005) STN8 protein kinase in *Arabidopsis thaliana* is specific in phosphorylation of photosystem II core proteins. *Journal of Biological Chemistry* **280**, 33679–33686.

Valladares F, Martinez-Ferri E, Balaguer L, Perez-Corona E, Manrique E. (2000) Low leaf-level response to light and nutrients in Mediterranean evergreeen oaks: a conservative resource-use strategy? *New Phytologist* **148**, 79–91.

Valladares F, Niinemets U. (2008) Shade tolerance, a key plant feature of complex nature and consequences. *Annual Review of Ecology, Evolution, and Systematics* **39**, 237–257.

van Wijk KJ, van Hasselt PR. (1993) Kinetic resolution of different recovery phases of photoinhibited photosystem II in cold-acclimated and non-acclimated spinach leaves. *Physiologia Plantarum* **87**, 187–198.

Vass I, Styring S, Hundal T, Koivuniemi A, Aro EM, Andersson B. (1992) Reversible and irreversible intermediates during photoinhibition of photosystem II: stable reduced Q_A species promote chlorophyll triplet formation. *Proceedings of the National Academy of Sciences of the United States of America* **89**, 1408–1412.

Vidal O, López-García J, Rendón-Salinas E. (2014) Trends in deforestation and forest degradation after a decade of monitoring in the monarch butterfly biosphere reserve in Mexico. *Conservation Biology* **28**, 177–186.

Vinyard DJ, Ananyev GM, Dismukes GC. (2013) Photosystem II: the reaction center of oxygenic photosynthesis. *Annual Review of Biochemistry* **82**, 577–606.

Vogelmann TC. (1993) Plant tissue optics. *Annual Review of Plant Biology* **44**, 231–251.

Vogelmann TC, Bornmann JF, Yates DJ. (1996a) Focusing of light by leaf epidermal cells. *Physiologia Plantarum* **98**, 43–56.

Vogelmann TC, Nishio JN, Smith WK. (1996b) Leaves and light capture: light propagation and gradients of carbon fixation within leaves. *Trends in Plant Science* **1**, 65–70.

Vogelmann TC, Han T. (2000) Measurement of gradients of absorbed light in spinach leaves from chlorophyll fluorescence profiles. *Plant, Cell & Environment* **23**, 1303–1311.

Vogt T, Ibdah M, Schmidt J, Wray V, Nimtz M, Strack D. (1999) Light induced betacyanin and flavonols accumulation in bladder cells of *Mesembryanthemum crystallinum. Phytochemistry* **52**, 583–592.

Voznesenskaya EV, Franceschi VR, Pyankov VI, Edwards GE. (1999) Anatomy, chloroplast structure and compartmentation of enzymes relative to photosynthetic mechanisms in leaves and cotyledons of species in the tribe Salsoleae (Chenopodiaceae). *Journal of Experimental Botany* **50**, 1779–1795.

Wagner GJ, Wang E, Shepherd RW. (2004) New approaches for studying and exploiting an old protuberance, the plant trichome. *Annals of Botany* **93**, 3–11.

Walker D. (1987) The use of the oxygen electrode and fluorescence probes in simple measurements of photosynthesis. Sheffield: Robert Hill Institute, The University of Sheffield, pp. 212.

Walters RG. (2005) Towards an understanding of photosynthetic acclimation. *Journal of Experimental Botany* **56**, 435–447.

Walters RG, Horton P. (1994) Acclimation of *Arabidopsis thaliana* to the light environment: changes in composition of the photosynthetic apparatus. *Planta* **195**, 248–256.

Wang CQ, Zhao JQ, Chen M, Wang BS. (2006) Identification of betacyanin and effects of environmental factors on its accumulation in halophyte *Suaeda salsa* L. *Journal of Plant Physiology and Molecular Biology* **32**, 195–201.

Wang CQ, Liu T. (2007) Involvement of betacyanin in chilling-induced photoinhibition in leaves of *Suaeda salsa*. *Photosynthetica* **45**, 182–188.

Ward DA, Woolhouse HW. (1986) Comparative effects of light during growth on the photosynthetic properties of NADP-ME type C4 grasses from open and shaded habitats. 1. Gas exchange, leaf anatomy and ultrastructure. *Plant, Cell & Environment* **9**, 261–270.

Webb MS, Green BR. (1991) Biochemical and biophysical properties of thylakoid acyl lipids. *Biochimica et Biophysica Acta*, **1060**, 133–158.

Weinhold A, Baldwin IT. (2011) Trichome-derived O-acyl sugars are a first meal for caterpillars that tags them for predation. *Proceedings of the National Academy of Sciences of the United States of America* **108**, 7855–7859.

Westphal S, Soll J, Vothknecht UC. (2003) Evolution of chloroplast vesicle transport. *Plant & Cell Physiology* **44**, 217–222.

Wilson KE, Ivanov AG, Öquist G, Grodzinski B, Sarhan F, Hüner NPA. (2006) Energy balance, organellar redox status, and acclimation to environmental stress. *Canadian Journal of Botany* **84**, 1355–1370.

Wise RR, Harris JB. (1984) The three-dimensional structure of the *Cyphomandra betacea* chloroplast peripheral reticulum. *Protoplasma* **119**, 222–225.

Wise RR. (2006) The diversity of plastid form and function. In: Wise RR, Hoober JK (eds) The Structure and Function of Plastids. Dordrecht: Springer, pp. 3–26.

Wientjes E, van Amerongen H, Croce R. (2013) LHCII is an antenna of both photosystems after long-term acclimation. *Biochimica et Biophysica Acta* **1827**, 420–426.

Wu LC, Hsu HW, Chen YC, Chiu CC, Lin YI, Ho JA (2006) Antioxidant and antiproliferative activities of red pataya. *Food Chemistry* **95**, 319–327.

Wybraniec S, Jerz G, Gebers N, Winterhalter P. (2010) Ion-pair high-speed countercurrent chromatography in fractionation of a high-molecular weight variation of acyl-oligosaccharide linked betacyanins from purple bracts of *Bougainvillea glabra*. *Journal of Chromatography B Analytical Technologies in the Biomedical and Life Science* **878**, 538–550.

Yamori W, Evans JR, von Cammerer S. (2009) Effects of growth and measurement light intensities on temperature dependence of CO_2 assimilation rate in tobacco leaves. *Plant, Cell & Environment* **33**, 332–343.

Yamori W, Shikanai T. (2016) Physiological functions of cyclic electron transport around photosystem I in sustaining photosynthesis and plant growth. *Annual Review of Plant Biology* **67**, 81–106.

Yokono M, Takabayashi A, Akimoto S, Tanaka A. (2015) A megacomplex composed of both photosystem reaction centres in higher plants. *Nature Communications* **6**, 6675.

Yu G, Nguyen TT, Guo Y, Schauvinhold I, Auldridge ME, Bhuiyan N, Ben-Israel I, Iijima Y, Fridman E, Noel JP, Pichersky E. (2010) Enzymatic functions of wild tomato methylketone synthases 1 and 2. *Plant Physiology* **154**, 67–77.

Yu G, Pichersky E. (2014) Heterologous expression of methylketone synthase1 and methylketone synthase2 leads to production of methylketones and myristic acid in transgenic plants. *Plant Physiology* **164**, 612–622.

Zarinkamar F. (2007) Stomatal observations in dicotyledons. *Pakistan Journal of Biological Sciences* **10**, 199–219.

Zhang D, Lanier SM, Downing JA, Avent JL, Lum J, McHale JL. (2008) Betalain pigments for dye-sensitized solar cells. *Journal of Photochemistry and Photobiology A: Chemistry* **195**, 72–80.

Zivcak M, Brestic M, Kalaji HM. (2014) Photosynthetic responses of sun-and shade-grown barley leaves to high light: is the lower PSII connectivity in shade leaves associated with protection against excess of light. *Photosynthesis Research* **119**, 339–354.

CHAPTER 8

8.0 APPENDICES

Table A1 Pigment analyses for red and green varieties of *Amaranthus.* Total chlorophyll (Chl), total carotenoid (Car), chlorophyll *a/b* ratios and chlorophyll/carotenoid ratios (Chl/Car) were determined from the fourth leaves of plants grown under HL and LL. Values represent means ± SE (*n* = 3). Values followed by different letters in each row indicate a significant difference at *P* = 0.05 using a Holm-Sidak post-hoc test. HL, high light; LL, low light; SE, standard error.

Parameter	Growth Irradiance and Variety			
	HL Red	HL Green	LL Red	LL Green
Total Chl ($\mu g\ g^{-1}$ FW)	1761.05 ± 23.78^{a}	750.87 ± 88.13^{c}	1530.11 ± 51.80^{b}	759.10 ± 61.93^{c}
Total Car ($\mu g\ g^{-1}$ FW)	350.15 ± 21.90^{a}	148.57 ± 25.74^{b}	256.96 ± 47.30^{a}	113.15 ± 15.01^{b}
Chl *a/b*	5.41 ± 0.67^{a}	6.49 ± 0.89^{a}	5.42 ± 0.36^{a}	4.79 ± 0.52^{a}
Total Chl/Car	4.8 ± 0.39^{b}	5.17 ± 0.28^{b}	5.3 ± 0.22^{b}	6.85 ± 0.47^{a}

Table A2 Total betalain content for red and green varieties of *Amaranthus*. Total betalain is the sum of betaxanthins and betacyanins. Total betalain (Bet), betacyanins (Bcy) and betaxanthins (Btx) were determined from the fourth leaves of plants grown under HL and LL. Values represent means ± SE (n = 3). Values followed by different letters in each row indicate a significant difference at P = 0.05 using a Holm-Sidak post-hoc test. HL, high light; LL, low light; SE, standard error.

Pigment ($\mu g\ g^{-1}$ DW)	Growth Irradiance and Variety			
	HL Red	HL Green	LL Red	LL Green
Bet	1243.35 ± 78.28[a]	255.68 ± 26.38[b]	1224.04 ± 24.43[a]	328.10 ± 44.10[b]
Bcy	643.55 ± 71.94[a]	21.36 ± 2.34[b]	492.86 ± 61.91[a]	29.89 ± 0.49[b]
Btx	599.80 ± 124.21[a]	234.32 ± 24.23[b]	731.18 ± 38.79[a]	298.21 ± 43.61[b]

Table A3 Stomatal density for red and green varieties of *Amaranthus.* Leaf imprints were obtained from fourth leaves of plants grown under HL and LL and used for the calculation of the stomatal index and trichome density. Values represent means ± SE (*n* = 3). Values followed by uppercase letters in each column and lowercase letters in each row indicate a significant difference at *P* = 0.05 using a Holm-Sidak post-hoc test. HL, high light; LL, low light; SE, standard error.

Stomatal Density (Stomata/mm^2)	Growth Irradiance and Variety			
	HL Red	HL Green	LL Red	LL Green
Adaxial	54.33 ± 5.24^{aB}	54.33 ± 3.42^{aB}	37.67 ± 6.36^{bA}	16.33 ± 0.887^{cB}
Abaxial	63.00 ± 4.73^{bA}	80.67 ± 7.24^{aA}	32.00 ± 6.51^{dA}	45.67 ± 2.40^{cA}

Table A4 Quantitative parameters of the leaf anatomy of the red and green varieties of *Amaranthus.* Fourth leaves were sampled at 20 and 23 DAS for the red and green variety under HL respectively and at 40 DAS under LL. Values represent means ± SE (*n* = 3 leaves). One transverse section containing 2 vascular bundles was obtained for each leaf. Values followed by different letters in each row indicate a significant difference at *P* = 0.05 using a Holm-Sidak post-hoc test. BSC, bundle sheath cell; DAS, days after sowing; HL, high light; LEC, lower epidermal cells; LMC, lower mesophyll cells; LL, low light; LT, leaf thickness; Max D, maximum diameter; Min D, minimum diameter; MC, mesophyll cell; Perim, perimeter; SE, standard error; UEC, upper epidermal cell; UMC, upper mesophyll cell.

Parameter	Growth Irradiance and Variety			
	HL Red	HL Green	LL Red	LL Green
UEC				
Area (μm^2)	515.94 ± 23.37^{a}	448.71 ± 36.26^{a}	256.87 ± 66.62^{b}	313.79 ± 27.52^{ab}
Perim (µm)	89.72 ± 2.11^{a}	76.31 ± 2.74^{a}	74.33 ± 10.19^{a}	75.66 ± 3.98^{a}
Max D (µm)	36.13 ± 0.98^{a}	27.36 ± 0.84^{a}	28.81 ± 5.11^{a}	30.14 ± 1.85^{a}
Min D (µm)	18.22 ± 0.44^{a}	19.83 ± 1.16^{a}	13.47 ± 1.27^{b}	13.94 ± 0.29^{b}
LEC				
Area (μm^2)	477.23 ± 30.29^{a}	392.95 ± 29.07^{b}	229.72 ± 12.41^{c}	182.92 ± 28.77^{c}
Perim (µm)	103.03 ± 0.48^{a}	78.71 ± 4.17^{b}	64.75 ± 5.79^{c}	51.21 ± 3.58^{d}
Max D (µm)	41.45 ± 0.80^{a}	30.36 ± 2.16^{b}	25.39 ± 2.41^{c}	19.58 ± 1.45^{d}
Min D (µm)	16.86 ± 0.79^{a}	16.74 ± 0.0.51^{a}	11.72 ± 0.39^{b}	10.86 ± 0.66^{b}
UMC				
Area (μm^2)	590.35 ± 91.68^{a}	350.11 ± 29.72^{ab}	311.43 ± 32.03^{b}	315.88 ± 14.41^{b}
Perim (µm)	101.27 ± 8.12^{a}	82.85 ± 3.56^{a}	80.12 ± 6.92^{a}	80.82 ± 0.62^{a}
Max D (µm)	38.35 ± 3.25^{a}	31.35 ± 1.26^{b}	27.28 ± 1.60^{b}	28.38 ± 0.69^{b}
Min D (µm)	20.98 ± 1.12^{a}	15.14 ± 0.45^{b}	17.26 ± 1.69^{b}	16.90 ± 0.40^{b}

LMC				
Area (μm^2)	356.79 ± 70.75[a]	185.48 ± 2.66[b]	127.08 ± 6.27[b]	106.94 ± 7.74[b]
Perim (µm)	82.63 ± 9.26[a]	52.60 ± 0.68[b]	47.28 ± 2.89[b]	40.95 ± 0.50[b]
Max D (µm)	29.36 ± 3.46[a]	19.43 ± 0.27[b]	17.36 ± 1.21[b]	15.51 ± 0.24[b]
Min D (µm)	17.61 ± 1.56[a]	12.23 ± 0.20[b]	10.19 ± 0.27[c]	8.81 ± 0.24[c]
BSC				
Area (μm^2)	705.35 ± 10.27[a]	668.43 ± 70.90[a]	399.0 ± 35.28[b]	358.98 ± 34.14[b]
Perim (µm)	105.65 ± 0.13[a]	98.83 ± 5.52[a]	92.25 ± 6.35[a]	85.78 ± 3.67[a]
Max D (µm)	37.52 ± 0.41[a]	35.91 ± 2.19[a]	32.66 ± 2.52[a]	32.27 ± 0.73[a]
Min D (µm)	26.50 ± 0.34[a]	25.33 ± 1.43[a]	21.77 ± 2.32[b]	18.54 ± 0.35[b]
Thickness Adaxial MC (µm)	41.92 ± 0.42[a]	39.83 ± 0.89[a]	24.66 ± 1.92[b]	25.12 ± 2.52[b]
Abaxial MC (µm)	38.01± 0.79[a]	31.54 ± 2.31[b]	15.94 ± 0.17[c]	17.24 ± 2.13[c]
Thickness LT (µm)	175.07 ± 1.77[a]	164.42 ± 4.26[b]	100.94 ± 4.19[c]	102.25 ± 1.03[c]

Table A5 Quantitative parameters of chloroplasts (C) and mitochondria (M) from profiles of BSC, MC, VPC and CC from sections of fourth leaves of the red and green varieties of *Amaranthus* grown under HL and LL. The plant material for the sections were sampled at 20 and 23 DAS for the red and green variety under HL respectively and at 40 DAS under LL. Values represent means ± SD (*n* = 3 to 50 organelles from multiple fields of view). Values followed by different letters in each row indicate a significant difference at *P* = 0.05 using a Holm-Sidak post-hoc test. BSC, bundle sheath cell; CC, companion cell; HL, high light; LL, low light; MC, mesophyll cell; Perim, perimeter; SD, standard deviation; VPC, vascular parenchyma cell.

Parameters	Growth Irradiance and Variety			
	HL Red	HL Green	LL Red	LL Green
C Area (μm^2)				
BSC	33.86 ± 17.10^a	20.36 ± 8.59^b	21.26 ± 9.30^b	21.38 ± 7.19^b
MC	12.41 ± 2.82^a	6.06 ± 2.86^b	13.05 ± 4.45^a	10.88 ± 4.90^a
VPC	8.89 ± 3.14^a	4.06 ± 0.83^b	5.67 ± 3.45^b	3.07 ± 1.07^b
CC	4.99 ± 1.56^a	3.77 ± 2.08^b	6.48 ± 2.36^a	3.61 ± 1.81^b
C Perim (μm)				
BSC	39.70 ± 16.47^a	21.70 ± 6.33^b	22.93 ± 5.38^b	24.07 ± 5.0^b
MC	16.10 ± 2.21^a	10.33 ± 2.09^b	18.02 ± 3.27^a	16.96 ± 4.88^a
VPC	13.63 ± 2.30^a	9.72 ± 1.71^b	12.88 ± 4.54^a	8.49 ± 1.92^b
CC	8.57 ± 1.33^a	7.38 ± 2.18^a	9.51 ± 1.64^a	7.96 ± 2.57^a
C Max D (μm)				
BSC	15.91 ± 5.26^a	8.92 ± 2.29^b	9.52 ± 2.28^b	10.46 ± 2.43^b
MC	6.95 ± 1.13^a	4.33 ± 0.89^b	7.99 ± 1.55^a	7.59 ± 2.34^a
VPC	5.53 ± 1.19^a	4.25 ± 0.86^b	5.80 ± 1.88^a	3.84 ± 0.95^b
CC	3.01 ± 0.42^a	2.83 ± 0.78^a	3.48 ± 0.77^a	3.29 ± 1.06^a
C Min D (μm)				
BSC	4.93 ± 2.46^a	3.39 ± 1.06^b	3.62 ± 1.38^b	3.26 ± 0.89^b

MC	2.43 ± 0.54[a]	1.81 ± 0.62[b]	2.36 ± 0.47[a]	2.07 ± 0.46[a]
VPC	2.49 ± 0.53[a]	1.40 ± 0.19[b]	1.55 ± 0.80[b]	1.05 ± 0.20[b]
CC	2.28 ± 0.58[a]	1.65 ± 0.66[b]	2.37 ± 0.42[a]	1.50 ± 0.43[b]
M Area (μm^2)				
BSC	0.94 ± 0.65[a]	0.86 ± 0.64[a]	1.23 ± 0.92[a]	1.34 ± 1.15[a]
MC	0.50 ± 0.30[a]	0.62 ± 0.35[a]	0.28 ± 0.16[b]	0.48 ± 0.31[a]
VPC	0.43 ± 0.20[a]	0.31 ± 0.14[a]	0.24 ± 0.14[b]	0.28 ± 0.16[ab]
CC	0.41 ± 0.14[a]	0.38 ± 0.14[a]	0.41 ± 0.17[a]	0.21 ± 0.10[b]
M Perimeter (µm)				
BSC	4.18 ± 1.64[a]	3.73 ± 1.41[a]	4.26 ± 1.72[a]	4.19 ± 1.61[a]
MC	2.62 ± 0.88[a]	3.00 ± 1.15[a]	2.03 ± 0.74[b]	2.63 ± 0.93[a]
VPC	2.46 ± 0.59[a]	2.18 ± 0.65[a]	1.90 ± 0.73[a]	1.93 ± 0.56[a]
CC	2.46 ± 0.42[a]	2.39 ± 0.59[a]	2.45 ± 0.54[ab]	1.71 ± 0.52[b]
M Max D (µm)				
BSC	1.58 ± 0.58[a]	1.48 ± 0.65[a]	1.63 ± 0.71[a]	1.54 ± 0.59[a]
MC	0.97 ± 0.38[a]	1.10 ± 0.50[ab]	0.75 ± 0.34[a]	1.02 ± 0.40[b]
VPC	0.90 ± 0.21[a]	0.82 ± 0.29[a]	0.63 ± 0.20[b]	0.69 ± 0.21[ab]
CC	0.92 ± 0.18[a]	0.89 ± 0.30[a]	0.92 ± 0.24[a]	0.63 ± 0.25[b]
M Min D (µm)				
BSC	0.85 ± 0.35[b]	0.75 ± 0.20[b]	0.90 ± 0.36[ab]	1.00 ± 0.45[a]
MC	0.64 ± 0.16[a]	0.72 ± 0.15[a]	0.49 ± 0.11[b]	0.57 ± 0.18[b]
VPC	0.59 ± 0.15[a]	0.49 ± 0.11[a]	0.49 ± 0.19[a]	0.50 ± 0.13[a]
CC	0.58 ± 0.12[a]	0.57 ± 0.07[a]	0.58 ± 0.11[a]	0.42 ± 0.08[b]

Table A6 Ultrastructural quantitative parameters of the chloroplasts (C) from sections of fourth leaves of the red and green varieties of *Amaranthus* grown under HL and LL. The plant material for the sections were sampled at 20 and 23 DAS for the red and green variety under HL respectively and at 40 DAS under LL. Values represent means ± SD (*n* = 3 to 9 chloroplasts from multiple fields of view). Values followed by different letters in each row indicate a significant difference at *P* = 0.05 using a Holm-Sidak post-hoc test. BSC, bundle sheath cell; CC, companion cell; CP, cytoplasmic protrusions; DAS, days after sowing; HL, high light; LL, low light; MC, mesophyll cell; PR, peripheral reticulum, SD, standard deviation; VPC, vascular parenchyma cell.

Parameters	Growth Irradiance and Variety			
	HL Red	HL Green	LL Red	LL Green
Area C (µm²)				
BSC	28.33 ± 4.03[a]	19.22 ± 10.83[a]	22.40 ± 6.71[a]	18.00 ± 4.47[a]
MC	11.72 ± 3.89[a]	7.79 ± 2.58[a]	9.86 ± 3.55[a]	6.17 ± 2.71[a]
VPC	9.78 ± 3.18[a]	3.80 ± 0.74[b]	5.52 ± 3.34[b]	3.30 ± 0.98[b]
CC	6.86 ± 0.72[a]	4.57 ± 0.69[ab]	6.55 ± 2.29[a]	3.11 ± 1.07[b]
Granal Index (%)				
BSC	52.62 ± 6.33[a]	26.22 ± 2.46[c]	42.29 ± 7.93[b]	46.40 ± 7.59[b]
MC	39.77 ± 5.82[a]	33.20 ± 6.64[a]	48.02 ± 4.97[ab]	48.55 ± 8.32[b]
VPC	54.57 ± 7.74[a]	32.21 ± 1.93[b]	57.91 ± 3.87[a]	53.71 ± 9.07[a]
CC	64.06 ± 3.06[a]	55.51 ± 4.65[a]	64.05 ± 5.11[a]	43.19 ± 4.09[a]
Granal Density (grana/µm)				
BSC	3.35 ± 0.43[b]	6.96 ± 1.55[a]	5.90 ± 1.91[a]	7.11 ± 1.79[a]
MC	7.89 ± 3.18[b]	13.50 ± 3.95[a]	7.70 ± 1.57[b]	12.66 ± 2.20[a]
VPC	3.96 ± 1.00[b]	17.31 ± 2.56[a]	8.77 ± 0.40[a]	12.86 ± 7.65[a]
CC	3.31 ± 1.34[b]	6.22 ± 1.46[b]	4.44 ± 1.23[b]	9.01 ± 3.01[a]

Appressed Thylakoid Density (μm/μm²)				
BSC	15.24 ± 2.93[a]	8.27 ± 1.77[b]	14.02 ± 4.87[a]	16.64 ± 6.08[a]
MC	20.56 ± 9.62[a]	20.38 ± 7.56[a]	24.37 ± 6.96[a]	29.61 ± 7.39[a]
VPC	15.01 ± 3.27[b]	13.12 ± 1.41[b]	25.50 ± 3.71[ab]	31.35 ± 12.57[a]
CC	8.94 ± 1.84[a]	14.22 ± 4.58[a]	14.41 ± 2.91[a]	12.01 ± 2.24[a]
Non-Apppressed Thylakoid Density (μm/μm²)				
BSC	13.83 ± 3.31[a]	22.49 ± 3.33[a]	19.35 ± 6.90[a]	19.46 ± 6.45[a]
MC	31.73 ± 13.63[a]	40.36 ± 9.12[a]	25.77 ± 3.30[a]	31.28 ± 6.49[a]
VPC	12.35 ± 1.87[b]	27.84 ± 4.85[a]	18.51 ± 2.54[b]	26.77 ± 12.45[a]
CC	5.10 ± 1.71[b]	11.57 ± 4.05[ab]	8.16 ± 2.10[b]	15.88 ± 3.20[a]
Total Thylakoid Density (μm/μm²)				
BSC	29.07 ± 5.01[a]	30.53 ± 4.71[a]	33.37 ± 10.55[a]	36.10 ± 10.80[a]
MC	52.29 ± 22.64[a]	60.73 ± 13.93[a]	50.14 ± 9.42[a]	60.90 ± 9.13[a]
VPC	27.36 ± 2.20[b]	40.95 ± 6.16[b]	44.01 ± 5.19[b]	72.29 ± 15.26[a]
CC	14.92 ± 2.93[a]	25.79 ± 8.42[a]	22.58 ± 4.60[a]	29.75 ± 5.67[a]
Thylakoids/Granum				
BSC	9.17 ± 2.67[a]	4.08 ± 1.21[c]	6.52 ± 1.11[b]	6.29 ± 0.61[b]
MC	7.44 ± 2.22[a]	4.78 ± 0.56[c]	9.13 ± 1.74[a]	6.95 ± 1.39[b]
VPC	9.45 ± 1.80[a]	3.47 ± 0.42[b]	7.32 ± 0.45[a]	6.98 ± 2.18[a]
CC	5.18 ± 1.25[a]	5.50 ± 0.69[a]	6.05 ± 1.79[a]	4.76 ±2.16[a]
Length Appressed Thylakoids/Non-Appressed Thylakoids				
BSC	1.14 ± 0.28[a]	0.37 ± 0.03[c]	0.76 ± 0.27[b]	0.90 ± 0.27[b]
MC	0.67 ± 0.16[b]	0.51 ± 0.15[b]	0.94 ± 0.21[ab]	0.98 ± 0.30[a]
VPC	1.26 ± 0.43[a]	0.48 ± 0.04[a]	1.39 ± 0.21[a]	1.25 ± 0.54[a]
CC	1.79 ± 0.24[a]	1.27 ± 0.24[a]	1.83 ± 0.41[a]	0.77 ± 0.12[a]
PR and CP Area from C Area				

BSC	0.00 [b]	2.73 ± 1.20[a]	0.00 [b]	1.92 ± 0.66[a]
MC	0.00 [b]	1.02 ± 0.84[a]	0.00 [b]	0.91 ± 0.44[a]
VPC	0.00 [b]	0.71 ± 0.23[a]	0.00 [b]	0.70 ± 0.32[a]
CC	0.00 [b]	0.00[b]	0.00 [b]	0.56 ± 0.26[a]
Stroma Area (µm²)				
BSC	16.21 ± 2.03[a]	10.04 ± 5.31[b]	13.56 ± 5.92[a]	9.44 ± 3.56[b]
MC	6.60 ± 4.61[a]	2.24 ± 1.04[a]	4.65 ± 1.71[a]	2.00 ± 0.66[a]
VPC	5.75 ± 2.11[a]	1.16 ± 0.20[b]	2.90 ± 1.55[b]	1.33 ± 0.54[b]
CC	5.16 ± 0.98[a]	2.64 ± 0.91[ab]	4.55 ± 1.59[a]	1.66 ± 0.59[b]
Starch Area (µm²)				
BSC	0.68 ± 1.27[a]	0.37 ± 0.65[a]	0.00[a]	0.00[a]
MC	0.06 ± 0.12[a]	0.05 ± 0.10[a]	0.00[a]	0.00[a]
VPC	0.10 ± 0.20[a]	0.00[a]	0.00[a]	0.00[a]
CC	0.01 ± 0.01[a]	0.00[a]	0.00[a]	0.00[a]
Plastoglobuli Area (µm²)				
BSC	0.16 ± 0.08[b]	0.36 ± 0.27[a]	0.04 ± 0.02[b]	0.12 ± 0.07[b]
MC	0.10 ± 0.03[a]	0.13 ± 0.05[a]	0.02 ± 0.01[b]	0.01 ± 0.00[b]
VPC	0.07 ± 0.04[a]	0.05 ± 0.01[a]	0.02 ± 0.01[b]	0.03 ± 0.03[ab]
CC	0.00 [b]	0.01 ± 0.00[b]	0.04 ± 0.02[a]	0.04 ± 0.03[ab]
Total Thylakoid Area (µm²)				
BSC	12.26 ± 1.42[a]	6.13 ± 4.63[b]	8.82 ± 1.12[b]	8.13 ± 2.00[b]
MC	7.56 ± 1.97[a]	4.19 ± 1.66[b]	5.08 ± 1.87[ab]	3.08 ± 1.69[b]
VPC	3.86 ± 1.22[a]	1.53 ± 0.29 [b]	2.60 ± 1.79[ab]	1.11 ± 0.39[b]
CC	1.69 ± 0.27[a]	1.92 ± 0.36[a]	1.96 ± 0.81[a]	0.93 ± 0.39[b]
Appressed Thylakoids Length (µm)				
BSC	244.76 ± 40.69[a]	74.60 ± 23.67[c]	172.17 ± 62.43[b]	141.83 ± 22.14[b]

MC	111.25 ± 32.01[a]	42.19 ± 12.79[b]	109.45 ± 37.36[a]	58.22 ± 19.80[b]
VPC	89.88 ± 50.23[a]	15.10 ± 2.12[b]	73.70 ± 36.89[ab]	37.31 ± 13.68[b]
CC	45.25 ± 0.78[b]	34.60 ± 3.33[b]	63.73 ± 16.06[a]	19.10 ± 3.91[b]
Non-Appressed Thylakoids Length (µm)				
BSC	226.48 ± 70.51[a]	214.77 ± 4.81[a]	233.21 ± 63.11[a]	167.49 ± 43.25[a]
MC	165.00 ± 18.69[a]	86.38 ± 28.23[b]	121.33 ± 50.11[a]	63.22 ± 26.92[b]
VPC	71.34 ± 28.72[a]	32.16 ± 7.04[b]	56.06 ± 34.97[ab]	32.37 ± 12.34[b]
CC	25.50 ± 3.82[a]	27.98 ± 5.66[a]	37.60 ± 16.51[a]	25.73 ± 8.32[a]
Appressed Thylakoids Area (µm²)				
BSC	5.15 ± 1.12[a]	1.35 ± 0.57[a]	3.96 ± 1.14[a]	3.22 ± 0.66[b]
MC	2.75 ± 0.67[a]	0.83 ± 0.19[b]	2.16 ± 0.83[a]	1.14 ± 0.50[b]
VPC	1.64 ± 0.55[a]	0.23 ± 0.07[b]	1.04 ± 0.48[ab]	0.66 ± 0.23[b]
CC	0.82 ± 0.19[a]	0.66 ± 0.09[a]	0.99 ± 0.26[a]	0.39 ± 0.10[a]

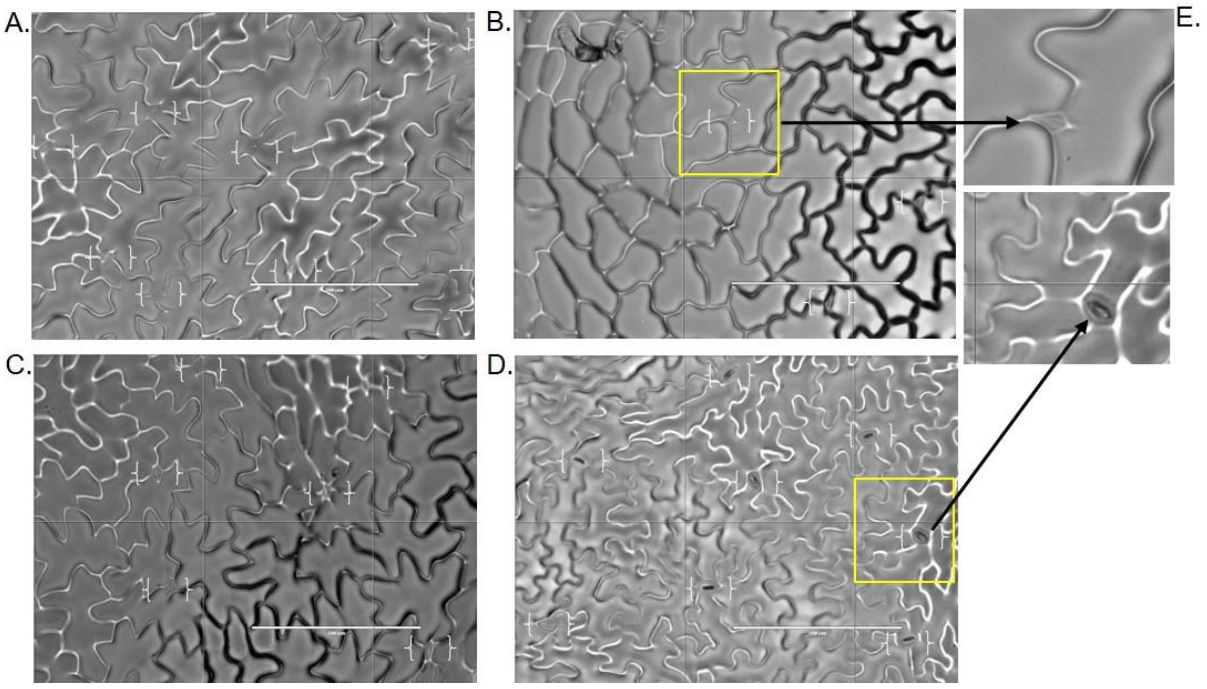

Figure A1 Distribution of stomata for *Amaranthus* grown under LL. Fourth leaves of the red (**A., C.**) and green (**B., D.**) varieties were analyzed on the adaxial (**A., B.**) and abaxial (**C., D.**) leaf surfaces. The insert (**E.**) shows a close up of the anomocytic stomatal (AS) complex. Scale bars indicate 200 µm. Representative images are shown. AS, anomocytic stomata; LL, Low light.

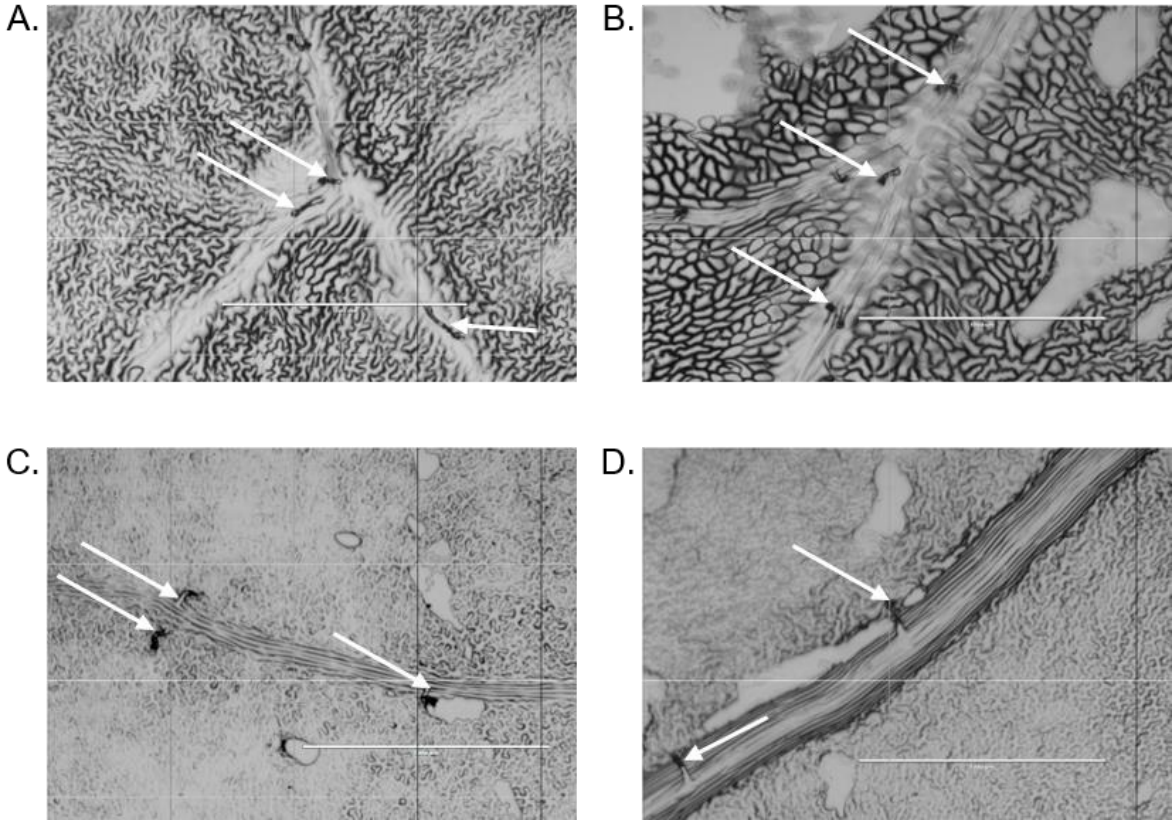

Figure A2 Distribution of trichomes for *Amaranthus* grown under LL. Fourth leaves of the red (**A., C.**) and green (**B., D.**) varieties were analyzed on the adaxial (**A., B.**) and abaxial (**C., D.**) leaf surfaces. Trichomes are indicated by arrows. Scale bars indicate 1 mm. Representative images are shown. LL, low light.

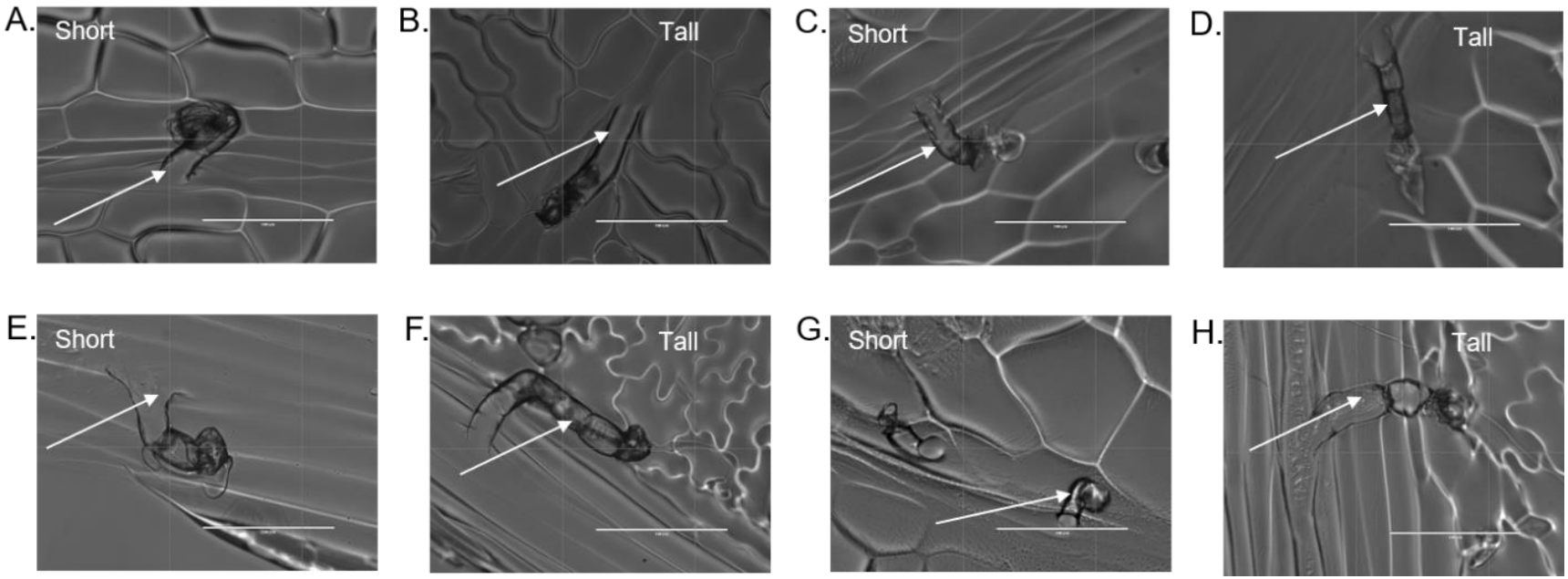

Figure A3 Short and tall, multicellular and uniseriate, glandular trichomes for *Amaranthus* grown under LL. Fourth leaves of the red (**A., B., E., F.**) and green (**C., D., G., H.**) varieties were analyzed from imprints taken on the adaxial (**A., B., C., D.**) and abaxial (**E., F., G., H.**) leaf surfaces. Trichomes are indicated by arrows. Scale bars indicate 100 µm. Representative images are shown. LL, low light.

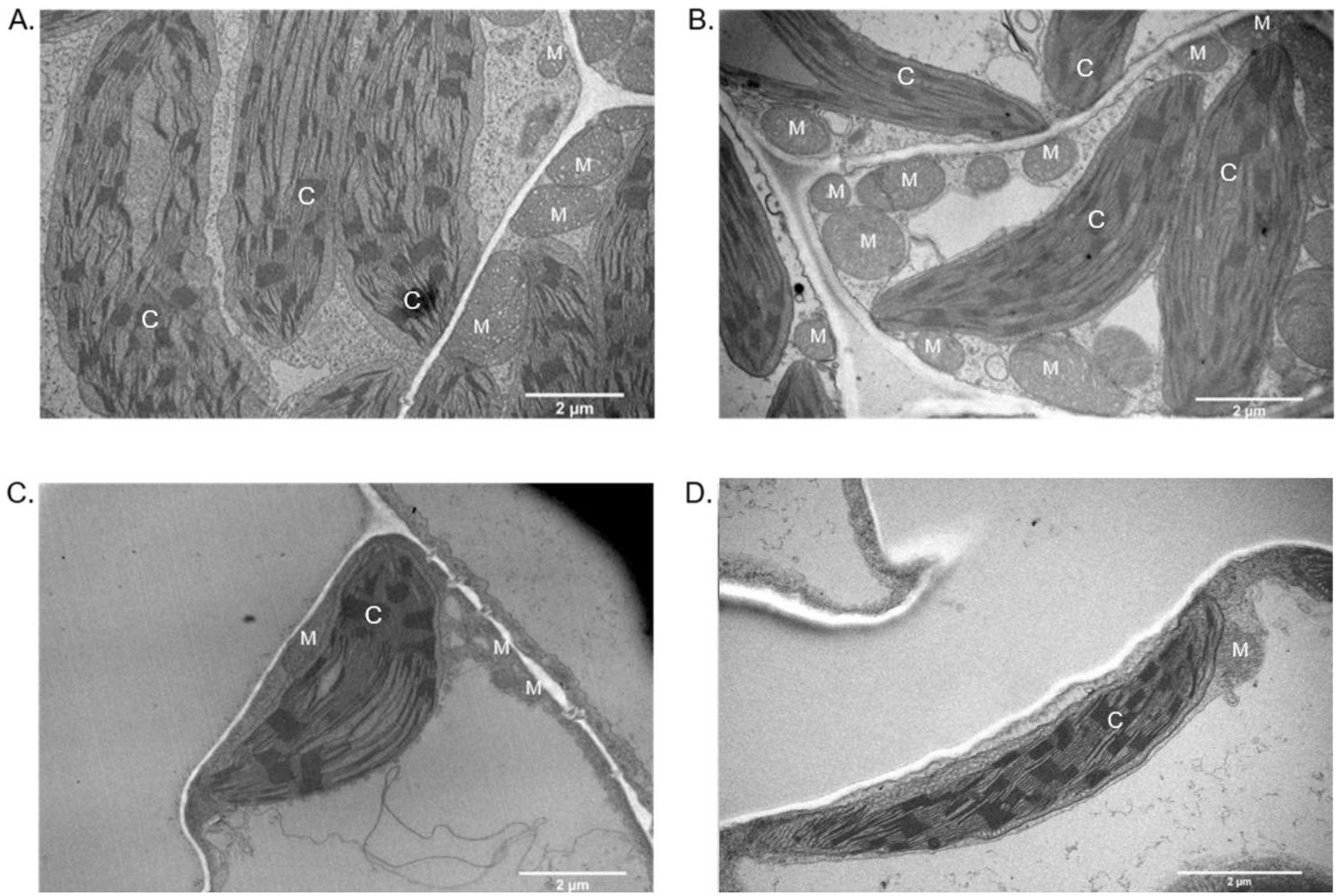

Figure A4 Ultrastructure of cells in leaves of *Amaranthus* grown under LL. Fourth leaf sections of the red (**A., C.**) and green (**B., D.**) varieties were analyzed from profiles of BSC (**A., B.**) and MC (**C., D.**). Scale bars indicate 2 µm. Representative images are shown. BSC, bundle sheath cell; C; chloroplast; LL, low light; MC, mesophyll cell; M, mitochondrion.

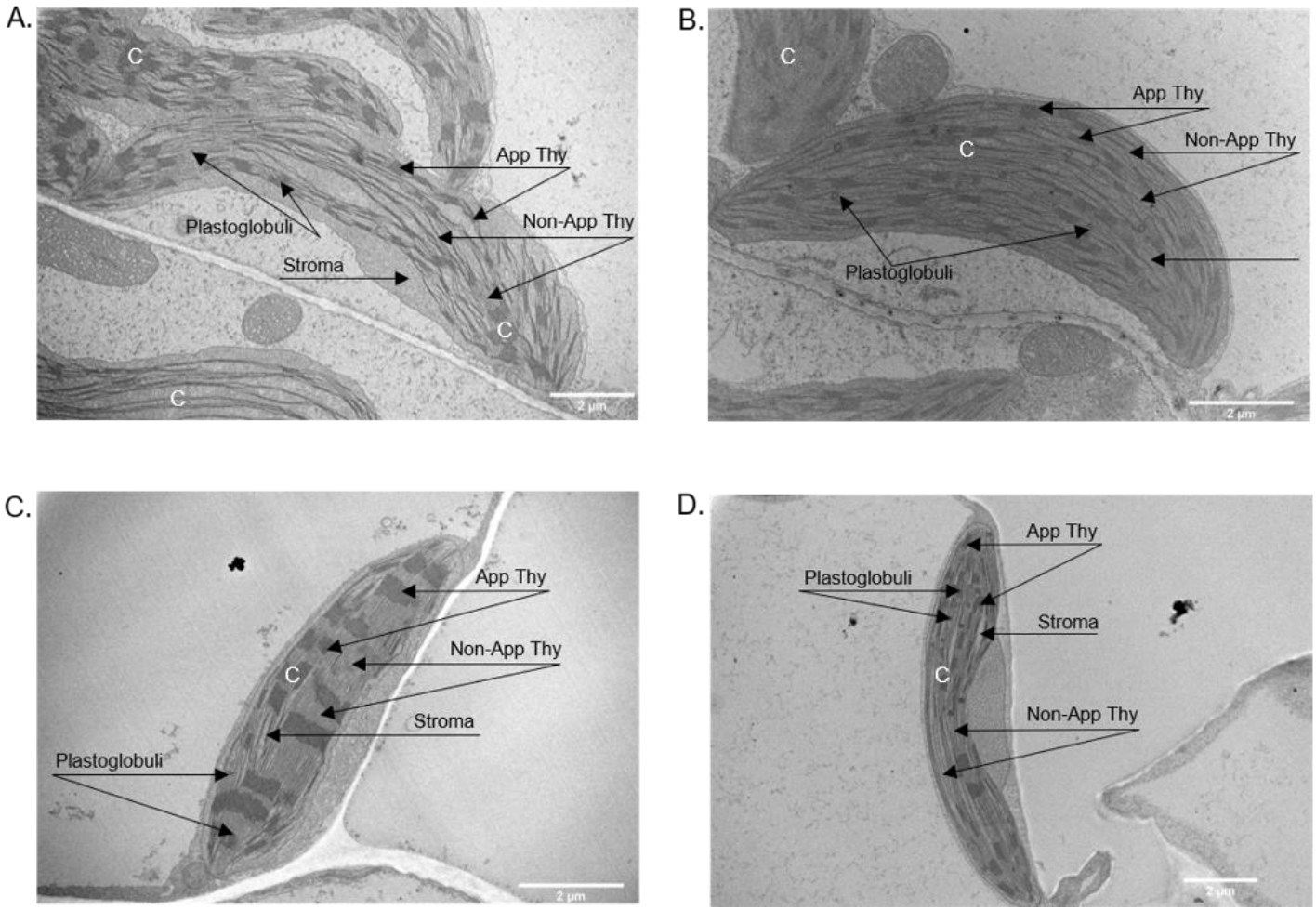

Figure A5 Chloroplasts ultrastructure of cells in leaves of *Amaranthus* grown under LL. Sections from fourth leaves of the red (**A., C.**) and green (**B., D.**) varieties were analyzed from profiles of BSC (**A., B.**) and MC (**C., D.**). Scale bars indicate 2 µm. Representative images are shown. App Thy, appressed thylakoids; BSC, bundle sheath cell; C, chloroplast; LL, low light; MC, mesophyll cell; Non-App, non-appressed thylakoids.